10-2022

Characterization of Nursery Habitats used by Black Sea Bass and Summer Flounder in Chesapeake Bay and the Coastal Lagoons

Mary C. Fabrizio
Virginia Institute of Marine Science

Troy D. Tuckey
Virginia Institute of Marine Science

Shannon C. Smith
Virginia Institute of Marine Science

Paige G. Ross
Virginia Institute of Marine Science

Richard A. Snyder
Virginia Institute of Marine Science

See next page for additional authors

Characterization of Nursery Habitats used by Summer Flounder and Black Sea Bass in Chesapeake Bay and the Coastal Lagoons

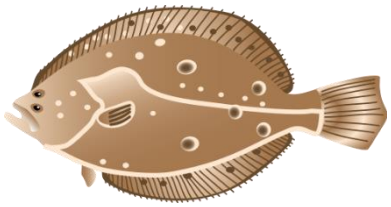

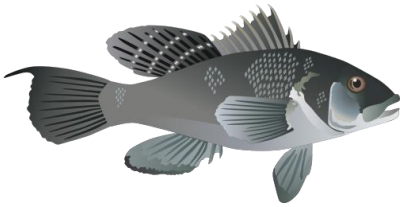

Mary C. Fabrizio	Fisheries Science Department
Troy D. Tuckey	Fisheries Science Department
Shannon C. Smith	Fisheries Science Department
Paige G. Ross, Jr.	Eastern Shore Laboratory
Richard A. Snyder	Eastern Shore Laboratory
Harry Wang	Physical Sciences Department
Aaron J. Bever	Anchor QEA, LLC

Final Report Submitted to:

NOAA Chesapeake Bay Office

Annapolis, MD

October 2022

DOI: 10.25773/PJCC-RG41

VIMS | William & Mary

Virginia Institute of Marine Science

Executive Summary: Characterization of Nursery Habitats used by Summer Flounder and Black Sea Bass in Chesapeake Bay and the Coastal Lagoons

M. C. Fabrizio, T. D. Tuckey, S. C. Smith, P. G. Ross, Jr., R. A. Snyder, H. Wang, and A. J. Bever

We studied the role of nursery areas at two spatial scales to determine how individual habitat types (oyster, marsh, seagrass, and soft-bottom habitats), as well as the seascape, support abundance, condition, and growth of juvenile fishes. In our small-scale field study conducted in 2019 and 2020, we found greater mean abundances of both species at Eastern Shore nursery sites relative to Piankatank River nursery sites, and in the case of black sea bass, that difference was an order of magnitude. These differences in relative abundance were likely associated with differences in the proximity of Eastern Shore sites to the coastal ocean, variations in physicochemical conditions, differences in seascape complexity, or a combination of two or more of these factors. Eastern Shore sites were characterized by a greater mean salinity, and more diverse seascapes; in particular, the Eastern Shore area had a greater percentage of structured habitats (especially seagrass), and less soft-bottom habitat than the Piankatank River area. Comparative evaluation of the quality of seaside and bayside nursery areas at a fine spatial scale can provide managers and policy makers with critical information on the importance of habitats and their placement in coastal systems. Proximity to the coastal ocean cannot be regulated or changed, but managers can develop and promote habitat conservation and restoration plans to ensure the availability of diverse and complex structured habitats. Such plans could promote the long-term sustainability of fishery resources by supporting production of abundant year classes.

Within the Eastern Shore and Piankatank seascapes, relative abundance of juvenile summer flounder was greatest in marsh habitats. Although consistent with reported habitat use, such associations have not been previously documented for the Chesapeake Bay region. We hypothesized that because marshes are highly productive systems, these habitats offer an abundance of prey for juvenile summer flounder. Marshes also provide tidally inundated, shallow areas that juvenile summer flounder may use as a refuge from predation. The protection and restoration of marsh habitats in Chesapeake Bay can directly benefit juvenile summer flounder by the provisioning of areas that contribute to the continued production of these fisheries. Looking ahead, conservation and protection of marshes as nursery grounds for fishes will require a holistic, ecosystem-based approach. Under climate change and sea-level rise, natural resource managers and land managers will need to work together to develop policies to address the transition of uplands (agricultural and forest lands) to marshes.

The body condition and recent growth of juvenile summer flounder and juvenile black sea bass were similar between the Eastern Shore and Piankatank River sites. We found no effect of seascape composition or complexity on juvenile summer flounder relative body condition or recent growth. Effects on recent growth and body condition of juvenile black sea bass were marginal, and the explanatory power of our models was low due to small sample sizes, which reflected the poor recruitment events observed in 2019 and especially in 2020 for these two species. Similarly, habitat type (marsh, oyster, seagrass, soft-bottom) had no effect on recent growth or body condition of juvenile black sea bass and summer flounder. Together,

these results suggest that juvenile fishes use multiple habitat types within the seascape to maximize growth and condition, and underscore the nursery value of complex seascapes.

We also explored habitat associations of juvenile fishes using long-term (1989 – 2019) catch records from surveys that sampled fishes during their duration of estuarine residency and over broad spatial scales. The three surveys considered here varied in terms of the window during which monthly sampling occurred, the depth range of habitats sampled, and the prevailing environmental conditions. We found that environmental differences among survey areas produced non-stationarity in the relationship between relative abundance and environmental conditions. To address this, we developed separate models for these relationships for each survey area. Bottom temperature and bottom salinity were significant predictors of relative abundance of juvenile summer flounder. Juvenile black sea bass abundance was affected by depth, bottom water temperature, salinity, and the proximity to structured habitats. The relationships of relative abundance to environmental conditions varied depending on the survey area – Virginia estuarine waters, Maryland estuaries, and the Maryland coastal bays.

Temperature, salinity, and distance to structure were important predictors of juvenile summer flounder growth. Indeed, thermal conditions that exceeded 25.9 °C were detrimental to growth of juvenile summer flounder and as such, we defined suitable thermal habitats for growth as those areas where bottom temperatures were less than 25.9 °C; these areas represent potential habitats for juvenile summer flounder. Local density of conspecifics was an important predictor of growth for juvenile summer flounder and black sea bass, reflecting possible density-dependent processes that limit growth of these species in nursery areas.

Juvenile summer flounder were larger on average in shallow habitats of the Choptank River and eastern bay in the Maryland portion of the bay, suggesting these areas better support growth of this species. The Choptank River is a NOAA Habitat Focus Area and is one of several areas benefitting from significant restoration of native oysters. This river appears to also support juvenile summer flounder that are larger than conspecifics from other areas of the bay. We caution, however, that greater growth rates may not indicate greater survival of juvenile summer flounder because information on mortality rates from these areas is lacking.

In summer, bottom-water temperatures in the Chesapeake Bay routinely exceeded the threshold for suitable thermal habitat for juvenile summer flounder growth. The proportion of the bay with suitable thermal conditions for this species declined between 47% and 64% since 1996. A greater proportion of Maryland waters tended to exceed the thermal threshold than waters in Virginia, and thus, proportionate loss of suitable potential habitat was greatest in Maryland. The greatest decline in the proportion of the bay with suitable conditions occurred in August, just prior to when juvenile summer flounder begin to leave coastal systems to migrate to their offshore wintering habitats on the shelf. The loss of suitable potential habitat in August since 1996 may trigger earlier emigration by juvenile summer flounder, and could explain the declining catches observed in September, October, and November in recent years in fishery-independent surveys. Thermal conditions of bottom waters in the Virginia portion of the bay responded on a fine temporal scale (daily) to the intrusion of cool bottom-water from the continental shelf. As the climate continues to warm, atmospheric conditions are likely to

change such that bottom-water intrusion events in summer may continue to decline, with the subsequent decline in suitable thermal conditions for juvenile summer flounder growth.

Median (annual) extent of suitable thermal habitat was not related to the annual relative abundance of juvenile summer flounder, suggesting that the extent of suitable habitats was sufficient to support the population of juvenile summer flounder that use Chesapeake Bay as a nursery area. Other factors are likely contributing to observed changes in recruitment of summer flounder to the bay. We suggest these factors include changes in the availability of prey resources in nursery areas, and the northward shift in the location of offshore spawning areas for summer flounder.

Characterization of Nursery Habitats used by Summer Flounder and Black Sea Bass in Chesapeake Bay and the Coastal Lagoons

Introduction

Coastal habitats are increasingly impacted by intersecting and often competing human activities overlaid on habitat loss and degradation. These demands have prompted resource managers to implement marine spatial-planning strategies (Foley et al. 2010), but the effectiveness of this approach depends on the quality and resolution of the ecological information considered in delineating best uses of public natural resources. Many economically and ecologically important species such as summer flounder and black sea bass depend on inshore nursery habitats, yet habitat-specific utilization patterns lack the resolution needed to protect critical areas and inform ecological restoration strategies. To address these data gaps, we investigated dynamic and static features that shape nursery habitat use by juvenile summer flounder and black sea bass in the Chesapeake Bay region and nearby coastal lagoons. The ability to evaluate environmental effects on the distribution and abundance of juvenile fishes is critical because nursery habitats are dynamic, and anticipating these changes is key to the success of ecosystem-based management in the Chesapeake Bay region. Management of species requires not just characterization of suitable habitat, but also knowledge of the extent of habitats that support production of juvenile fishes, because these extents will change as the climate continues to warm and as precipitation amounts and patterns change in the watershed (Najjar et al. 2010).

With the exception of a handful of species (Fabrizio et al. 2021), we lack a quantitative understanding of habitat relationships for juvenile fishes in the Chesapeake Bay region. At best, fish-habitat relationships are described in broad terms, e.g., juvenile summer flounder occupy soft-sediment, marsh creek, and seagrass habitats in inshore areas (Packer et al. 1999). Such characterizations are insufficient for evaluation of proposed management actions that directly or indirectly affect environmental conditions in coastal and estuarine systems. In particular, the ecosystem-based approach to fisheries recognizes that alterations to aquatic habitats may have profound effects on productivity of fish stocks. Maintaining the functional integrity of nursery areas used by fishes is critical to ensuring their continued production.

Habitats suitable for growth and survival of juvenile fishes are spatially dynamic, changing through time as environmental conditions change (Manderson et al. 2002) and as physiological optima change with ontogeny. Fishes with complex life histories may thus use multiple habitat types during ontogeny and the ensemble of habitats used by early-life stages should be considered when delineating nursery areas (Nagelkerken et al. 2015). This spatial approach, termed the ‘nursery seascape’, explicitly considers linkages among habitat patches used by early-life stages and recognizes the dynamic nature of patch use. Functional connections among habitat patches within the mosaic occurs through ontogenetic habitat shifts and movement of juveniles (Nagelkerken et al. 2015). The nursery seascape concept is particularly relevant for flatfishes because the larvae of some species settle in habitats that differ from those used by older juveniles (e.g., Curran & Able 2002; Furey & Rooker 2013).

The dynamic seascape approach is useful for understanding nursery habitats in the Chesapeake Bay and the coastal lagoons because early-life stages may use a multitude of habitat types in these coastal systems. In this region, coastal lagoons and estuaries present markedly different habitat mosaics and range of environmental conditions, yet a similar suite of juvenile fishes uses these areas during their first year of life. Many factors can shape nursery habitat use by juvenile fishes. Features such as depth, substrate, and the presence and type of structure are often used to characterize fish habitats because these features are known to affect fish distributions and habitat use (Day et al. 1989). For some demersal species, structured habitats support higher densities, growth, and survival of juveniles, and the benefits of associations with such habitats may be realized beyond the settlement stage (e.g., juvenile Atlantic cod, Grabowski et al. 2018). Because of their small size and abundance, juvenile fishes are particularly vulnerable to predation, and indeed, structural complexity of bottom habitats may enhance the ability of juveniles to escape predation (Scharf et al. 2006).

Seagrass beds, intertidal marshes (i.e., marsh habitats that are inundated during high tide), oyster reefs, and soft-bottom habitats are common habitat types in mid-Atlantic coastal areas. In these areas, seagrass and marsh habitats are known to be used by juvenile summer flounder (Rountree & Able 1992) and juvenile black sea bass (Able & Hales 1997). Oyster reefs may provide shelter and feeding opportunities for small fishes, but to date, most studies of ecosystem services of oyster reefs have focused on the diversity and abundance of invertebrate macrofauna associated with oyster reefs (e.g., Gain et al. 2017; Karp et al. 2018). This limitation is likely due to the type of gear used to sample macrofauna on oyster reefs; for example, many studies use settling trays (e.g., Karp et al. 2018), which are ineffective at capturing highly mobile fishes, although drop nets and traps may also be used. In a few studies, experimental gill nets were used to understand the value of Chesapeake Bay oyster reefs for mobile foragers such as striped bass, Atlantic croaker, and spot (Harding & Mann 2003; Pfirrmann & Seitz 2019), but the use of oyster reefs by juvenile summer flounder and black sea bass remains unexplored. Soft-bottom habitats are known to be used by juvenile fishes and unlike structured habitats, soft-bottom habitats are effectively sampled by bottom trawl gear (Tuckey & Fabrizio 2022).

Within the dynamic seascape of the bay and coastal lagoons, habitat use by fishes is constrained by their physiological tolerances to thermal, salinity, dissolved oxygen (DO), and other environmental conditions; furthermore, these tolerances may change with ontogeny. Because temperature and salinity conditions exert direct effects on fish metabolism and thereby on growth and survival, habitat associations of juvenile fishes are generally described in these terms (e.g., Vasconcelos et al. 2010; Furey & Rooker 2013). For example, growth and survival of juvenile summer flounder that enter the estuary in winter are negatively affected by low temperatures at that time (Packer et al. 1999), and in summer, temperatures that exceed 26°C negatively affect growth of juvenile summer flounder in Chesapeake Bay (Nys et al. 2015). Environmental conditions are often used to describe fish-habitat relationships but the role of structural components in the seascape and the connectivity between habitats have only recently been considered (e.g., Cristiani et al. 2021). Such consideration is important because human activities may impair functional habitats by curtailing access of organisms to structural habitat components, or by temporally or spatially uncoupling structural components from dynamic components (Peterson 2003).

Nursery habitats for summer flounder and black sea bass in Chesapeake Bay and the coastal lagoons are not well described, and the low resolution of current descriptions hampers the understanding of the role of estuaries and lagoons in sustaining production of these stocks. Summer flounder and black sea bass, both of which support important fisheries in the mid-Atlantic region, are coastal-shelf spawners with protracted spawning periods. Early-life stages of these species use coastal systems for development and first-year growth.

Summer flounder, which range from Nova Scotia to the east coast of Florida, spawn on the continental shelf from September to January (Murdy et al. 1997); pelagic larvae enter coastal systems where they metamorphose to the juvenile stage and become demersal. Summer flounder larvae are found in coastal and estuarine waters of the mid-Atlantic Bight from October to May; larvae primarily use selective tidal stream transport to arrive in shallow coastal waters (Hare et al. 2005), where they metamorphose to the benthic, juvenile stage. The majority of juveniles emigrate from the Chesapeake Bay in late fall, but some juveniles may remain in the bay throughout the year (Norcross & Wyanski 1994; Tuckey and Fabrizio, *personal observation*). The inner continental shelf is also used as a nursery by juvenile summer flounder, however, juvenile densities are greater in Chesapeake Bay than in shelf habitats (Woodland et al. 2012). The pattern of use of multiple habitat types (shelf, lagoons, estuaries) as nursery areas during ontogeny characterizes a number of flatfish species (e.g., Fodrie et al. 2009; Primo et al. 2013; Li et al. 2022), and connectivity between habitats on the coastal shelf and those in estuaries and lagoons is critical to sustaining production of these populations.

The black sea bass population which ranges from the Gulf of Maine south to Cape Hatteras, North Carolina, is considered a single genetically distinct stock (Roy et al. 2012). In the mid-Atlantic region, spawning can occur from April to October at inshore reef sites on the continental shelf (Musick & Mercer 1977; see review in McBride et al. 2018), and larvae develop in nearshore continental shelf waters (Kendall 1972; Able et al. 1995). Juvenile black sea bass are found on structured habitats on the continental shelf, as well as in high salinity (generally > 20 psu) coastal areas, although the mechanism by which they enter estuaries and lagoons is unknown (Able et al. 1995). Once a habitat is selected, juvenile black sea bass exhibit a high degree of fidelity to localized sites (on the scale of 30 m; Able & Hales 1997). In October-November, juveniles undertake cross-shelf migrations to their wintering grounds near the edge of the shelf (Moser & Shepherd 2009).

Nursery habitat quality is highly variable within and among coastal systems, reflecting the availability of resources (prey, shelter) and environmental conditions conducive to growth and survival of juvenile fishes (Schloesser & Fabrizio 2019; Li et al. 2022). Characteristics of nursery areas such as proximity to the ocean, and abundance of prey are also important for determining habitat use by juvenile flatfishes (Burke 1995; LePape et al. 2007; Vasconcelos et al. 2010; Furey & Rooker 2013). The quality of nursery habitats is most commonly assessed using density or abundance of juveniles, but this approach does not account for vital processes that contribute to production, namely, growth and survival (Johnson et al. 2013). Metrics such as body condition and growth rates (determined, e.g., from otolith marginal increments) provide a more integrative assessment of habitat quality and are preferred approaches (e.g., LePape et al. 2003; Vasconcelos et al. 2009; Taylor et al. 2016; Li et al. 2022). Fish body condition reflects the general health and nutritional status of individuals (Lloret et al. 2014), as

well as ecological interactions (diet and predation), activity, and environmental stress experienced by fish. In the Chesapeake Bay region, the quality of summer flounder nurseries varies spatially and on average, coastal lagoons near Oyster, VA, support fish in better condition than nurseries in Chesapeake Bay (Schloesser & Fabrizio 2019).

Like body condition, growth rates of juvenile fish also exhibit spatial differences; for example, juvenile summer flounder from Chesapeake Bay are larger than contemporaneously collected conspecifics from tidal tributaries, implying that bay habitats are more favorable to summer flounder growth than habitats in tidal tributaries (Nys et al. 2015), an inference consistent with summer flounder growth variation in Narragansett Bay (Taylor et al. 2016). Furthermore, variable thermal conditions in nursery habitats in Chesapeake Bay may influence production of summer flounder year classes through effects on maturation and survival (Nys et al. 2015). This is because some of the fast-growing juveniles may reach maturity by the end of their first year of life. Thus, thermal habitat conditions can affect the proportion of fish that mature, and the proportion that survive winter (Nys et al. 2015). Here, we extend the Nys et al. (2015) study to describe the dynamics of thermal habitats suitable for growth of juvenile summer flounder in the Chesapeake Bay region.

Because annual and seasonal variations in the extent of suitable habitat may help explain variation in juvenile fish abundance in the Chesapeake Bay, we investigated the relationship between extent of suitable nursery habitat and annual recruitment to the bay. To our knowledge, only one study (Le Pape et al. 2003) has related recruitment success of flatfishes to changes in the extent of suitable nursery habitat. As waters in Chesapeake Bay continue to warm, juvenile fishes will experience a decrease in the availability of cooler bottom waters in Chesapeake Bay in summer; this decreased availability may limit production of juvenile summer flounder (Nys et al. 2015). One mechanism that contributes to cooler (optimal) water temperatures in summer in the lower Chesapeake Bay and the coastal lagoons is the periodic surge of cool, bottom waters from the inner continental shelf (Ye et al. 2018). This intrusion of bottom-water in summer is driven by the prevailing southwesterly winds and can reduce bottom-water temperatures by 5°C from midsummer maxima of 28-30°C. Bottom-water intrusion in summer may increase optimal thermal conditions for growth of juvenile summer flounder, and we tested this hypothesis by regressing the extent of thermally suitable habitat against an index of bottom-water intrusion.

In this study, we characterized habitats and environmental conditions that support production of juvenile summer flounder and black sea bass in coastal marine and estuarine ecosystems in the Chesapeake Bay region. The objectives were to:

(1) Evaluate the quality of habitat types in seaside and bayside nursery areas used by juvenile summer flounder and black sea bass,

(2) Delineate nursery habitats used by summer flounder and black sea bass in Chesapeake Bay and the coastal lagoons, and

(3) Identify the relationship between habitat conditions in nursery areas and annual recruitment of summer flounder and black sea bass.

To address these objectives, we applied complementary approaches at two spatial scales. First, we conducted an intensive field study in 2019 and 2020 to investigate nursery habitat quality at a small spatial scale. The quality of structured (seagrass, oyster, marsh) and unstructured (soft-bottom) habitats was assessed using characteristics of juvenile summer flounder and black sea bass collected from the Piankatank River, a tributary to Chesapeake Bay, and a coastal lagoon on Virginia's eastern shore. Specifically, we examined abundance, individual fish condition, and recent growth determined from otolith increments as indicators of habitat quality. Observed spatial variation in condition of juvenile fishes suggests that factors other than environmental conditions measured at the sampling site may be important (Schloesser & Fabrizio 2019). Thus, we evaluated the effect of proximity to structured habitats, and the diversity of habitats in the vicinity of each sampling site for summer flounder and black sea bass in the bay and in the coastal lagoons. Second, large-scale delineation and characterization of nursery habitats (objectives 2 and 3) were addressed using a retrospective analysis of fisheries-independent survey data collected from 1989 to 2019 by VIMS and the MD Department of Natural Resources, as well as existing GIS coverages that delineate seagrass, oyster, and marsh habitats. Nursery habitat delineation was described in terms of dynamic environmental conditions and proximity to structured habitats. This multiscale hierarchical approach allowed us to assess the importance of spatial scale in shaping relationships between juvenile fish abundance and abiotic and biotic characteristics of the nursery environment. Finally, we evaluated relationships between the extent of suitable habitat and relative abundance of juvenile fishes as such relationships may be used to develop spatial thresholds that could serve as spatial reference points for management (Reuchlin-Hugenholtz et al. 2016).

Methods

Identification of juvenile (age-0) summer flounder was based on monthly length thresholds developed by the VIMS Juvenile Fish Trawl Survey (Table 1; Tuckey & Fabrizio 2022). For the purposes of this study, juvenile black sea bass were defined as late age-0 or early age-1 individuals who hatched the previous calendar year and survived their first winter. The presence of multiple black sea bass cohorts in a given year was apparent based on the large size range of individuals in a given month (e.g., 40 mm – 160 mm in August and September). This was common among the trawl surveys and was especially noted in the small-scale field study (Figure 1). The presence of multiple cohorts is not surprising given that black sea bass spawning peaks between June and August in the mid-Atlantic region (VanderKooy et al. 2020) and young-of-the-year fish enter Chesapeake Bay along with individuals from older cohorts. Black sea bass juveniles were separated from other cohorts based on monthly length thresholds developed by the VIMS Juvenile Fish Trawl Survey (Table 1; Tuckey & Fabrizio 2022) and on estimated spring-summer growth of young-of-the-year black sea bass (0.42 mm/day; Able & Hales 1997). These thresholds excluded newly hatched fish as well as age-2 fish; age-2+ black sea bass usually do not re-enter estuaries.

Methods to Address Objective (1): Evaluate the quality of habitat types in seaside and bayside nursery areas used by juvenile summer flounder and black sea bass

Habitat quality for juvenile summer flounder and black sea bass was assessed in multiple habitats from South Bay, a coastal bay near Oyster, VA (37.29°N) and the lower Piankatank River, VA (37.50°N; Figure 2). Habitat quality was evaluated for four habitat types often associated with nursery areas and commonly found in the mid-Atlantic region: seagrass beds, oyster reefs or on-bottom oyster aquaculture, tidal marshes, and unstructured soft-bottom. Each habitat type was sampled in triplicate (i.e., 3 oyster habitats, 3 marsh habitats, 3 seagrass beds, 3 soft-bottom habitats) in South Bay (hereafter, Eastern Shore or ES study area) and in the lower Piankatank River (hereafter, PK study area). Sampling occurred biweekly from April to October in 2019 and 2020 to assess annual and seasonal variation in habitat use. No sampling occurred in October 2020 because inclement weather prevented safe and effective sampling. In ES, one sampling event in September 2019 was missed because of inclement weather, and in PK one sampling event in June 2020 was missed because of complications arising from the COVID-19 pandemic. Early juvenile fish (April-May) were sampled with standard monitoring units for the recruitment of reef fish (SMURFs; Ammann 2004). SMURFs are effective samplers of small-bodied fishes that associate with structured habitats. Each sampling site (12 sites per area, total=24) was sampled with 2 SMURFs at biweekly intervals corresponding with the spring-neap tidal cycles during April and May. SMURFs were deployed for 48 hours to reduce the bias associated with sampling only in the daytime. To assess use of habitat types by late juvenile stages (June-October), we used a fyke net constructed of 1.75-cm mesh net. Fyke nets are a passive gear that use a series of funnels to allow movement of fishes into the net but restrict outward movement; nets were set for 24 hours to capture diurnal movements of fishes and eliminate day/night bias. All fishes captured in both gear types were identified to species and enumerated. At each site during each sampling event, summer flounder and black sea bass were euthanized in accordance with procedures approved by William & Mary's Institutional Animal Care and Use Committee (protocol: IACUC-2019-03-25-13564-mcfabr). Summer flounder and black sea bass were returned to the lab, measured to the nearest millimeter (mm), and weighed to the nearest tenth of a gram (g).

At the time of gear retrieval, we measured instantaneous environmental conditions (water temperature [°C], DO [mg/L], salinity [psu]) with a multiparameter sonde (YSI Inc, Yellow Springs, OH). To capture fluctuations in water temperature common in shallow areas, we deployed a HOBO Tidbit temperature logger (Onset Computer Corporation, Bourne, MA) on each net that recorded water temperature every five minutes for the duration of gear deployment. Depth of each sampling site was estimated from NOAA's National Center for Environmental Information's Continuously Updated Digital Elevation Model (referenced to mean high water [MHW] vertical datum). Data collected in this small-scale field study in 2019 and 2020 allowed us to address the following null hypotheses for each species: (1) ***there is no difference in the mean abundance, body condition, or recent growth of juveniles between areas or among habitat types***; and (2) ***seascape features near capture locations do not affect body condition, or recent growth.***

To assess seascape features such as proximity to structured habitats, area of structured habitats, and habitat diversity, the spatial extent of habitat types within each study area was mapped in a GIS (ESRI ArcGIS Desktop 10.7) using available coverages modified by on-site GPS and drone surveys to enhance resolution (e.g., see Ross & Luckenbach 2009). Marsh habitat coverage (fringe, embayed, detached, and island marshes) was sourced from VIMS' Center for Coastal Resource Management (CCRM) Tidal and Shoreline Inventory program; spatial features were verified by CCRM field surveys conducted between 2002 and 2016. VIMS' Submerged Aquatic Vegetation (SAV) Program provided assessments of seagrass spatial coverage in 2019 and 2020 using aerial imagery (standard 1:24,000 USGS quadrangles) and verified with field surveys. Oyster habitat coverage was sourced from NOAA's seaside patch reefs dataset (ES) and from VIMS' Virginia Oyster Stock Assessment and Replenishment Archive (VOSARA) data (PK). Drone survey images provided additional coverage of on-bottom oyster aquaculture in PK; on-bottom oyster aquaculture is not surveyed by VOSARA. All habitat feature layers were converted to rasters using the highest resolution common to all coverages (5 meters). All rasters were projected to North American Datum 1983 Universal Transverse Mercator Zone 18N, which is standard for conducting spatial analyses in this geographic region. Rasters were spatially matched to a base raster to reduce distance calculation errors incurred during geoprocessing. Proximity (distance in meters) to structured habitats (oyster, seagrass, marsh habitat) was calculated from each site's GPS coordinates to the nearest habitat feature. Proximity was calculated based on the shortest-distance path around land features. In addition to estimating proximity of each sampling site to structured habitats, we calculated the percent area of each habitat type and habitat diversity within the surrounding area of each sampling site; these calculations were performed for the 2019 and 2020 sampling events separately as some features (such as seagrass coverage) exhibited annual changes. We calculated percent area and diversity at two spatial scales around each site: 500 meters, which reflects an estimate of juvenile black sea bass home range (Able & Hales 1997), and 1 km, which reflects juvenile summer flounder home range and larger nocturnal movements corresponding with tides (Szedlmayer & Able 1993). These range estimates do not include movements associated with seasonal migrations. Habitat percent area calculations excluded areas that fish cannot traverse (e.g., land). Habitat diversity was calculated with Simpson's diversity index:

$$Simpson's\ diversity = 1 - \sum_{i=1}^{m} P_i^2$$

where P_i is the proportion of habitat type *i* and *m* is the number of habitat types present in the area around each site.

Relative abundance of juveniles was used to determine the importance of the four habitat types to juvenile fish abundance and production. Indices of abundance were calculated separately for SMURFs and fyke nets because of differences in time deployed and area fished for each gear. We compared the proportion of nets that successfully captured juvenile summer flounder and juvenile black sea bass between study areas and among habitat types using Fisher's exact tests with Bonferroni adjustments for multiple comparisons. This method of evaluating abundance is recommended for data with a high proportion of zeros and non-normal distributions (Hubert & Fabrizio 2007), properties that characterized both the summer

flounder and black sea bass catch data. To account for the variation in gear deployment times (SMURFs: 44-49 hours; fyke nets: 19-27 hours), we standardized catch (numbers of juvenile fish) by the number of hours each gear was deployed (catch per hour). Species-specific catch per hour was further standardized to the minimum number of hours fished for each gear type (44 hours for SMURFs, 19 hours for fykes) to obtain an estimate of relative abundance. To estimate mean relative abundance of juvenile fishes across study areas and habitat types and account for the proportion of positive (non-zero) catches in each unique area-habitat combination, we used the delta-lognormal method (Lo et al. 1992) with confidence intervals estimated following Fletcher (2008). We investigated interannual differences in abundance by calculating species-specific delta-lognormal indices for each sampling area-habitat-year combination but found none, therefore, indices were estimated by pooling the data from the two years.

Individual body condition and growth of juvenile fishes can provide robust assessments of habitat quality as well as information about the functional roles of a particular habitat (Nys et al. 2015; Olson et al. 2019; Schloesser & Fabrizio 2019; Schwartzkopf et al. 2021). To estimate body condition of juvenile summer flounder and black sea bass, we used total length (nearest mm) and weight (nearest 0.1 gram) to calculate relative condition (K_n) of each fish as follows:

$$K_n = \frac{observed\ weight}{estimated\ weight}$$

Species-specific estimated weights were obtained from length-weight regressions specific to the fishes collected in this study. Relative condition is consistent across fish body size, does not assume isometric growth, and is suitable for population-level and regional analyses (Lloret et al. 2014).

We estimated recent growth using otolith daily increment analysis as an additional indicator of habitat quality because daily increment analysis is more sensitive to recent growth conditions than body condition of fish (LePape et al. 2003). Daily formation of increments has been validated for summer flounder (Szedlmayer & Able 1992) and black sea bass (Hales & Able 1995; McBride et al. 2018). Although summer flounder otoliths exhibit non-daily increments during the pre-metamorphic stage (Szedlmayer & Able 1992), all individuals captured in this study were post-metamorphic. Whole sagittal otoliths were removed from fish and mounted in embedding molds using epoxy resin. Once hardened, the molds were sectioned transversely with a low-speed Buehler isomet saw and affixed to a microscope slide using Crystalbond. Each otolith was polished with P320-P400 grit wet/dry grinding paper until daily increments were visible at 200x magnification. A thin layer of immersion oil was applied to otoliths to enhance the visibility of daily increments. Otoliths with uninterpretable increments were excluded from analyses. Two independent readers without knowledge of fish size or capture location identified daily increments and measured increment widths (microns, µm). NIS Elements BR 3.2 imaging software was used to mark a transect from the otolith's outer edge inward where consecutive daily increments were clearly visible from edge to core; both readers identified and measured daily increments along this same transect to facilitate consistency. The middle of each increment served as the delineation point for increment measurements. Recent otolith

growth was defined as the distance measured from the otolith's edge to the seventh daily increment (Figure 3); the distance measured (µm) from edge to the seventh daily increment is related to growth accrued over the seven days prior to capture. Use of this time span aimed to describe growth when exposed to conditions in the area of capture as opposed to growth during immigration, which is reasonable given the relatively limited movements exhibited by juvenile individuals of both species (Szedlmayer & Able 1993; Able & Hales 1997).

Between-reader agreement in increment identification was evaluated by calculating the percent and absolute differences in increment distances measured for each otolith, using the more experienced reader (reader 1) as the reference reader, i.e.,

$$percent\ difference = \left(\frac{Reader\ 2\ total\ distance\ measured - Reader\ 1\ total\ distance\ measured}{Reader\ 1\ total\ distance\ measured}\right) * 100$$

Otoliths where readers differed by 25% or more in their measurements were co-read by both readers until a consensus was reached. Bland-Altman plots were used to assess between-reader differences in increment measurements and evaluate reader biases. Bland-Altman plots do not *a priori* assume one reader to be more accurate (in this case, the "true" increment distance is unknown). Instead, these plots regress the difference between readers against the mean of both readers (Bland & Altman 1986). For the majority of otoliths, the distances measured were averaged between two readers to yield the distance used for recent growth estimation. In the case of co-read otoliths, the distance agreed upon by both readers was used.

To interpret recent growth in the context of fish size instead of otolith size, we first confirmed the association between fish size (total length, mm) and otolith maximum diameter (µm) using linear regression. We then developed predictive linear models relating fish size to otolith radial distance (distance measured from the otolith's edge along the transect where daily increments were measured to the otolith's core), with the goal of estimating recent growth of the fish in mm based on recent growth of the otolith (distance measured from otolith's edge to the seventh daily increment in µm). Models predicting fish size based on otolith radial distance took the general form L = a + bx, where L was fish size in mm, a and b were the intercept and slope in mm, and x was otolith radial distance in µm. We estimated recent growth of each fish in mm as:

$$recent\ growth = \frac{(\ (b * 1000) * recent\ otolith\ growth)}{1000}$$

where the numerator is the product of otolith recent growth in µm and *b* is the slope in mm converted to µm. This product was converted to mm to yield recent growth of each fish in mm estimated from recent otolith growth in µm.

Linear mixed models (fitted using the *lme4* package in R, Bates et al. 2015) were used to relate juvenile fish relative condition and recent growth with habitat type and area (ES and PK). We hypothesized that ***habitat quality (as measured by relative condition and recent growth of juvenile fishes) is greater at the Eastern Shore.*** The same habitat type in each area (e.g., marsh in ES and marsh in PK) are likely not directly comparable between areas given differences in

environmental context (i.e., proximity to the Atlantic Ocean and relative size of habitat patches), therefore, our main effect of interest encompassed every unique area-habitat type combination and treated habitat types separately for each area (e.g., ES-marsh and PK-marsh). SMURF and fyke net collections were treated as subsamples within each replicated habitat type in ES or PK. We identified effects that best described random variation in the data using restricted maximum likelihood estimation (REML). Random effects included (1) a unique site identifier (site nested in each area-habitat type combination) to address potential correlations between fish captured at the same location throughout the study, and (2) a temporal sampling event identifier to explicitly account for potential correlations resulting from repeated (biweekly) sampling. Models estimating summer flounder and black sea bass relative condition initially included both of these random effects, however, there was no support for the inclusion of the temporal dependency (sampling event explained <1% of the variance in relative condition of summer flounder and black sea bass) so this random effect was removed for the sake of parsimony. The random effect of site nested in area-habitat type was removed in the model that estimated summer flounder recent growth for the same reason (site nested within area-habitat type explained < 1% of the variance). Models predicting recent growth included fish size (total length, mm) at the time of capture as a covariate. The relative contribution of main effects was evaluated using maximum likelihood estimation and models were selected using an information theoretic approach with Akaike's Information Criterion corrected for small sample sizes (AIC_C, Burnham & Anderson 2002). We used REML estimation to fit the selected model. We hypothesized that ***seascape features such as close proximity to structured habitat, high habitat diversity, and high proportions of structured habitat near sampling sites are associated with good relative condition and fast growth.*** We explored this with Generalized Additive Models (GAMs) fitted using thin-plate regression splines (R package *mgcv*; Wood 2011); GAMs were used to investigate non-linear responses of relative condition, and recent growth to seascape features (e.g., proximity to structured habitats, percent area of structured habitats surrounding sampling sites, and habitat diversity).

Methods to Address Objective (2): Delineate nursery habitats used by summer flounder and black sea bass in Chesapeake Bay and the coastal lagoons

Trawl surveys are commonly used to examine habitat associations of juvenile fishes and to delineate nursery habitats (e.g., LePape et al. 2007; Nys et al. 2015; Fabrizio et al. 2021). Trawl survey observations from the Chesapeake Bay region were used to explore the hypothesis that ***relative abundance is related to environmental conditions and seascape metrics (e.g., proximity to structured habitats) in nursery areas*** using Generalized Additive Mixed Models (GAMMs). For the abundance models, we chose to use the *GAMLSS* package in R, which allows for a wider range of distributions for the response variable and the ability to model additional components (σ, ν, and τ) that represent the variance, skewness, and kurtosis of the distribution as a function of explanatory variables. In addition, we modeled the effect of environmental conditions, local density, and seascape metrics on the mean length of fish using GAMMs; local density was considered in this model because juvenile fish growth may exhibit

density-dependent effects (Nys et al. 2015), and because juvenile densities must be considered when using fish size to assess nursery habitat quality for flatfishes (LePape et al. 2003).

We used catch and fish size information from monthly collections spanning a maximum of 31 years (1989-2019) from the Chesapeake Bay and its subestuaries (VIMS Juvenile Fish Trawl Survey, MD Small Trawl Survey) and from the Maryland coastal lagoons (MD Coastal Bays Survey). Measures of dynamic environmental conditions (temperature, salinity) in near-bottom waters were obtained from *in situ* observations collected during the time of sampling; missing values were imputed from surface conditions when possible, and estimates of environmental conditions based on hindcasts from a 3-D hydrodynamic model were used in the absence of *in situ* measures (Table 2). We used available GIS coverages for the region to characterize proximity of trawl survey sites to structured habitat features (oyster, seagrass, and marsh habitats).

To accurately calculate the proximity of trawl survey sites to structured habitat features, coordinates of each tow were inspected in a GIS (ESRI ArcGIS Desktop 10.7). After verifying the accuracy of tow coordinates, midpoints were calculated for each tow ([latitude + longitude] / 2) and used to calculate distance to habitat features. We identified inaccurate coordinates for the start and end of each tow as (1) coordinates located on land more than 0.1 km from the water, or (2) outside the spatial bounds of the area surveyed. Inaccurate or missing coordinates were present in all three surveys: MD Coastal Bays Survey, MD Small Trawl Survey, and VIMS Juvenile Fish Trawl Survey. For the MD Coastal Bays and MD Small Trawl surveys, inaccurate or missing coordinates were addressed by calculating the spatial mean center of each fixed station using verified tow coordinates for that station from other sampling dates. The mean center coordinates for each station were then used to calculate distance to habitat features in place of the inaccurate tow coordinates. The MD Coastal Bays Survey data included 68.57% unavailable or inaccurate tow locations. Spatial data were either unavailable or inaccurate for 16.8% of tows in the MD Small Trawl data. Three tows (0.04% of all tows) were located between 5 and 50 meters inland and were corrected by relocating coordinates to the nearest water feature while preserving tow distance, depth, and direction. The remaining 16.76% of inaccurate tow coordinates were corrected using the mean-center approach described above. Tows with inaccurate coordinates comprised only 0.4% of the VIMS Juvenile Fish Trawl Survey tows, and these locations were corrected using coordinates from sampling events on the same date that shared the same conditions (depth, tide, tow direction, and vessel speed).

Marsh habitat spatial features in MD and VA were sourced from VIMS' CCRM Tidal and Shoreline Inventory program; features were verified by field surveys conducted between 2002 and 2016. Marsh habitat features were defined as either fringe, embayed, detached, or island marshes. Annual surveys of marsh habitat were not available for the spatial scale of this project, therefore, the same marsh habitat spatial features were used to describe annual marsh habitat coverage for 1989 to 2019. VIMS' Submerged Aquatic Vegetation (SAV) Program provided annual assessments of the spatial coverage and location of seagrass beds using aerial imagery along with field surveys to classify and digitize seagrass beds from 1989-2019. Aerial imagery was based on standard 1:24,000 USGS quadrangles. The years 1999, 2001, 2005, 2016, 2018, and 2019 each had one missing quadrangle due to incomplete survey coverage. These areas were treated as missing data when calculating distance to seagrass habitat features.

Annual spatially comprehensive surveys of oyster reef location and coverage are not available for Chesapeake Bay or the coastal bays, therefore, we estimated reef locations and area covered for each year (1989-2019) based on multiple GIS coverages. Indeed, to our knowledge this study was the first to bring together a comprehensive annual time-series of GIS coverages for oyster reefs throughout the entire Chesapeake Bay for 1989 to 2019. We excluded on-bottom oyster aquaculture (e.g., cages) in our definition of oyster reefs. We defined oyster reefs in 1989 based on historic MD and VA surveys of oyster bottom (Yates and Baylor grounds, respectively). Historic GIS data were sourced from MD Department of Natural Resources' Maryland Shellfish - Historic Oyster Bottom data, NMFS Office Of Habitat Conservation's Chesapeake Bay Coastal Marine Ecological Classification Standard Component Geodatabase (CMECS), and the Virginia Oyster Productivity Information Tool (Mann et al. 2021). The CMECS dataset contains historic as well as more recent substrate surveys distinguishing biogenic shell substrates from sedimentary substrates. Recent CMECS surveys spanned different areas of Chesapeake Bay from 2003 to 2016; we used these to sequentially update oyster reef locations and coverage for all years post-1989. If an area was re-surveyed in a given year, the spatial locations and area of oyster reefs would reflect this in that year and in subsequent years. If an area was not re-surveyed, the oyster reef coverage in that area remained static through time based on the last available survey. Oyster reef locations were also updated using NOAA's seaside patch reefs dataset (coastal bays only) and VOSARA polygons (Mann et al. 2021). Given the available data and the challenges that oyster reefs faced in recent decades, we acknowledge that this approach may be generous in its estimations of oyster reefs in Chesapeake Bay. However, there has been no inclusive, comprehensive survey of MD oyster reefs since the Yates survey (1906-1977) and this survey continues to be used for management today (Allison Colden, Chesapeake Bay Foundation, *personal communication*). Similarly, in VA there has been no recent baywide survey of oyster reefs, although increased spat set in the seaside coastal lagoons in recent years (Ross and Snyder, *personal observation*) may indicate that the estimates we used for the coastal bays are conservative.

After characterizing marsh, seagrass, and oyster reef features for each year, the final GIS layers consisted of (1) a single marsh habitat feature layer used for all years, 1989-2019, (2) annual seagrass locations and coverage for 1989 to 2019, and (3) annual oyster reef locations and coverage for 1989 to 2019. Distance to shore was also calculated for each year; shorelines remained the same for 1989-2019 and shoreline spatial data were provided by CCRM and MD DNR. All habitat feature layers were converted to raster datasets using the highest resolution common to all habitat surveys (5 meters). All rasters were projected to North American Datum 1983 Universal Transverse Mercator Zone 18N, which is standard for conducting spatial analyses in this geographic region. Rasters were spatially matched to a base raster to reduce distance calculation errors incurred during geoprocessing. Proximity (distance in meters) of tows to habitat features (oyster reefs, seagrass, marsh habitat, shoreline) was calculated from the midpoint of each tow to the nearest habitat feature while accounting for land features. To account for land features, we created a cost raster that made crossing land features (e.g., islands) prohibitive, thereby calculating the shortest-distance path around land features instead of through them. All geoprocessing and spatial analyses were conducted with ESRI ArcGIS Desktop 10.7.

VIMS Juvenile Fish Trawl Survey: Catch and Environmental Conditions

The VIMS Juvenile Fish Trawl Survey uses a stratified random survey design to sample juvenile fishes throughout estuarine waters of Virginia, from the Atlantic Ocean to waters south of the Potomac River, and in tidal waters in the James, York, and Rappahannock rivers (Figure 4). Fish are sampled monthly from January to December at 111 stations using a 9.1-m semi-balloon bottom trawl deployed for 5 minutes at each site (further details of sampling methods are provided in Tuckey & Fabrizio 2022). We used catch (numbers of juvenile fish), fish length (measured to the nearest mm), temperature (°C), and salinity (psu) observations from April to October from this survey; both surface and bottom conditions were recorded at the time of the tow.

As described previously, juvenile summer flounder and black sea bass were identified from observed lengths using monthly length thresholds for the cohort of interest developed for each species (Table 1; Tuckey & Fabrizio 2022). For each tow, catch-per-unit-effort (CPUE, #fish/km^2) of juvenile summer flounder and black sea bass was estimated using numbers captured divided by the area swept by the trawl. Because the distribution of summer flounder and black sea bass varies throughout Chesapeake Bay, different strata were included in the calculation of abundance for each species. For juvenile summer flounder, strata included all bay stations and stations that occurred in the lower James, York, and Rappahannock rivers, as few juvenile summer flounder are found in the upper portions of these Virginia tributaries. Strata considered in the estimates of abundance for juvenile black sea bass included all bay stations and those in the lower James River. Stratum-specific, monthly (April – October), and annual mean relative abundance for each survey was calculated using a design-based estimator to account for stratification in the CPUE estimates; stratum-specific means were obtained using model-based estimates calculated from the delta-lognormal model (Tuckey & Fabrizio 2022). The delta-lognormal model permits estimation of abundance in the presence of a large number of zero catches (Lo et al. 1992).

Because observations of bottom conditions were missing for a few observations (<1%), we used a multiple linear regression to impute bottom temperature and bottom salinity from observed surface temperature and surface salinity, while accounting for time of year, depth, and location:

$$\theta_{bottom,ijkl} = \mu + \beta_1\theta_{surface,i} + \beta_2 season_j + \beta_3 depth_k + \beta_4 system_l + \varepsilon_{ijkl}$$

where $\theta_{bottom,ijkl}$ is either the i^{th} bottom temperature or bottom salinity value observed in the j^{th} season, at the k^{th} depth, in the l^{th} system; μ is the overall mean; β_1, β_2, β_3, and β_4 are the partial regression coefficients; season is spring (April, May, June), summer (July, August, September), or fall (October); depth is in meters; system is either James River, York River, Rappahannock River, or lower Chesapeake Bay; and ε_{ijkl} is the random unexplained error assumed to be normally distributed with a mean of 0 and a variance of σ_ε^2. The estimate of bottom condition from the multiple linear regression is adjusted to account for season, depth, and general location of the sample site, because the bottom-to-surface relationship varies depending on time of year (season), water depth, and regional hydrodynamics (system). No evidence of collinearity was detected among the predictors, and temperature and salinity regressions were significant ($F_{temperature}$=48647.8, P<0.01, $N_{temperature}$ = 21,019; $F_{salinity}$=29351.2,

P<0.01, $N_{salinity}$ = 20,968); 94.2% of the variation in bottom temperature, and 90.7% of the variation in bottom salinity was explained by the models. Diagnostic plots of the residuals from these models were reasonable, but indicated that bottom temperatures in the bay tended to be overestimated slightly, and bottom salinities less than 5 psu were overestimated slightly. Although a model for bottom DO was constructed in a similar manner (N_{DO} = 20,905), the variation explained by the DO model was low (r^2=0.555) and estimates of bottom DO were unreliable for bottom DO < 5 mg/L or > 7.5 mg/L. The DO model performed worse for sites in the Rappahannock River in summer, where seasonal hypoxia is pronounced. Thus, we did not attempt to interpolate bottom DO for the surveys considered in this study. All imputations were obtained using the *GLM* procedure in SAS.

MD Small Trawl Survey: Catch and Environmental Conditions

The MD DNR samples fixed sites in MD waters using a 4.9-m semi-balloon bottom trawl towed for 6 minutes at each site. Sampling is conducted monthly from May to September in the Chester River, Patuxent River, Choptank River, Eastern Bay, Tangier Sound, and Pocomoke Sound. In 2002 and thereafter, additional sites were sampled in the Little Choptank River, Fishing Bay, and the Nanticoke River (Figure 4). Fish catches are available from 37 monthly samples from 1991 to 2001, and from 53 monthly samples from 2002 to 2019; sampling was conducted in 1989 and 1990, but those records were not available electronically. Extensive QA/QC procedures were performed with the 1991 – 2019 data due to inconsistent coding, incorrect data entry (e.g., a depth of 23.5 m), and juxtaposition of temperature and salinity data (e.g., surface temperature of 6°C and surface salinity of 27 psu in August in the Choptank River).

Although the MD Small Trawl Survey primarily targets blue crabs, all juvenile fishes are counted and measured to the nearest mm (up to 20 individuals per site; additional fishes are counted). We used the length thresholds from the VIMS Juvenile Fish Trawl Survey to identify juvenile summer flounder and black sea bass cohorts of interest in the catches. For each tow, catch-per-unit-effort (CPUE, #fish/km^2) of juvenile summer flounder and black sea bass was estimated using numbers captured divided by the area swept by the trawl. For summer flounder, all Maryland strata were included in the analysis, however for black sea bass only stations in Tangier Sound and Pocomoke Sound were included as black sea bass were not found outside of these strata. Estimation of stratum-specific, monthly (May – September), and annual relative abundances were based on the delta-lognormal mean to account for the large number of zeros in the data.

We considered observations from 6,397 unique tows from this survey, where surface temperature ranged between 10.4 and 32.8 °C, surface salinity ranged between 0 and 31.4 psu, and depth ranged between 0.6 and 6.1 m. None of the samples included bottom water conditions, so we used the hindcast estimates of bottom temperature and bottom salinity at the location of the MD Small Trawl sites for 5,325 samples collected between 1996, which was the first year in the temporal domain of the hydrodynamic model, and 2019. To impute bottom conditions for samples collected between 1991 and 1995, we modeled the relationship between surface and bottom conditions using a 'shallow water' subset of the VIMS Juvenile Fish Trawl Survey data. The VIMS survey data were restricted to sites that ranged between 0.6

and 6.1 m that exhibited surface temperatures greater than or equal to 10 °C between May and September. This VIMS 'shallow water' subset, comprised of 5,613 observations, was used to construct the multiple linear regression:

$$\theta_{bottom,ijk} = \mu + \beta_1\theta_{surface,i} + \beta_2 season_j + \beta_3 depth_k + \varepsilon_{ijk}$$

where all symbols are as described previously; we found no evidence of collinearity among the predictors. The temperature and salinity models were significant ($F_{temperature}$=93802.1; P<0.01; $F_{salinity}$=56947.8; P<0.01) and explained 98.0% of the variation in bottom temperature and 96.8% of the variation in bottom salinity. Residuals from the bottom temperature and bottom salinity models were reasonable. We imputed 708 bottom temperatures and 670 bottom salinity values for the MD Small Trawl Survey from 1991 to 1995 using recorded values of surface temperature and surface salinity; the discrepancy in number of imputations is due to missing values for surface conditions. All imputations were obtained using the *GLM* procedure in SAS.

MD Coastal Bays Survey: Catch and Environmental Conditions

Isle of Wight Bay, Chincoteague Bay, Assawoman Bay, and Sinepuxent Bay were sampled monthly at 20 fixed sites from April to October (n= 140 tows/yr); in this survey, Isle of Wight Bay and Assawoman Bay were combined into a northern sampling region and Chincoteague Bay and Sinepuxent Bay were combined into a southern sampling region (Figure 4). We treated these data in a manner similar to the VIMS Juvenile Fish Trawl Survey using these sampling regions as strata as described above and supported by analyses in Tuckey and Fabrizio (2013). At each site, a 4.9-m semi-balloon otter trawl was deployed for 6 min. The MD Coastal Bays are shallow systems, and sampling sites ranged in depth from 0.8 to 5.2 m. All fishes were identified and measured to the nearest mm (up to 20 individuals per site; additional fishes were counted).

As before, summer flounder and black sea bass cohorts of interest were identified from observed lengths using monthly length thresholds developed for each species (Table 1; Tuckey & Fabrizio 2022). For each tow, catch-per-unit-effort (CPUE) of juvenile summer flounder and black sea bass was estimated using numbers captured divided by the area swept by the trawl. Stratum-specific, monthly (April – October), and annual mean relative abundances were calculated using model-based estimates calculated from the delta-lognormal model (Tuckey & Fabrizio 2022).

We imputed missing values for bottom temperature and bottom salinity for all sampling events in April to October between 1989 and 2005 using a multiple linear regression fit to the April to October data from 2006 to 2019 (n=1,960):

$$\theta_{bottom,ijkl} = \mu + \beta_1\theta_{surface,i} + \beta_2 season_j + \beta_3 depth_k + \beta_4 system_l + \varepsilon_{ijkl}$$

In this regression, all symbols were as defined previously, and system was Isle of Wight Bay, Chincoteague Bay, Assawoman Bay, or Sinepuxent Bay. We found no evidence of collinearity for the bottom temperature model, which explained 98.6% of the variation in bottom temperature ($F_{temperature}$ = 18,740.1; P< 0.01; n=1,868); nor was there evidence of collinearity for

the bottom salinity model, which explained 89.6% of the variation in bottom salinity ($F_{salinity}$=2,285.96; P<0.01; n=1,867). Diagnostic plots of the residuals from these models were reasonable. For these data, we imputed 2,323 values of bottom temperature and 2,315 values of bottom salinity; discrepancies in sample size were due to missing surface values. All imputations were obtained using the *GLM* procedure in SAS.

Delineation of Nursery Habitats Based on Relative Abundance from Trawl Surveys

Generalized Additive Mixed Models (GAMMs; fit using the *GAMLSS* package in R) were used to ***describe relationships between juvenile fish abundance (tow-level CPUE) and habitat conditions, including depth, temperature, salinity, and distance to the nearest structure***. These distances allowed us to describe the spatial relationships between sample sites and structured habitats using GIS coverages of seagrass, oyster, and marsh habitats. GAMMs were based on multidecadal observations from broad spatial scales and as such, provided robust indicators of nursery conditions that support summer flounder and black sea bass in Chesapeake Bay and the coastal lagoons.

Because catch data from all surveys spanned the period May to September from 1989 to 2019 (1991 - 2019 in the case of MD Small Trawl), and because we wished to consider information from all surveys, we standardized each time series by dividing each survey's CPUE by the maximum CPUE + 0.1 within each survey (i.e., standardized each tow so that CPUEs were ≥ 0 and < 1.0 for each survey), resulting in comparable indices of abundance (Rubec et al. 2016). Residuals from models fit to observations from the three surveys combined indicated a poor fit, thus relative abundance was modeled separately for each survey. Abundance of juvenile summer flounder and black sea bass (# fish/km^2) was the response variable and the model included bottom water temperature, bottom salinity, and depth. Some of the bottom conditions were imputed (as described above) or obtained as hindcasts from a hydrodynamic model of Chesapeake Bay developed by Anchor QEA, LLC (Fabrizio et al. 2021). Year was included as a random effect to account for variation in year-class strength. Distance to structure was defined as a categorical variable with three levels (0 - 500 m, 0 - 1000 m, > 1000 m). Distances greater than 1000 m were unlikely to influence abundance and we considered those tows as occurring in unstructured habitats. Multiple candidate models were tested and model comparisons were made using AIC; model fit was assessed by examining residuals. We compared several statistical distributions for the response variable (identified through the *fitDist* function in GAMLSS) including Pareto Type 2, t Family, and zero-inflated gamma (ZAGA) distributions and found that only ZAGA models converged. Significance of the final model terms was tested using stepGAIC function in GAMLSS.

Methods to Address Objective (3): Identify the relationship between habitat conditions in nursery areas and annual recruitment of summer flounder and black sea bass

Thermal Conditions Suitable for Growth of Juvenile Summer Flounder and Black Sea Bass

GAMMs (*mgcv* package in R) were used to ***examine sizes of fish (May to September) relative to environmental conditions*** (temperature, salinity) following methods in Nys et al. (2015). ***Local*** (individual subestuaries) and ***regional*** (bay vs coastal lagoons) ***effects,*** as well as ***fish densities*** (CPUE at each site) were considered because spatial and density-dependent effects on growth have been observed for juvenile summer flounder (Nys et al. 2015). Individual tows were considered random effects in the models to account for the clustered nature of the length data; distance to structure was binned into five categories: 0 - 250 m, 251 - 500 m, 501 - 750 m, 751 - 1000m, and > 1000 m. GAMM results were used to delineate suitable nursery habitat by identifying the range of conditions that supported growth of juvenile summer flounder and black sea bass during their residency in the Chesapeake Bay and coastal lagoons. The bottom temperature threshold for designating suitable habitat for summer flounder represents the upper temperature limit that supports growth of juveniles in Chesapeake Bay. We were unable to designate a thermal threshold for black sea bass because our GAMM model indicated that in the Chesapeake Bay and the coastal lagoons, temperature did not exert a negative effect on the size of juvenile black sea bass (see results, below).

Extent of Suitable Habitat for Juvenile Summer Flounder in Chesapeake Bay

The areal extent (m^2) of potential habitats that support growth of juvenile summer flounder was computed daily for 1996 to 2019 using the daily mean bottom temperature from the 3-D hydrodynamic model of Chesapeake Bay (Fabrizio et al. 2021). Hindcast estimates for each day between 1 May and 30 November were obtained from the hydrodynamic model for the entire bay and the lower portion of the major tributaries of Chesapeake Bay (i.e., the sampling domain for juvenile summer flounder). The hydrodynamic model does not extend to the MD Coastal Bays so we were unable to estimate suitable habitat extent in that system. Annual and monthly estimates of the extent of suitable habitat in Chesapeake Bay were computed as median values from the daily extent. These values represent the extent of potential habitat for juvenile summer flounder (Fabrizio et al. 2022).

Preliminary graphical inspection indicated annual and monthly variation in the extent of suitable habitat, and this variation was not consistent across months. Greater loss rates of suitable habitat through time were observed in August and very little to no loss of suitable habitat through time occurred in October or November, when bottom water temperatures rarely or never exceeded the thermal threshold in these months (Figure 5). Therefore, we focused our analysis of the extent of suitable habitats between May and September when bottom water temperatures were observed to exceed the thermal threshold in 1996 to 2019. Because changes in the mean monthly suitable habitat extent varied across years and months, we fitted the monthly mean extent data to the following non-additive linear model:

$$Y_{ij} = \mu + Month_i + \beta_i(Year_{ij} - \overline{Year_i}) + \varepsilon_{ij}$$

where Y_{ij} is the j^{th} observation of the mean extent of suitable habitat in month *i*, $Month_i$ is the effect of the i^{th} month, β_i is the partial regression coefficient describing the change in mean

extent of suitable habitat with year for month *i*, $Year_{ij}$ is the *j*th observation in month *i*, $\overline{Year_i}$ is the mean year in month *i,* and ε_{ij} is the random unexplained error assumed to be normally distributed with a mean of 0 and a variance of σ_ε^2. We interpreted the slope parameters (β_i) as the rate of annual change in suitable thermal habitat in month *i*. The model was fitted using the *GLM* procedure in SAS. Temporal dependency among years was added to the above model and fitted using the *MIXED* procedure in SAS, but there was no support for this additional complexity (Likelihood ratio χ^2= 0.19, P=0.667); therefore, we used the more parsimonious model with independent errors. Residuals from the model (combined across months) exhibited a random pattern around zero, indicating that the homogeneity of variance assumption was reasonable.

To further explore the variability in suitable habitat extent in Chesapeake Bay, we examined the relationship between habitat extent and two indices of bottom-water intrusion which represent the time scales of the dynamic processes whereby bottom waters intrude from the continental shelf into the bay. Bottom-water intrusion (BWI) events were identified by the following criteria: (a) wind direction from the south or southwest (155 degree – 250 degree measured from the north), (b) wind speed between 5 m/sec and 30 m/sec, (c) wind conditions that satisfy (a) and (b) and were persistent for 12 hours or more. We note that these conditions are sufficient for BWI events to occur, but it is yet to be shown that they are also necessary conditions. Based on observed wind speed and direction at the Chesapeake Bay Bridge Tunnel weather station (NOAA station ID: 8638863), we calculated the average wind speed and direction every 6 hours from 1989 to 2019 to identify time periods when conditions were favorable for a BWI event, and to calculate the duration of each BWI event (event = consecutive 6-hour time periods with favorable BWI conditions). The product of duration and average wind speed for each event resulted in the magnitude of each BWI event (hereafter termed fetch). Median fetch was calculated on a monthly basis and total (sum) fetch was calculated for each month and day.

We hypothesized that ***the daily and monthly BWI indices (i.e., daily or monthly fetch) predict the extent of suitable thermal habitat for summer flounder growth***. Furthermore, because BWI events are limited to the area near the mouth of the Chesapeake Bay, we examined extents of suitable habitats in Virginia waters only, reasoning that BWI events were likely to have less effect on bottom-water temperatures in the Maryland portion of the bay. The daily BWI indices for May to September were considered in the following repeated measures mixed effects model:

$$Y_{ijk} = \beta_0 + \beta_1 BWI + Day_i + Year_j + \varepsilon_{ijk}$$

where Y_{ij} is the *k*th observation of the mean extent of suitable habitat in Virginia on day *i* in year *j*, β_0 is the overall mean extent, β_1 is the partial regression coefficient describing the effect of the daily BWI on extent of suitable habitat, Day_i is the effect of the *i*th day of the year, $Year_j$ is the random effect of the *j*th year, and ε_{ij} is the random unexplained error assumed to be normally distributed with a mean of 0 and a variance of σ_ε^2. In this model, which was fitted using the *MIXED* procedure in SAS, year was treated as the "subject" from which repeated (daily) observations of the BWI index were obtained. We used a first-order autoregressive model to describe the decreasing correlations between adjacent observations through time.

The diagnostic plot of the residuals from this model was reasonable. We similarly constructed a model for examining the monthly BWI indices from May to September; monthly residuals from this model were reasonable.

Relationship of Suitable Habitat Extent to Relative Abundance

We hypothesized that ***the annual extent of suitable nursery habitat affects the annual production of juvenile fish***. To address this hypothesis, we related the annual time series of extent of suitable thermal habitat for growth (from the GAMMs, above) to estimates of annual juvenile abundance for Chesapeake Bay using a simple linear model:

$$Index_i = \mu + \beta Extent_i + \varepsilon_i$$

where $Index_i$ is the annual relative abundance of juvenile summer flounder in Chesapeake Bay in year *i*, μ is the overall mean index, $Extent_i$ is the annual extent of suitable thermal habitat in Chesapeake Bay calculated as the median of the daily extents from June to October in year *i*, β is the regression coefficient relating the change in the index for every unit change in suitable habitat extent, and ε_i is the random unexplained error, assumed to follow a Normal distribution with a mean of 0 and a variance of σ_ε^2. We used the *GLM* procedure in SAS to fit the model to observations of baywide relative abundance of juvenile summer flounder from 1996 to 2019 (24 years) with each cohort treated as an independent observation. The residuals from this model were randomly spread around zero, indicating that the assumption of homogeneity of variance was reasonable. No information on suitable habitat extent was available for juvenile black sea bass or for years prior to 1996. For this analysis, we considered CPUE data from the VIMS Trawl Survey and the MD Small Trawl Survey only because extent of suitable habitat could not be estimated from the MD Coastal Bays Survey (see above). The two survey indices for juvenile summer flounder were combined using the Conn (2010) hierarchical method, which uses a Bayesian approach to produce a single overall index from catch rates obtained from multiple fishery-independent surveys. The Conn method was implemented in R using the *R2WinBugs* package and code obtained from Conn. The Conn (2010) approach assumes each index is subject to process error (due to variation in catchability, spatial distribution, etc.) and sampling error (i.e., within-survey variance; Conn 2010). Simulations using this approach indicate good performance under a number of scenarios, including violation of assumptions (Conn 2010). Conn indices were estimated annually using survey indices from June to September as this is the period during which small summer flounder are most vulnerable to the trawl gear. Conn indices were also estimated for each month (June to September) to investigate finer temporal scale relationships between habitat extents and relative abundance.

Results

Some of the physicochemical characteristics of the study areas exhibited differences between ES and PK, but generally appeared similar within each study area. In particular, ES habitats were characterized by higher mean salinity compared with PK habitats (Table 3), and average salinity in PK was greater in 2020 compared with 2019 (Figure 6). Average water

temperature was similar between areas, among habitats, and across years (Table 3; Figure 7). Although we recorded slightly higher DO levels in PK compared with ES, DO appeared to be suitable (> 3 mg/L) across all habitat types and areas (Figure 8).

Seascape composition varied between ES and PK. On average, sampling sites in ES were characterized by a greater percentage of structured habitats (particularly seagrass) in the surrounding seascape, and a lower percentage of soft-bottom habitat (Figure 9). In addition to the increased availability of structured habitats in ES, sampling sites in ES were closer to structured habitats compared with PK sampling sites (Table 4). On average, ES sites were closer to marsh creeks by approximately 209 m, closer to oyster habitats by approximately 401 m, and closer to seagrass beds by approximately 449 m. Mean habitat diversity within 500 m of sampling sites was greater in ES (0.28 ± 0.04) compared with PK (0.11 ± 0.02); mean habitat diversity within 1 km of sampling sites was also greater in ES (0.41 ± 0.02) compared with PK (0.09 ± 0.01; also see Table 4). Sites in ES were also in deeper water (1.14 ± 0.08 m) on average compared with PK sites (0.49 ± 0.07 m). Seagrass sites in ES were dominated by eelgrass (*Zostera marina*), while seagrass beds in PK contained both eelgrass and widgeon grass (*Ruppia maritima*; Smith and Ross, *personal observation*).

During the two-year field study, we captured 58 fish species on the Eastern Shore and 62 fish species in the Piankatank River (Table 5, see also Table 6 for a comprehensive list of species). Species richness was remarkably similar despite differences in geographic location (i.e., proximity to the Atlantic Ocean), salinity conditions (Table 3), and habitat extents (Figure 9) between the two areas. We also note that the number of individual fishes captured was nearly equal between the two areas; we captured 31,255 individuals on the Eastern Shore and 31,243 individuals in the Piankatank River. Summer flounder (N=183) and black sea bass (N=138) were the 8th and 9th most abundant fish in ES (Table 6). In PK, summer flounder (N=62) and black sea bass (N=12) were the 19th and 33rd most abundant (Table 6).

Hypothesis 1 Results: Effect of Habitat Type and Area on Relative Abundance

Summer flounder

During the field study, we captured juvenile and (presumed) mature adult summer flounder ranging from 41 to 500 mm total length in both areas (Figure 10). A total of 87 juvenile summer flounder was captured in the Eastern Shore (ES) study area and 49 were captured in the Piankatank River (PK). No summer flounder were captured in April or May during either year of the study, suggesting that SMURFs were not effective for sampling early juvenile summer flounder. Monthly length-frequency histograms did not suggest the presence of sub-cohorts within a given year in either area (Figure 11). A low proportion of fyke nets captured juvenile summer flounder in both ES and PK and no difference was detected in the proportion of nets that captured fish between areas (Fisher's exact test P=0.154). In ES, fyke nets deployed in marsh habitats captured a greater proportion of juvenile summer flounder compared with nets deployed in all other habitat types (Fisher's exact test with Bonferroni adjustment: $P_{\text{marsh vs. oyster}} < 0.001$; $P_{\text{marsh vs. soft-bottom}} = 0.008$, $P_{\text{marsh vs. seagrass}} < 0.001$; Table 7, Figure 12). In PK, nets in marsh habitats captured a greater proportion of juvenile summer flounder compared with nets

in seagrass habitats (P=0.050, Table 7, Figure 12). Delta-lognormal estimates of abundance exhibited a similar pattern of higher mean abundance in ES marsh habitats compared with all other ES habitats and all habitats in PK (Figure 13). We found no significant differences in delta-lognormal mean abundance of ES juvenile summer flounder in 2019 (mean = 0.32, 95% confidence interval 0.17 – 0.49) compared with 2020 (mean = 0.41, 95% confidence interval 0.23 – 0.63). In contrast, delta-lognormal mean abundances of PK juvenile summer flounder were greater in 2019 (mean = 0.35, 95% confidence interval 0.22 – 0.49) compared with 2020 (mean = 0.04, 95% confidence interval 0.009 – 0.07); only four juvenile summer flounder were captured in PK in 2020.

Juvenile summer flounder captured in ES were smaller on average compared with fish captured in PK (141.7 ± 5.7 mm and 180.4 ± 7.6 mm respectively; ANOVA F = 6.55, P = 0.012). This result may be partially explained by the fact that we consistently captured juvenile summer flounder earlier in the year in ES compared with PK (average date of arrival was 9.3 days earlier in 2019 and 5.3 days earlier in 2020). Mean length of juvenile summer flounder was similar between years (F = 3.39, P = 0.078; Table 8). Mean length was also similar among habitats within a study area (F = 0.38, P = 0.763; Table 9), indicating a lack of size-based habitat use.

Black sea bass

Black sea bass ranging from age-0 to older juveniles (42-200 mm) were captured during the field study (Figure 10). We captured 129 juvenile black sea bass in ES and 12 in PK. In ES, a greater proportion of SMURFs (deployed April-May) captured juvenile black sea bass compared with SMURFs in PK (Fisher's exact test P = 0.003; Figure 14). Within ES, we found significant differences in the proportion of SMURFs that captured black sea bass among habitat types (Fisher's exact test P = 0.030). We found marginal evidence that juvenile black sea bass were captured in a greater proportion of SMURFs deployed in ES oyster habitat compared with those deployed in ES seagrass habitat (Bonferroni adjusted Fisher's exact test P = 0.060). None of the SMURFs deployed in 2020 captured black sea bass despite sampling effort that was equal to that in 2019. Delta-lognormal estimates of abundance based on SMURF captured fish indicated a greater mean abundance of black sea bass in ES habitats compared with PK habitats, along with a weak indication of greater mean abundance in ES oyster habitat compared with other ES habitats, although variation around these means was high (Figure 15).

Similar to SMURFs, a greater proportion of fyke nets (deployed June-October) captured juvenile black sea bass in ES compared with PK (Figure 14, Fisher's exact test P <0.001). Within each study area, we did not detect a difference among habitats in the proportion of net sets that captured fish, however, a greater proportion of fyke net deployments in ES seagrass habitat captured juvenile black sea bass compared with fyke nets in PK seagrass habitat (Figure 14; Bonferroni adjusted P = 0.002). The variation around the delta-lognormal estimates of mean abundance of black sea bass was high. Nevertheless, our results suggested greater mean abundance in ES habitats compared with PK habitats, as well as a greater mean abundance in ES seagrass habitat compared with other ES habitats (Figure 15). Furthermore, mean abundances of ES juvenile black sea bass in 2019 (mean = 0.62, 95% confidence interval 0.34 –

0.98) and 2020 (mean = 0.26, 95% confidence interval 0.15 – 0.37) were not significantly different.

Juvenile black sea bass in ES were smaller on average in 2019 (94.6 ± 2.1 mm) compared with 2020 (117.4 ± 4.2 mm; F = 19.9, P<0.001). We note that juvenile black sea bass in ES were captured 19 days earlier in 2019 compared with 2020, and this likely explained the difference in mean size between years. The average date of arrival of black sea bass in PK in the two years differed by one day (8 August 2019 and 7 August 2020). Mean length of individuals also differed among ES habitats (F = 3.57, P = 0.020): fish captured in ES seagrass habitats were larger on average compared with fish captured in ES marsh habitats (Table 10, seagrass-marsh adjusted P = 0.002). The mean length of black sea bass captured in PK appeared greater than that of fish captured in ES in 2019 and 2020 (Table 10) although low sample size in PK (9 and 3 individuals captured in 2019 and 2020, respectively) precluded meaningful comparisons. We note that fish were captured later in the year in PK compared with ES (average date of arrival was 50.3 days later in 2019, and 30.2 days later in 2020), a finding that partially explains the differences in mean size we observed among PK and ES fish.

Hypothesis 1 Results: Habitat Quality Assessed by Fish Condition and Recent Growth

Summer flounder

Relative condition (K_n) was calculated for 136 of the 141 juvenile summer flounder captured. Five fish were omitted because of unreliable length measurements resulting from partial net predation. Observations of mean K_n among areas and habitats ranged from 0.93 in ES oyster habitat to 1.04 in PK seagrass habitat (Table 9). Differences in body weight for fish with $K_n < 0.95$ compared with fish with $K_n > 1.05$ were 28.5% for individuals 100-150 mm and 27.7% for individuals 150-200 mm. Relative condition was highly variable in some instances. For example, individual K_n ranged from 0.79 to 1.29 within the same ES marsh site in early June. Area-habitat type was not an important predictor of summer flounder K_n and the model was not informative (likelihood ratio χ^2= 4.57, P=0.712; Table 11) and model-based estimates of mean K_n did not differ between study areas or among habitat types (Table 12; Figure 16). The random effect of site nested in area-habitat type explained minimal variance (5.2%). The assumptions of normality and homogeneity of variance were met and no patterns in model residuals were observed.

A total of 116 otoliths from juvenile summer flounder was used to estimate recent growth. Otoliths from a small number (n=13) of juvenile summer flounder were excluded from growth analyses because of damage during handling or poor increment interpretability. The mean between-reader difference in distance measured from otolith edge to the 7th increment (averaged across all otoliths) was less than 1 µm (Table 13). Twenty-nine of the 116 (25%) otoliths had between-reader disagreement greater than 25% and required both readers to reach consensus. Bland-Altman plots revealed no discernible bias between readers (Figure 17). We used ordinary least-squares regression to establish relationships between fish size and otolith maximum diameter, and fish size and otolith radial diameter. Otolith maximum diameter and fish length were strongly associated ($F_{1,112}$ = 1488, P<0.001, r^2 = 0.93; Table 14).

Otolith radial diameter and fish length were strongly associated, but radial diameter explained a relatively smaller amount of the variation in fish length ($F_{1,113}$ = 57.42, P<0.001, r^2 = 0.33; Table 14; Figure 18). Because the assumptions of linear regression were reasonable for both models, we used these regressions to estimate recent growth of each fish, where recent growth is the cumulative growth (in mm) a fish experienced during the seven days prior to capture. Estimation of recent growth for juvenile summer flounder was not improved by the inclusion of area-habitat type in the model (likelihood ratio χ^2= 6.921, P=0.437; Table 15), indicating that we were unable to detect a habitat-type effect on recent growth. Marginal mean-scaled estimates of recent growth were highly variable and did not differ between areas or habitat types (estimates based on the "full" model in Table 15; Table 16; Figure 19). The assumptions of normality and homogeneity of variance were met and no patterns in model residuals were observed.

Black sea bass

Relative condition was calculated for 129 fish from ES and 12 fish from PK. The small number of black sea bass captured in PK precluded meaningful comparisons of K_n among habitats in PK or between sampling areas (Table 17). We therefore focused subsequent analyses on ES fish only. Mean K_n for ES fish ranged from 0.95 ± 0.03 in soft-bottom habitats to 1.05 ± 0.03 in oyster habitats (Table 17). Black sea bass mean K_n in ES was not explained by habitat type (likelihood ratio χ^2= 0.19, P=0.658) or year (likelihood ratio χ^2= 4.88, P=0.180). Models including these main effects were generally uninformative (Table 18). Marginal mean-scaled estimates of K_n among habitat types and between years were highly variable and did not appear to differ (estimates based on the "full" model in Table 18; Figure 20). The random effect of site nested in habitat type explained 22.2% of the variance. The assumptions of normality and homogeneity of variance were met and no patterns in model residuals were observed.

Fifteen black sea bass otoliths were omitted from recent growth analyses because of poor increment interpretability. Our growth analyses were based on 105 black sea bass otoliths. The mean between-reader difference in the distance between the otolith edge and the 7th increment (averaged across all otoliths) was 1.01 ± 0.08 µm (Table 13) based on 83 otoliths for which we achieved reasonable between-reader agreement. Twenty-two (20.9%) of the 105 otoliths had between-reader disagreement greater than 25% and were co-read by two readers. Bland-Altman plots revealed no discernible bias between readers (Figure 17). The relationship between otolith maximum diameter and fish length was significant and explained 91% of the variation in fish length ($F_{1,95}$ = 988.1, p<0.001, r^2= 0.91; Table 14). Although the relationship between otolith radial diameter and fish length was significant, the variation in fish length explained by the radial diameter was relatively low ($F_{1,98}$ = 70.18, p<0.001, r^2 = 0.41; Table 14; Figure 21). The assumptions of linear regression were reasonable for both models. Therefore, these models allowed us to estimate recent growth of the fish, where recent growth is the cumulative growth (in mm) a fish experienced during the seven days prior to capture. PK fish were not included in black sea bass recent growth analysis because of low sample size; 99 fish from ES were used for this analysis. Models fit to the recent growth data for ES black sea bass were generally uninformative (Table 19). Mean recent growth of black sea bass was not explained by habitat type (likelihood ratio χ^2=2.080, P=0.556) or year (likelihood ratio

χ^2=3.274, P=0.071). The random effects of sampling event and site nested in habitat type explained 6.9% and 10.9% of variation in the full model. Marginal mean-scaled estimates of recent growth among habitat types and between years were highly variable (estimates based on the "full" model in Table 19; Figure 22). The assumptions of normality and homogeneity of variance were met for all models.

Hypothesis 1 Results: Seascape Effects on Fish Condition and Recent Growth

Despite the differences in seascape composition between ES and PK, no relationships were detected between seascape features and habitat-quality metrics (relative condition or recent growth) for juvenile summer flounder (Table 20). Unlike habitat quality for juvenile summer flounder, habitat quality for juvenile black sea bass appeared to have an association with seascape features. Mean relative condition of juvenile black sea bass was positively associated with the availability of oyster habitat within 500 m of capture locations when oyster habitats covered between 0 and 5% of the area under consideration; when the percent area of oyster habitat exceeded 5%, relative condition was negatively associated with oyster habitat (F=9.509, P<0.001, deviance explained=19.7%, N=141). We note, however, that this pattern was likely driven by a few individual observations and a lack of sites characterized as 5 to 15% oyster habitat (Figure 23). The mean recent growth of black sea bass was greater at capture locations with a high percentage of soft-bottom habitat (F=2.708, P=0.039, deviance explained=8.77%, N=106), and a low percentage of seagrass habitat (F=3.829, P=0.034, deviance explained=8.52%, N=106; Figure 24). Distance to seagrass habitat was also associated with mean recent growth of black sea bass (F=3.066, P=0.027, deviance explained=8.87%, N=106) and suggested that recent growth may be greater in areas away from seagrass (Figure 24). Model assumptions were met for all of these models, but we note the low proportion of deviance explained, and hence, the lack of explanatory power. Black sea bass habitat quality was not associated with habitat diversity in the seascape, nor with the proximity or availability of other structured habitats (Table 20).

Hypothesis 2 Results: Factors Affecting Relative Abundance

The number of tows conducted by each survey varied during the early years and stabilized after about 2000 (Figure 25). Data from different regions of Chesapeake Bay were used for juvenile summer flounder and black sea bass based on salinity and knowledge of their early life history such that more tows were included in the analysis for summer flounder compared with black sea bass. All sample sites in the MD Coastal Bays were included for each species.

The number of fish captured by each survey varied among years and species, with the VIMS survey capturing the most of each species followed by the MD Coastal Bays (Figure 26). The MD Small Trawl captured only 32 black sea bass and thus data from this survey were not included in the abundance analysis.

<u>Summer flounder</u>

The best fitting model describing the abundance of juvenile summer flounder in the MD Coastal Bays (Table 21) assumed a zero-inflated gamma distribution and included significant smooths for bottom water temperature, salinity, and depth, and a random effect of structure (<500 m) nested within year. Additionally, the σ or scale parameter (variance) was modeled with the significant effects of temperature and salinity and the shape parameter (skewness and kurtosis) was modeled with the significant effects of temperature only. In the MD Coastal Bays, abundance of juvenile summer flounder was significantly affected by bottom temperature, salinity, and depth (Table 22; Figure 27). Higher mean relative abundances of summer flounder were observed at temperatures exceeding 19 °C, and at salinities less than 27 psu. Depths between 2 and 3 m appeared to support fewer summer flounder compared with other depths that were sampled (range 0.8 – 4.6 m), however, we caution that this may be an artifact of the fixed-station design of the MD Coastal Bays survey.

The best fitting model for the abundance of juvenile summer flounder in the VIMS survey domain (Table 21) assumed a zero-inflated gamma distribution and included significant smooths for bottom water temperature, salinity, and depth, and the random effect of year. Additionally, the shape parameter (skewness and kurtosis) was modeled with the significant effects of temperature and salinity. Mean abundance of juvenile summer flounder from the VIMS survey was significantly affected by water temperature with fewer summer flounder found at temperatures < 17.5 °C (Table 22; Figure 28). In the VIMS survey, greater mean abundances of summer flounder were found at relatively high salinities (> 29 psu), which contrasts with results from the MD Coastal Bays. Additionally, greater abundances of juvenile summer flounder were observed at shallow depths (< 5 m) in the VIMS survey.

The best fitting model for the abundance of juvenile summer flounder captured by the MD Small Trawl Survey (Table 21) assumed a zero-inflated gamma distribution and included significant smooths for bottom water temperature and salinity, and the random effect of year. Additionally, the σ parameter (variance) was modeled with the significant effect of salinity, and the ν parameter (skewness) was modeled with the significant effects of temperature and salinity. In the MD portion of the bay, the mean abundance of summer flounder was significantly influenced by water temperature and salinity (Table 22; Figure 29). However, patterns were less evident than those observed in the MD Coastal Bays and the Virginia portion of Chesapeake Bay. For example, in the MD Small Trawl Survey, greater relative abundances of summer flounder occurred in habitats with water temperatures between 19 and 21 °C, and with salinities between 10 and 15 psu.

Black sea bass

In the MD Coastal Bays, the best fitting model for the abundance of juvenile black sea bass (Table 23) assumed a zero-inflated gamma distribution and included significant smooths for bottom water temperature and depth, and a random effect of structure (<500 m) nested within year. Additionally, σ and shape parameters (variance, skewness and kurtosis) were modeled with the effects of temperature and salinity. In the MD Coastal Bays, juvenile black sea bass were significantly less abundant at water temperatures less than about 18 °C and in depths shallower than 1.5 m (Table 24; Figure 30).

The best fitting model for the relative abundance of juvenile black sea bass in the VIMS survey domain (Table 23) was similar to the best fitting model for the MD Coastal Bays with the exception that salinity was also a significant smoothed term in the model. Mean relative abundance of black sea bass captured by the VIMS survey increased at water temperatures exceeding 15 °C, with greatest abundances occurring between 17 and 22 °C (Table 24; Figure 31). Salinity was also important and greater mean relative abundances of black sea bass were found at salinities between 18 and 34 psu. Additionally, juvenile black sea bass were more abundant at depths exceeding 10 m in the Virginia portion of Chesapeake Bay.

Only 32 black sea bass in 30 tows were observed from the MD Small Trawl samples, which prevented the fitting of abundance models for this survey.

Hypothesis 3 Results: Factors Affecting Fish Length

Mean length of juvenile summer flounder was significantly affected by bottom water temperature and salinity, day of the year, local density, stratum, and distance to structure; the model explained 91.7% of the deviance (Table 25). As expected, mean length of summer flounder increased throughout the summer growing season (Table 25). However, summer flounder mean length decreased at water temperatures exceeding 25.9 °C indicating that these temperatures negatively influenced growth (Figure 32). Salinities less than about 12 psu had a negative influence on summer flounder length, and intermediate summer flounder densities had a positive effect on summer flounder length. Relative to the Choptank River, all other strata except for the Eastern Bay had significantly smaller juvenile summer flounder. Summer flounder size as it relates to distance to structure showed varied responses with no clear patterns indicating that structure did not influence mean fish length.

Mean length of juvenile black sea bass was significantly affected by day of the year, depth, stratum, and local density with the model explaining 79.8% of the deviance (Table 26). Unlike summer flounder, we found no effect of water temperature or salinity on mean size of black sea bass. Mean length of juvenile black sea bass increased with day of the year, and larger black sea bass were found in depths greater than 15 m (Figure 33). Relative to the James River, juvenile black sea bass were significantly larger in the northern region of the MD Coastal Bays and significantly smaller in the Virginia portion of Chesapeake Bay.

Hypothesis 3 Results: Extents of Suitable Thermal Habitats for Growth & Relationship to BWI

The spatial domain of the 3D hydrodynamic model for Chesapeake Bay and its tributaries comprised 914,192.6 hectares, with 66.0% (603,588.9 hectares) in Maryland and 34.0% (310,603.7 hectares) in Virginia; this domain includes only those areas that could be potentially occupied by juvenile summer flounder, that is, the bay and lower portions of the major tributaries. Suitable habitat extents varied annually, and on average, the minimum extent of suitable habitat occurred in mid-August (Figure 34). The linear model describing changes in potential habitat extent across years indicated the presence of a significant interaction between year and month ($F=4.56$, $P=0.002$); therefore, monthly models were constructed to estimate change in suitable habitat extent. Baywide, we found no evidence of

annual changes in the extent of suitable thermal habitat in May (F=2.89, P=0.103), which exhibited a mean of 911,554.3 hectares (95% confidence interval: 910,094.4 – 913,014.1) across years. Similarly, we found no change in suitable habitat extent in October (F=1.75, P=0.199), when the mean extent was 913,204.0 hectares (95% confidence interval: 912,172.5 – 914,192.6), or in November when bottom temperatures in the bay never exceeded the upper thermal threshold for growth of juvenile summer flounder (extent=914,192.6 hectares). In contrast, we found significant declines in the mean extent of suitable thermal habitats in June (F=7.20, P=0.014), July (F=24.80, P<0.001), August (F=6.47, P=0.019), and September (F=39.67, P<0.001; Figure 35). The annual loss in mean extent of suitable habitats was 2,858.9 hectares/year in June, 16,475.0 hectares/year in July, 18,764.0 hectares/year in August, and 8,797.8 hectares/year in September for the period 1996 to 2019 (Figure 35). The model-based extent of suitable thermal habitat for growth of juvenile summer flounder in August 2019 was 247,614.4 hectares, which represents a 63.5% decline from that predicted in August 1996 (679,191.6 hectares). Similarly, suitable habitat extent in July 2019 (428,643.5 hectares) was 46.9% lower than that predicted in July 1996 (807,573.0 hectares).

The monthly BWI (median monthly fetch) was not a significant predictor of the mean monthly extent of suitable thermal habitats in Virginia (F=1.37, P=0.244, N=120 observations). In this model, month was a significant predictor (F=57.23, P<0.001) and the correlation between adjacent observations of monthly extents was relatively low (r=0.224).

The daily BWI was a significant predictor of the daily extent of suitable thermal habitats for juvenile summer flounder in Virginia (F=21.24, P<0.001); this model was based on 3,672 observations from May to September, 1996-2019. The correlation between daily observations was 0.962, suggesting that consecutive daily BWI events are highly correlated with one another.

Hypothesis 3 Results: Relationship between Extent of Thermal Habitat and Annual Relative Abundance

The distribution of the estimated extent of suitable thermal habitat for juvenile summer flounder in the bay was highly left skewed, indicating a greater proportion of observations with large extents from June to October (N=3,672 daily observations from 1996 to 2019). Because of the skewness in the data, we used medians as measures of central tendency for a given month or year. On an annual basis, the median percent suitable habitat in Chesapeake Bay decreased significantly since 1996 (F=15.69, P<0.001, Figure 36). Closer inspection of the daily extents of suitable habitat in Chesapeake Bay revealed that declines through time were most pronounced in July and August (Figure 37).

Annual and daily changes in the extent of suitable habitat in Maryland and Virginia were not proportional, such that the percent of the total available habitat that was considered suitable was lower in MD waters relative to VA waters, and this was especially evident in late summer (Figure 38).

The linear model relating the median extent of suitable thermal habitat in Chesapeake Bay for juvenile summer flounder and the annual abundance index was not significant (F=0.93, P=0.346, N=24), suggesting that the amount of suitable habitat did not limit the abundance of juvenile summer flounder in the bay (Figure 39). This model used the Conn abundance index

based on catches from the VIMS Juvenile Fish Trawl Survey and the MD Small Trawl Survey. We attempted to fit the regression to annual abundances for age-0 summer flounder reported by ChesMMAP for 2002 to 2018 (the 17 years during which ChesMMAP sampled the bay with the same research vessel), but this regression also yielded a non-significant model ($F=0.83$, $P=0.378$). We next examined the relationship between extent of suitable thermal habitat and relative abundance on a finer temporal scale using monthly values. Although we found a significant relationship between the baywide index of relative abundance and the median extent of suitable thermal habitat for juvenile summer flounder in June ($F=5.00$, $P=0.036$), this relationship was driven by a single influential observation from 2015 (Cook's $D > 1$), and therefore we deemed this model unreliable. Relationships in July ($F=0.76$, $P=0.392$), August ($F=1.70$, $P=0.205$), and September ($F=1.12$, $P=0.302$) were not significant, indicating that the relative abundance of juvenile summer flounder was not explained by variation in the extent of suitable thermal habitat in any month.

Discussion

Juvenile summer flounder and black sea bass use nursery areas in the Chesapeake Bay and the Delmarva coastal bays for feeding and growth during their first year of life. We studied the role of nursery areas at two spatial scales to determine how individual habitat types (oyster, marsh, seagrass, and soft-bottom habitats), as well as the seascape, support abundance, condition, and growth of juvenile fishes. In our small-scale field study, we found greater mean abundances of both species at ES nursery sites relative to PK nursery sites, and in the case of black sea bass, that difference was an order of magnitude. This is noteworthy because recruitment of these species in the mid-Atlantic region was low in 2019 and 2020. Nevertheless, marked differences in relative abundance were noted and are likely associated with differences in proximity of ES nurseries to the coastal ocean (ES is closer than PK), variations in habitat conditions, differences in seascape complexity, or a combination of two or more of these factors.

Juvenile summer flounder and black sea bass were captured earlier in the year in ES nurseries than in PK nurseries, and may reflect the shorter distance between offshore spawning areas and areas used as nurseries. Conditions at ES and PK sites were similar in terms of bottom water temperature, but ES sites were characterized by a greater mean salinity. ES seascapes were more diverse, i.e., more complex, and offered slightly deeper habitats than PK seascapes; in particular, the ES area had a greater percentage of structured habitats (especially seagrass), and less soft-bottom habitat than the PK area. As a result, ES sampling sites were closer to structured habitats such as marsh creeks, oyster habitats, and seagrass beds, than PK sites. Comparative evaluation of the quality of seaside (ES) and bayside (PK) nursery areas at a fine spatial scale can provide managers and policy makers with critical information on the importance of habitats and their placement in coastal systems. Proximity to the coastal ocean cannot be regulated or changed, but managers can develop and promote habitat conservation and restoration plans to ensure the availability of diverse and complex structured habitats. Such plans could promote the long-term sustainability of fishery resources by supporting production of abundant year classes.

In ES habitats, relative abundances of black sea bass were marginally associated with oyster habitats during early summer (April-May) but showed no association with habitat type in late summer-fall. This may be indicative of a stronger association of small-bodied individuals with oyster habitats, and a lack of association with a particular habitat type as body size increases. This finding supports previous work that documented small black sea bass (< 70 mm) residing in oyster habitats (Able & Fahay 1998a; Steimle et al. 1999).

Within the ES and PK seascapes, relative abundance of juvenile summer flounder was greatest in marsh habitats. This is consistent with reported habitat use (Rountree & Able 1992; Able & Fahay 1998b; Packer et al. 1999; Sackett et al. 2008), but such associations based on sampling of multiple habitat types have not been previously documented for the Chesapeake Bay region. For juvenile summer flounder, we hypothesized that because marshes are highly productive systems (Kennish 2015), these habitats offer an abundance of prey. Marshes also provide tidally inundated, shallow areas that juvenile summer flounder may use as a refuge from predation (Manderson et al. 2004). Although there has been a historical loss of marsh habitats in the Chesapeake Bay region since the mid-19th century due to sea-level rise, the conversion of upland areas to marshes compensated for these losses (Schieder et al. 2018). Accelerating rates of sea-level rise in the region, however, threaten the resiliency of marshes, unless marshes can migrate landward at a rate that keeps pace with rising seas. Some have argued that the extent of marshes and other wetlands may actually increase as these systems migrate inland (Kirwan et al. 2016). The response of marshes to inundation depends primarily on local topography and upland land use (Gedan et al. 2020; Molino et al. 2022), and because much of the land along the US mid-Atlantic coast is suitable for the conversion of upland areas to marsh (Holmquist et al. 2021), an overall gain in the extent of marshes and other types of wetlands may be expected under climate change (Molino et al. 2022). In areas characterized by urbanization and extensive shoreline armoring, marsh resilience is reduced and the landward migration of marshes will be impeded (Molino et al. 2022). In the near term, protection and restoration of marsh habitats in Chesapeake Bay can directly benefit juvenile summer flounder by the provisioning of areas that support high abundances of juveniles; protected and restored marshes can thereby contribute to the continued production of these fisheries. Looking ahead, conservation and protection of marshes as nursery grounds for fishes will require a holistic, ecosystem-based approach. Under climate change, natural resource managers and land managers will need to work together to develop policies to address the likely conversion of agricultural and forest lands that are adjacent to Chesapeake Bay to marshes and other wetlands. Whether newly formed marshes will be functionally equivalent to contemporary marshes, however, remains unknown (Molino et al. 2022).

At the small-scale, the effect of seascape composition on the fitness proxies that we examined – recent growth and relative body condition – varied by species. We observed a positive relationship between oyster habitat availability and black sea bass relative condition, but emphasize that this effect was likely driven by a select few observations and a lack of sites with intermediate amounts of oyster habitat (relative to the range of oyster habitat coverage in our sites). We also observed a positive association between black sea bass recent growth and the availability of soft-bottom habitats and, conversely, a negative association between recent growth and seagrass habitat availability and proximity. However, we note that the models

suggesting these associations of seascape features with recent growth lacked explanatory power (only ~8% of deviance explained). Juvenile black sea bass are known to feed on benthic and epibenthic invertebrates typically found in soft-bottom habitats (Steimle et al. 1999), and adult black sea bass also make use of sandy bottoms for foraging (Lindquist et al. 1994; Steimle & Figley 1996). Additional work is needed, however, to confirm similar use of soft-bottom habitats for juveniles in shallow waters. There was no effect of seascape composition or complexity on juvenile summer flounder relative body condition or recent growth.

Unlike the differences in relative abundance observed between the two study areas, body condition and recent growth of juvenile summer flounder and black sea bass were similar between ES and PK. This differs from the findings of Schloesser and Fabrizio (2019), who reported greater mean body condition of summer flounder in ES coastal lagoons compared with fish from the James, York, and Rappahannock rivers. Although the tributaries we sampled were different than those sampled by Schloesser and Fabrizio (2019), similarities in mean body condition observed in our study might also be attributed to differences in the habitats sampled. Schloesser and Fabrizio (2019) used an otter trawl to sample habitats 2 - 27 m deep whereas this study used passive gears to sample shallow habitats < 2 m in depth. Schloesser and Fabrizio (2019) observed healthier individuals in deeper habitats and related the effect of depth to potential ecological effects such as increased prey availability or fewer predators. This finding may indicate different factors affecting summer flounder body condition in shallow and deep habitats and highlights the importance of comprehensive sampling of a species' occupied habitats. Similarly, habitat type (marsh, oyster, seagrass, soft-bottom) had no effect on recent growth or body condition of juvenile black sea bass and summer flounder. Together, these results suggest that juvenile fishes use multiple habitat types within the seascape to maximize growth and condition, and that for black sea bass, fidelity to habitat type is low or zero (recall that relative abundance of juvenile summer flounder was greatest in marsh habitats). The effect of movement of individuals among habitat types on fitness proxies was a concern when we designed the field study, and thus, we used reported estimates of home ranges to account for movement within the seascape and its effect on recent growth and body condition. We offer four possibilities to explain our results: (1) published home ranges are not applicable to fishes in the Chesapeake Bay region, (2) recent growth and body condition metrics are insensitive to recent feeding, (3) prey resources were sufficiently abundant to support similar growth in the two study areas and among habitats, or (4) sample sizes are insufficient to detect true differences in fitness proxies. Home range estimates may be affected by the study system such that fish may exhibit smaller home ranges in highly productive systems (e.g., fish need not move large distances to find forage or refuge); the home ranges used in our study were obtained from studies of juvenile summer flounder and black sea bass in Little Egg Inlet and Great South Bay, both of which are mid-Atlantic estuaries. We cannot know if home ranges would be different in the Chesapeake Bay region without a field study (e.g., using acoustic telemetry). Body condition metrics may be insensitive to recent feeding in juvenile fishes if individuals allocate a relatively larger portion of their energy to growth, which would result in less energy available for storage in the liver or as body fat (Schloesser & Fabrizio 2016). Moreover, body condition of juvenile fishes (thus, the allocation of energy to different tissues) varies within and among years (Schloesser & Fabrizio 2016). We were unable to conduct a

comprehensive survey of prey resources at our study sites, but in the future, sampling of benthic epifauna and infauna concurrent with fish collection may help determine the relative abundance and type of prey resources available to fishes. For example, we observed juvenile summer flounder predation on penaeid shrimps in multiple habitat types in both study areas, suggesting that summer flounder generally take advantage of this prey species (Smith and Ross, *personal observation*). We acknowledge that sample size could be improved and that with more fish, we may have been able to detect the effects of seascape features or habitat types on recent growth and relative body condition. Our low sample size, however, was not a result of our sampling design or sampling effort, but rather, a reflection of the poor recruitment events observed in 2019 and especially in 2020 for these two species.

In this study, habitat associations of juvenile fishes were also described using long-term catch records from surveys that sampled fishes during their duration of estuarine residency and over broad spatial scales. The three surveys considered here varied in terms of the window during which monthly sampling occurred, the depth range of habitats sampled, and the prevailing environmental conditions. Although the VIMS Juvenile Fish Trawl Survey and the MD Coastal Bays Survey conducts sampling from April to October when juvenile summer flounder and black sea bass are present in these systems, we restricted the period of study to coincide with the MD Small Trawl Survey, that is, May to September. The MD Small Trawl Survey does not measure DO concentrations; therefore, we could not consider this environmental parameter in models that related abundance and fish size to environmental conditions. Nonetheless, bottom DO and bottom temperature are highly correlated, and as such, bottom temperature may provide an adequate descriptor of conditions. Although all surveys sampled relatively shallow waters (<2 m), the mean depth of sites sampled by the VIMS Juvenile Fish Trawl Survey (8.8 m; range 0.9 to 40.5 m) between May and September was greater than that of the MD Small Trawl Survey (2.2 m; range 0.6 to 7.6 m) and the MD Coastal Bays Survey (2.0 m; range 0.8 to 4.6 m). As surveys that sampled mostly in shallow areas, mean bottom temperature between May and September was 24.0 °C for the MD Small Trawl (range: 12.3 – 35.5 °C) and the MD Coastal Bays (range: 12.5 – 35.0 °C) surveys. The mean bottom temperature between May and September was slightly lower, 23.2 °C, for the VIMS Juvenile Fish Trawl Survey (range: 8.9 – 35.0 °C). Unlike temperature, bottom salinity conditions were highly divergent among the surveys: mean bottom salinity was 11.5 psu for the MD Small Trawl Survey (range: 0 – 22.1 psu), 17.0 psu for the VIMS Juvenile Fish Trawl Survey (range: 0 – 37.1 psu), and 27.5 for the MD Coastal Bays Survey (range: 5.7 – 36.2 psu). Coastal lagoons receive relatively little freshwater input, and most of that is from ground water (Kennish & Paerl 2010), thus, higher salinities are often observed in these systems.

These environmental differences among survey areas may produce non-stationarity in the relationship between relative abundance and environmental conditions, that is, different relationships are required for each survey area. Spatially-dependent relationships can be addressed by treating the models for relative abundance separately for each survey domain (e.g., Behan et al. 2021). Bottom temperature and bottom salinity were significant predictors of relative abundance of juvenile summer flounder, but the conditions that supported high abundances varied, depending on the system: in the shallow, relatively warmer waters of the MD Coastal Bays, juvenile summer flounder abundance was greatest in salinities less than 27

psu, but greater abundances were observed in the cooler waters of the VIMS survey where salinity exceeded 29 psu. Salinity is a factor driving relative abundance, but its effect likely depends on bottom temperature. Based on the MD Small Trawl Survey, juvenile summer flounder are more likely to be found in a narrow temperature range (19 – 21 °C) and narrow salinity range (10 – 15 psu). We note, however, that abundance of summer flounder in the MD Small Trawl Survey was lower than that observed in the MD Coastal Bays and in Virginia waters of the Chesapeake Bay. Although depth was an important driver of juvenile summer flounder abundance in the Coastal Bays and in the VIMS survey domain, this was not the case for the MD Small Trawl Survey. The limited range of depths sampled may have hindered the ability to detect depth effects in the marginal salinity conditions of the northern waters of the Chesapeake Bay.

Our understanding of habitat effects on abundance of juvenile black sea bass was derived from observations from the VIMS Juvenile Fish Trawl Survey and the MD Coastal Bays Surveys, because catches were extremely low for the MD Small Trawl Survey. This suggests that salinity in the areas sampled by the MD Small Trawl may be too low to support black sea bass. In the MD Coastal Bays, where bottom salinity during the period 1989 to 2019 averaged 27.5 psu, high abundances of juvenile black sea bass were observed in waters exceeding 18 °C and depths greater than 1.5 m. This finding is consistent with findings reported by Peters & Chigbu for the MD Coastal Bays (2017). In the lower Chesapeake Bay, juvenile black sea bass abundance was greater in deep waters (> 10 m), where temperature exceeded 15 °C and salinity was relatively high (18 – 34 psu). The proximity to structure was also a driver of relative abundance of juvenile black sea bass.

Models to describe the variation in juvenile fish lengths explained 92% (summer flounder) and 80% (black sea bass) of the deviance, and indicated that growth of these species responded to different factors. Temperature and salinity were important predictors of summer flounder growth, but had no effect on black sea bass growth. Local density of conspecifics was an important predictor for both species, reflecting possible density-dependent processes that limit growth. Growth of juvenile summer flounder, but not black sea bass, was influenced by distance to structure; juvenile black sea bass growth responded positively to depth, but depth had no effect on summer flounder growth. Thermal conditions that exceeded 25.9 °C were detrimental to growth of juvenile summer flounder and as such, we defined suitable thermal habitats for growth as those areas where bottom temperatures were less than 25.9 °C. This thermal threshold was similar to the threshold (25.0 °C) reported for juvenile summer flounder in Narragansett Bay, Rhode Island (Taylor et al 2016). No relationships were observed between length and temperature or length and salinity for juvenile black sea bass, suggesting that salinity and temperature conditions in the sampling domains considered in Chesapeake Bay and the MD Coastal Bays supported growth. We note, however, that we restricted our analysis to catch data from areas where salinity exceeded 12 psu, because we did not observe black sea bass in lower salinity waters. We suggest that the 12 psu threshold may be used to estimate extent of suitable habitats for juvenile black sea bass; these extents may be altered under climate change because the amount and timing of freshwater inputs in the Chesapeake Bay region are likely to change. We speculate that under climate change, extents will be fairly stable for the MD Coastal Bays due to the relatively large exchange of waters with the coastal

ocean and because coastal bays receive little input from rivers. In the Chesapeake Bay, juvenile black sea bass were captured in the Virginia waters of the bay and in the Maryland portion of the bay near the Pocomoke River and Tangier Sound. These areas in Maryland exhibit relatively higher salinities because tidal exchange in the bay is not spatially uniform; higher salinity waters enter the bay along the eastern portion during flood tides and only a few small rivers discharge freshwater into this part of the bay.

Spatial variations in environmental and biotic conditions (e.g., prey availability) across the areas we sampled resulted in spatial differences in the relative mean lengths of juvenile summer flounder and black sea bass. Black sea bass attained a greater size in the northern portion of the MD Coastal Bays relative to other areas, and deep waters (>15 m) also supported larger fish. Because the Coastal Bays are relatively shallow (<4.6 m), and the MD Small Trawl Survey does not sample water greater than 7.6 m deep, the depth effect on length was driven by our observations of fish captured by the VIMS Juvenile Fish Trawl Survey. Juvenile summer flounder were larger on average in the Choptank River and the eastern bay stratum sampled by the MD Small Trawl Survey, suggesting these areas better support growth of this species. The Choptank River is a NOAA Habitat Focus Area and is one of several areas benefitting from significant restoration of native oysters. This river appears to also support juvenile summer flounder that are larger than conspecifics from other areas of the bay. We caution, however, that greater growth rates may not indicate greater survival of juvenile summer flounder because predation mortality must be considered (Taylor et al. 2016). Mean length of summer flounder was positively affected by intermediate densities of conspecifics; areas characterized by low densities of juvenile summer flounder may reflect the lack of prey availability or availability of less energetically rich prey and hence, juvenile fish may be less likely to occupy such habitats. Areas with high densities of juvenile summer flounder were associated with lower growth rates, suggesting density-dependent effects, for example, due to prey limitation. Finally, low salinity areas (<12 psu) were not supportive of summer flounder growth; this finding is consistent with Nys et al. (2015) and with our observations that juvenile summer flounder are not captured in areas with salinities < 10 psu (Tuckey and Fabrizio, *personal observation*).

Suitable thermal habitat for juvenile summer flounder was defined as waters with temperatures less than 25.9 °C, and these areas represented potential habitats; temperatures exceeding this threshold negatively affected growth of juvenile fish. Bottom-water temperatures in the Chesapeake Bay routinely exceed this threshold in summer, but by October, such occurrences are extremely rare. The proportion of the bay with suitable thermal conditions for juvenile summer flounder declined between 47 and 64% since 1996. The greatest decline in the proportion of the bay with suitable conditions occurred in August, just prior to when juvenile summer flounder begin to leave coastal systems to migrate to their offshore wintering habitats on the shelf. The loss of suitable potential habitat in August since 1996 may trigger earlier emigration by juvenile summer flounder, and could explain the declining catches observed in September, October, and November in recent years in the VIMS Juvenile Fish Trawl Survey (Tuckey and Fabrizio, *personal observation*). A greater proportion of Maryland waters tended to exceed the thermal threshold than waters in Virginia, and thus, proportionate loss of suitable potential habitat was greatest in Maryland. Changes in thermal

suitability of habitats for juvenile summer flounder were related to daily changes in the physical processes (wind direction, speed, and duration) that controlled the intrusion of offshore bottom-water into the lower Chesapeake Bay. Thermal conditions of bottom waters in the Virginia portion of the bay responded on a fine temporal scale (daily) to bottom-water intrusion, and as the climate continues to warm, atmospheric conditions are likely to change such that bottom-water intrusion events in summer may continue to decline. Also, on average, the water temperature of the Chesapeake Bay has been warming (Ding and Elmore 2015; Hinson et al. 2021). As a consequence, bottom waters in summer will continue to warm, thereby potentially amplifying the loss of suitable habitat for juvenile summer flounder. The median (annual) extent of suitable thermal habitat, however, was not related to the annual relative abundance of juvenile summer flounder, suggesting that the extent of suitable habitats was sufficient to support the population of juvenile summer flounder that use Chesapeake Bay as a nursery area. Other factors are likely contributing to observed changes in recruitment of summer flounder to the bay. We suggest these factors include changes in the availability of prey resources in nursery areas, and the northward shift in the location of offshore spawning areas for summer flounder (Perretti & Thorson 2019). Although it is unclear which factors account for the observed distributional shifts of the summer flounder population (Perretti & Thorson 2019), such a shift in the spawning location could result in the advection of newly hatched larvae to estuaries other than Chesapeake Bay.

Considerations for the Future

(1) We were unable to impute bottom DO conditions from surface DO conditions, particularly in summer, even though we adjusted our models to account for depth and time of year (e.g., stratified in summer, mixed in fall). Because DO affects not just the spatial distribution of fishes, but also their metabolic rates, growth, and reproduction (Buchheister et al. 2013; Campbell & Rice 2014; Lapointe et al. 2014; Tuckey & Fabrizio 2016; Cottingham et al. 2018), DO should be considered in models that examine the quality of nursery areas for fishes. Unfortunately, many long-term fisheries surveys that operate in the Chesapeake Bay and MD Coastal Bays either do not record *in situ* DO conditions (e.g., MD Small Trawl survey), or began doing so only in the mid-2000s (e.g., bottom DO in the MD Coastal Bays survey). We recommend continued monitoring of surface and bottom DO by the VIMS Juvenile Fish Trawl survey and the MD Coastal Bays survey, and the initiation of DO measures in surface and bottom waters by the MD Small Trawl survey. Alternatively, high-resolution coupled hydrodynamic and biogeochemical models of Chesapeake Bay could be used to hindcast bottom DO conditions at sampling sites. Currently, the resolution of these models limits their application in shallow waters, where many fisheries surveys operate. Furthermore, these models can provide hindcasts to the early 2010s, constraining the time series of fisheries catches that can be used to address climate change questions (some fisheries surveys can be queried as far back as the late 1980s). Continued progress on DO models for the bay and its tributaries will require additional sentinel sites that measure bottom DO (e.g., profiles of DO), and this is a topic of discussion among scientists and managers at the Chesapeake Bay Program.

(2) SMURFs and fyke nets were effective gears for sampling black sea bass during their residency in estuarine systems. Although juvenile summer flounder were captured effectively by fyke nets, SMURFs were not efficient samplers of the younger juveniles in estuarine nurseries in April and May. This suggests that once summer flounder undergo metamorphosis to the benthic juvenile stage, their use of the water column diminishes, and hence, the probability of capture also declines.

(3) The effects of seascape diversity and proximity to the coastal ocean were confounded in our study, but such effects may be teased apart by replicating the small-scale study in multiple coastal lagoons, selecting lagoons with different levels of seascape diversity. For example, South Bay has extensive restored seagrass beds, but Burton's Bay does not have appreciable seagrass beds, and as such, would likely be characterized by a lower seascape diversity. Other coastal bays and bayside areas (e.g., Cape Charles) could be considered for study to ensure a wide range of seascape diversity.

(4) The ES coastal sites sampled in 2019 and 2020 were located in an area of undeveloped coastal wilderness. Extrapolations of our results about seascape effects on relative abundance, recent growth, or fish body condition to juvenile summer flounder and black sea bass from coastal bays associated with developed areas are not warranted. We recommend future studies to address the role that coastal development plays in defining nursery habitat quality.

(5) With rising rates of sea-level rise in the Chesapeake Bay, and the transformation of upland areas to marshes and other wetlands, we recommend studies to compare the functional role of established and newly formed marshes. For example, the relative contribution of these areas to juvenile summer flounder abundance may be evaluated using methods from our study (recent growth, relative condition, relative abundance) and properly designed surveys that incorporate sufficient replication and effective randomization.

(6) The home ranges of juvenile summer flounder and juvenile black sea bass in the Chesapeake Bay region have not been assessed. Home range refers to the area used by fishes for daily activities such as foraging and sheltering (Nagelkerken et al. 2015), and in some species, fish body size affects home range size (larger fish have larger home ranges; Kramer and Chapman 1999). Others have reported home ranges that are invariant to fish size (e.g., Lowe et al. 2003; Afonso et al. 2008; Bellquist et al. 2008; Farmer and Ault 2011; Fabrizio et al. 2014). Here, we suggest that home range size may be a function of seascape complexity and diversity. In general, such a relationship has not been studied for fishes, but could provide a spatial context for consideration of baywide restoration efforts (e.g., seagrass restoration) and formation of marshes in response to sea-level rise.

Acknowledgments

We thank the many field and lab assistants who supported our research in the Piankatank River and the Eastern Shore: Chris Bentley, Destiny Blow, Jack Buchanan, Nick Coleman, Jasmine

Evans, Sean Fate, Anna Hartman, Darian Kelley, PJ LeBel, John Leonard, Connor Lovett, Katie Nickerson, Matthew Oliver, Dylan Orlando, Daniel Royster, Edward Smith, Rebecca Smith, Edward Smith, Benjamin Szykman, Braeden Thompson, Kirsten Travis, and Connor Van Vorren. A special appreciation is extended to Charlie Jordan who provided field support to Shannon Smith during the COVID-19 epidemic. We appreciate the many field scientists from MD DNR and VIMS who collected the fisheries data from the Chesapeake Bay and coastal bays. We thank Chris Walstrum (MD DNR) and Angel Willey (MD DNR) for providing data from the MD Small Trawl Survey and the MD Coastal Bays Survey. The VIMS Juvenile Fish Trawl survey was supported by funds from the Virginia Marine Resources Commission, the US Fish & Wildlife Service, and NOAA – Fisheries. Breanna Maldonado (VIMS) compiled and collated wind speed and direction data in support of BWI index calculation. Tamia Rudnicky (VIMS Center for Coastal Resource Management) and Marcia Berman (VIMS Center for Coastal Resource Management) provided GIS files; we appreciate all the VIMS CCRM scientists who collected and digitized these spatial data. We are grateful to Melissa Southworth (VIMS) for assistance in identifying viable Piankatank oyster sites and for oyster GIS data consultations. Tracey Saxby and Jane Thomas (Integration and Application Network) provided the black sea bass and summer flounder artwork (ian.umces.edu/media-library). We appreciate Andrew Larkin (NOAA Program Officer) for working with us during the COVID-19 pandemic to ensure continuity of research. Finally, we acknowledge funding for this study from the Fisheries Habitat Conservation Program Office, NOAA Fisheries (award NA18NMF4570254 to VIMS).

References

Able, K. W., M. P. Fahay, & G. R. Shepherd. 1995. Early life history of black sea bass in the Mid-Atlantic Bight and a New Jersey estuary. Fish Bull 93: 429-445.

Able, K.W. & M. P. Fahay. 1998a. *Centropristis striata* (Linneaus) Black sea bass. Pages 152-156 in The first year of life of estuarine fishes in the Middle Atlantic Bight. Rutgers University Press, New Jersey.

Able, K.W. & M. P. Fahay. 1998b. *Paralichthys dentatus* (Linneaus) Summer flounder. Pages 240-245 in The first year of life of estuarine fishes in the Middle Atlantic Bight. Rutgers University Press, New Jersey.

Able, K. W., & L. S. Hales, Jr. 1997. Movements of juvenile black sea bass *Centropristis striata* (Linnaeus) in a southern New Jersey estuary. J Exp Mar Bio Eco 213: 153-167.

Afonso, P., J. Fontes, K. N. Holland, & R. S. Santos. 2008. Social status determines behavior and habitat usage in a temperate parrotfish: implications for marine reserve design. Mar Ecol Prog Ser 359: 215–227.

Ammann, A. J. 2004. SMURFs: standard monitoring units for the recruitment of temperate reef fishes. J Exp Mar Bio Eco 299: 135-154.

Bates, D., M. Mächler, B. Bolker, & S. Walker. 2015. Fitting linear mixed-effects models using lme4. J of Stat Softw 1: 1–48.

Behan, J., B. Li, & Y. Chen. 2021. Examining scale dependent environmental effects on American lobster (*Homarus americanus*) spatial distribution in a changing Gulf of Maine. Front Mar Sci 8:680541.

Bellquist, L. F., C. G. Lowe, & J. E. Caselle. 2008. Fine-scale movement patterns, site fidelity, and habitat selection of ocean whitefish (*Caulolatilus princeps*). Fish Res 91: 325–335.

Bland, J.M. & D.G. Altman. 1986. Statistical methods for assessing agreement between two methods of clinical measurement. Lancet 1:307-310.

Buchheister, A., C. F. Bonzek, J. Gartland, & R. J. Latour. 2013. Patterns and drivers of the demersal fish community of Chesapeake Bay. Mar Ecol Progr Ser 481: 161-180.

Burke, J.S. 1995. Role of feeding and prey distribution of summer and southern flounder in selection of estuarine nursery habitats. J Fish Biol 47:355-366

Burnham, K. P. & D. R. Anderson. 2002. Model selection and multimodel inference: a practical information-theoretic approach, 2nd edition. Springer-Verlag, New York, New York.

Campbell, L. A., & J. A. Rice. Effects of hypoxia-induced habitat compression on growth of juvenile fish in the Neuse River estuary, North Carolina, USA. Mar Ecol Progr Ser 497: 199-213.

Conn, P. B. 2010. Hierarchical analysis of multiple noisy abundance indices. Can J Fish Aqua Sci 67: 108-120.

Cottingham, A., P. Huang, M. R. Hipsey, N. G. Hall, E. Ashworth, J. Williams, & I. C. Potter. 2018. Growth, condition, and maturity schedules of an estuarine fish species change in estuaries following increased hypoxia due to climate change. Ecol Evol 8: 7111-7130.

Cristiani J., E. Rubidge, C. Forbes, B. Moore-Maley, & M. I. O'Connor. 2021. A biophysical model and network analysis of invertebrate community dispersal reveals regional patterns of seagrass habitat connectivity. Front Mar Sci 8:717469.

Curran, M. C. & K. W. Able. 2002. Annual stability in the use of coves near inlets as settlement areas for winter flounder (*Pseudopleuronectes americanus*). Est 25: 227-234.

Day, Jr., J. W., C. A. S. Hall, W. M. Kemp, & A. Yáñez-Arancibia. 1989. Estuarine ecology. John Wiley & Sons, New York.

Ding, H., & A. J. Elmore. 2015. Spatio-temporal patterns in water surface temperature from Landsat time series data in the Chesapeake Bay, U.S.A. Remote Sensing of Environment 168: 335-348.

Fabrizio, M. C., M. J. Henderson, K. Rose, & P. Petitgas. 2022. Editorial: Habitat and distribution models of marine and estuarine species: Advances for a sustainable future. Front Mar Sci 9:1050548.

Fabrizio, M. C., J. P. Manderson, & J. P. Pessutti. 2014. Home range and seasonal movements of black sea bass (*Centropristis striata*) during their inshore residency at a reef in the mid-Atlantic Bight. Fish Bull 112: 82-97.

Fabrizio, M. C., T. D. Tuckey, A. J. Bever, & M. L. MacWilliams. 2021. The extent of seasonally suitable habitats may limit forage fish production in a temperate estuary. Front Mar Sci 8: 706666.

Farmer, N. A., & J. S. Ault. 2011. Grouper and snapper movements and habitat use in Dry Tortugas, Florida. Mar Ecol Prog Ser 433: 169–184.

Fletcher, D. 2008. Confidence intervals for the mean of the delta-lognormal distribution. Environ Ecol Stat 15: 175-189.

Fodrie, F. J., L. A. Levin, & A. J. Lucas. 2009. Use of population fitness to evaluate the nursery function of juvenile habitats. Mar Ecol Prog Ser 385:39-49.

Foley, M. M., & 20 coauthors. 2010. Guiding ecological principles for marine spatial planning. Mar Pol 34: 955-966.

Furey, N. B. & J. R. Rooker. 2013. Spatial and temporal shifts in suitable habitat of juvenile southern founder (*Paralichthys lethostigma*). J Sea Res 76: 161-169

Gain, I. E., R. A. Brewton, M. M. R. Robillard, K. D. Johnson, D. L. Smee, & G. W. Stuntz. 2017. Macrofauna using intertidal oyster reef varies in relation to position within the estuarine habitat mosaic. Mar Bio 164: 8.

Gedan, K.B., R. Epanchin-Niell, & M. Qi. 2020. Rapid land cover change in a submerging coastal county. Wetlands 40:1717-1728.

Grabowski, J. H., & 6 coauthors. 2018. Habitat associations of juvenile cod in nearshore waters. Rev Fish Sci & Aqua 26: 1-14.

Hales, L. S., & K. W. Able. 1995. Effects of oxygen concentration on somatic and otolith growth rates of juvenile black sea bass. Pages 135–154 in D.H. Secor, J.M. Dean and S.M. Campana, eds., Recent developments in fish otolith research. University of South Carolina Press, Columbia, SC.

Harding, J. M., & R. Mann. 2003. Influence of habitat on diet and distribution of striped bass (*Morone saxatilis*) in a temperate estuary. Bull Mar Sci 72: 841–851.

Hare, J. A., S. Thorrold, H. Walsh, C. Reiss, A. Valle-Levinson, & C. Jones. 2005. Biophysical mechanisms of larval fish ingress into Chesapeake Bay. Mar Ecol Prog Ser 303: 295-310.

Hinson, K.E., M.A.M. Friedrichs, P. St-Laurent, F. Da, & R.G. Najjar. 2021. Extent and causes of Chesapeake Bay warming. Journal of the American Water Resources Association. https://doi.org/10.1111/1752-1688.12916.

Holmquist, J.R., L. N. Brown, & G. M. MacDonald. 2021. Localized scenarios and latitudinal patterns of vertical and lateral resilience of tidal marshes to sea-level rise in the contiguous United States. Earth's Future 9, e2020EF001804.

Hubert, W.A., & M.C. Fabrizio. 2007. Relative abundance and catch per unit effort. Pages 279 – 326 in C.S. Guy & M.L Brown, eds. Analysis and interpretation of freshwater fisheries data. American Fisheries Society.

Johnson, A. F., S. R. Jenkins, J. G. Hiddink, & H. Hinz. 2013. Linking temperate demersal fish species to habitat: scales, patterns and future directions. Fish & Fish 14: 256-280.

Karp, M. A., R. D. Seitz, & M. C. Fabrizio. 2018. Faunal communities on restored oyster reefs: effects of habitat complexity and environmental conditions. Mar Ecol Prog Ser 590: 35-51.

Kendall, A. W., Jr. 1972. Descriptions of black sea bass larvae and their occurrences north of Cape Lookout, North Carolina. Fish Bull 70: 1243-1260.

Kennish, M. J. 2015. Coastal lagoons. Chapter 5 in M. J. Kennish, ed., Encyclopedia of Estuaries. Springer.

Kennish, M. J. & H. W. Paerl. 2010. Coastal lagoons: critical habitats of environmental change. Chapter 1 in Kennish, M. J., and H. W. Paerl, eds., Coastal lagoons: critical habitats of environmental change. CRC Press, Taylor & Francis Group, Boca Raton, FL.

Kirwan, M. L., D. C. Walters, W. G. Reay, & J. A. Carr. 2016. Sea level driven marsh expansion in a coupled model of marsh erosion and migration. Geophys Res Lett 43: 4366-4373.

Kramer, D. L., & M. R. Chapman. 1999. Implications of fish home range size and relocation for marine reserve function. Env Biol Fishes 55: 65-79.

Lapointe, D., W. K. Vogelbein, M. C. Fabrizio, D. T. Gauthier, & R. W. Brill. 2014. Temperature, hypoxia, and mycobacteriosis: effects on adult striped bass *Morone saxatilis* metabolic performance. Dis Aquat Org 108: 113-127.

LePape, O., F. Chauvet, S. Mahevas, P. Lazure, D. Guerault, & Y. Desaunay. 2003. Quantitative description of habitat suitability for the juvenile common sole in the Bay of Biscay (France) and the contribution of different habitats to the adult population. J Sea Res 50: 139-149.

LePape, O., L. Baulier, A. Cloarec, J. Martin, F. Le Loc'h, & Y. Desaunay. 2007. Habitat suitability for juvenile common sole in the Bay of Biscay: A quantitative description using indicators based on epibenthic fauna. J Sea Res 57: 126-136.

Li, C., L. Ciannelli, M. Bancroft, J. Rooker, C. Ryer, & H. Liu. 2022. Interplay of temperature and hypoxia in habitat quality for a juvenile demersal fish in a coastal upwelling system. Can J Fish Aquat Sci 79: 1667-1680.

Lindquist, D. G., & 7 coauthors. 1994. Reef fish stomach contents and prey abundance on reef and sand substrata associated with adjacent artificial and natural reefs in Onslow Bay, North Carolina. Bull Mar Sci 55:308-318.

Lloret, J. G. Shulman, & R. M. Love. 2014. Condition and health indicators of exploited marine fishes. John Wiley, Chichester, UK.

Lo, N. C., L. D. Jacobson, & J. L. Squire. 1992. Indices of relative abundance from fish spotter data based on delta-lognormal models. Can J Fish Aquat Sci 49: 2515-2526.

Lowe, C. G., D. T. Topping, D. P. Cartamil, & Y. P. Papastamatiou. 2003. Movement patterns, home range, and habitat utilization of adult kelp bass *Paralabrax clathratus* in a temperate no-take marine reserve. Mar Ecol Prog Ser 256: 205–216.

Manderson, J. P., & 8 coauthors. 2002. Spatial dynamics of habitat suitability for the growth of newly settled winter flounder in an estuarine nursery. Mar Ecol Prog Ser 228: 227-239.

Manderson, J. P., J. Pessutti, J. G. Hilbert, & F. Juanes. 2004. Shallow water predation risk for a juvenile flatfish (winter flounder; *Pseudopleuronectes americanus*, Walbaum) in a northwest Atlantic estuary. J Exp Mar Biol Ecol 304:137–157.

Mann, R., M. Berman, J. Wesson, M. Southworth & T. Rudnicky. 2021. Expanding Virginia's oyster industry while minimizing user conflict. Final Report submitted to Virginia Coastal Zone Managment Program, Department of Environmental Quality, Richmond, VA. https://cmap2.vims.edu/OysterInfoToolVa/

McBride, R.S., M.K. Tweedie, & K. Oliveira. 2018. Reproduction, first-year growth, and expansion of spawning and nursery grounds of black sea bass (*Centropristis striata*) into a warming Gulf of Maine. Fish B-NOAA 116: 323-336.

Molino, G.D., J.A. Carr, N.K. Ganju, & M.L. Kirwan. 2022. Variability in marsh migration potential determined by topographic rather than anthropogenic constraints in the Chesapeake Bay region. Limnol Oceanogr-Letters 7:321-331.

Moser, J., & G. R. Shepherd. 2009. Seasonal distribution and Movement of black sea bass (*Centropristis striata*) in the Northwest Atlantic as determined from a mark-recapture Experiment. J Northw Atl Fish Sci 40: 17–28.

Murdy, E. O., R. S. Birdsong & J. A. Musick. 1997. Fishes of Chesapeake Bay. Smithsonian Institution Press.

Musick, J. A., & L. P. Mercer. 1977. Seasonal distribution of black sea bass in the Mid-Atlantic Bight with comments on the ecology and fisheries of the species. Tran Amer Fish Soc 106: 12-25.

Nagelkerken, I., M. Sheaves, R. Baker, & R. M. Connolly. 2015. The seascape nursery: a novel approach to identify and manage nurseries for coastal marine fauna. Fish & Fish 16: 362-371.

Najjar, R. G., C. R. Pyke, M. B. Adams, D. Breitberg, C. Hershner, M. Kemp, R. Howarth, M. R. Mulholland, M. Paolisso, D. Secor, K. Sellner, D. Wardrop, & R. Wood. 2010. Potential climate-change impacts on the Chesapeake Bay. Est Coast Shelf Sci 86: 1-20.

Norcross, B. L. & D. M. Wyanski. 1994. Interannual variation in the recruitment pattern and abundance of age-0 summer flounder, *Paralichthys dentatus*, in Virginia estuaries. Fish Bull 92: 591-598.

Nys, L., M. C. Fabrizio, & T. D. Tuckey. 2015. Multi-decadal variation in size of juvenile summer flounder (*Paralichthys dentatus*) in Chesapeake Bay. J Sea Res 103: 50-58.

Olson, A. M., M. Hessing-Lewis, D. Haggarty, & F. Juanes. 2019. Nearshore seascape connectivity enhances seagrass meadow nursery function. Ecol Appl e01897

Packer, D. B., S. J. Griesbach, P. L. Berrien, C. A. Zetlin, D. L. Johnson, & W. W. Morse. 1999. Essential fish habitat source document: Summer flounder, *Paralichthys dentatus*, life history and habitat characteristics. NOAA Technical Memorandum NMFS-NE-151.

Perretti, C. T., & J. T. Thorson. 2019. Spatio-temporal dynamics of summer flounder (*Paralichthys dentatus*) on the Northeast US shelf. Fish Res 215:62-68

Peters, R., & P. Chigbu. 2017. Spatial and temporal patterns of abundance of juvenile black sea bass (*Centropristis striata*) in Maryland coastal bays. Fish Bull 115: 504-516.

Peterson, M. S. 2003. A conceptual view of environment-habitat-production linkages in tidal river estuaries. Rev Fish Sci 11: 291-313.

Pfirrmann, B. W. & R. D. Seitz. 2019. Ecosystem services of restored oyster reefs in a Chesapeake Bay tributary: abundance and foraging of estuarine fishes Mar Ecol Prog Ser 628: 155-169.

Primo, A. L., U. M. Azeiteiro, S. C. Marques, F. Martinho, J. Baptista, & M. A. Pardal. 2013. Colonization and nursery habitat use patterns of larval and juvenile flatfish species in a small temperate estuary. J Sea Res 76: 126-134.

Reuchlin-Hugenholtz, E., N. L. Shackell, & J. A. Hutchings. 2016. Spatial reference points for groundfish. ICES J Mar Sci 73: 2468-2478.

Ross, P.G. & M. W. Luckenbach. 2009. Population assessment of Eastern oysters in the seaside coastal bays. Final report submitted to NOAA-Va Coastal Zone Management Program. 101 pp.

Rountree, R. A. & K. W. Able. 1992. Foraging habits, growth, and temporal patterns of salt-marsh creek habitat use by young-of-the-year summer flounder in New Jersey. Trans Amer Fish Soc 121: 765-776.

Roy, E. M., J. M. Quattro, & T. W. Greig. 2012. Genetic management of Black sea bass: influence of biogeographic barriers on population structure. Mar Coast Fish 4: 391-402.

Rubec, P. J., R. Kiltie, E. Leone, R. O. Flamm, L. McEachron, & C. Santi. 2016. Using delta-generalized additive models to predict spatial distributions and population abundance of juvenile pink shrimp in Tampa Bay, Florida. Mar Coast Fish 8: 232-243.

Sackett, D. K., K. W. Able, & T. M. Grothues. 2008. Habitat dynamics of summer flounder *Paralichthys dentatus* within a shallow USA estuary, based on multiple approaches using acoustic telemetry. Mar Eco Prog Ser 364:199–212.

Scharf, F. S., J. P. Manderson, & M. C. Fabrizio. 2006. The effects of seafloor habitat complexity on survival of juvenile fishes: species-specific interactions with structural refuge. J Exp Mar Bio Eco 335:167-176.

Schieder, N. W., D. C. Walters, & M. L. Kirwan. 2018. Massive upland to wetland conversion compensated for historical marsh loss in Chesapeake Bay, USA. Est Coasts 41: 940-951.
Schloesser, R. W., & M. C. Fabrizio. 2016. Temporal dynamics of condition for estuarine fishes in their nursery habitats. Mar Ecol Prog Ser 557: 2017-219.
Schloesser, R. W., & M. C. Fabrizio. 2019. Nursery habitat quality assessed by the condition of juvenile fishes: not all estuarine areas are equal. Est Coast 42: 548-566.
Schwartzkopf, B. D., L. Ciannelli, J. C. Garza, & S. A. Heppell. 2021. Growth of juvenile black rockfish (*Sebastes melanops*) during estuarine residence. Environ Biol Fish 104:851–865.
Steimle, F.W. & W. Figley. 1996. The importance of artificial reef epifauna to black sea bass diets in the Middle Atlantic Bight. N Am J Fish Mange 16:433-439.
Steimle, F.W., C.A. Zetlin, P.L. Berrien, & S. Chang. 1999. Essential fish habitat source document: Black sea bass, *Centropristis striata*, Life history and habitat characteristics. National Ocean and Atmospheric Administration Technical Memorandum NMFS-NE-143.
Szedlmayer, S. T., & K. W. Able. 1992. Validation studies of daily increment formation for larval and juvenile summer flounder, *Paralichthy dentatus*. Can J Fish Aq Sci 49: 1856-1862.
Szedlmayer, S. T., & K. W. Able. 1993. Ultrasonic telemetry of age-0 summer flounder, *Paralichthys dentatus,* movements in a southern New Jersey estuary. Copeia 1993(3):728.
Taylor, D. L., J. McNamee, J. Lake, C. L. Gervasi, & D. G. Palance. 2016. Juvenile winter flounder and summer flounder utilization of southern New England nurseries: comparisons among estuarine, tidal river, and coastal lagoon shallow-water habitats. Est Coast 39: 1505-1525.
Tuckey, T. D., & M. C. Fabrizio. 2013. Influence of survey design on fish assemblages: implications from a study in Chesapeake Bay tributaries. Trans Amer Fish Soc 142:957-973.
Tuckey, T. D., & M. C. Fabrizio. 2016. Variability in fish tissue proximate composition is consistent with indirect effects of hypoxia in Chesapeake Bay tributaries. Mar Coast Fish 8: 1-15.
Tuckey, T. D. & M. C. Fabrizio. 2022. Estimating relative juvenile abundance of ecologically important finfish in the Virginia portion of Chesapeake Bay. Final report to Virginia Marine Resources Commission.
VanderKooy, S., J. Carroll, S. Elzey, J. Gilmore, & J. Kipp, eds. 2020. A practical handbook for determining the ages of Gulf of Mexico and Atlantic Coast fishes. Third Edition. Gulf States Marine Fisheries Commission Publication No. 300.
Vasconcelos, R. P., P. Reis-Santos, V. Fonseca, M. Ruano, S. Tanner, M. J. Costa, & H. N. Cabral. 2009. Juvenile fish condition in estuarine nurseries along the Portuguese coast. Estuar Coast Shelf S 82:128-138
Vasconcelos, R. P., & 7 coauthors. 2010. Nursery use patterns of commercially important marine fish species in estuarine systems along the Portuguese coast. Est Coast Shelf Sci 86: 613-624.
Wood, S.N. 2011. Fast stable restricted maximum likelihood and marginal likelihood estimation of semiparametric generalized linear models. J R Stat Soc B 73: 3-36.
Woodland, R. J., D. H. Secor, M. C. Fabrizio, & M. J. Wilberg. 2012. Comparing the nursery role of inner continental shelf and estuarine habitats for temperate marine fishes. Est Coast Shelf Sci 99: 61-73.
Ye, F. & 10 coauthors. 2018. A 3D unstructured-grid model for Chesapeake Bay: importance of bathymetry. Ocean Mod 127: 16-39.

Table 1. Monthly length (mm) thresholds for juvenile (age-0) summer flounder and juvenile black sea bass.

	April	**May**	**June**	**July**	**August**	**September**	**October**
Summer flounder	0-100	0-140	0-170	0-200	0-225	0-250	0-275
Black sea bass	35-110	50-110	65-150	75-175	85 - 200	95 - 220	105 - 240

Table 2. Number of tows during which environmental conditions were measured at the time of fish sampling, imputed from linear regression, or estimated by hindcasts of the hydrodynamic model for April - October. Note that the domain of the hydrodynamic model includes Chesapeake Bay and tributaries only, therefore, hindcast estimates are not available for the MD Coastal Bays. Additionally, the hydrodynamic model temporal domain is 1996 to 2019. The MD Coastal Bays Survey did not record environmental conditions prior to 2006 (though records of fish catches extend to 1989). Sampling records for the MD Small Trawl Survey are available beginning in 1991; this survey sampled from May to September. The VIMS Trawl Survey sampled fishes and recorded environmental conditions from 1989 to 2019.

	Apr	May	Jun	Jul	Aug	Sep	Oct
	MD Coastal Bays: 2006 – 2019 (n=4,308)						
	Bottom temperature						
Observed during sampling	280	280	280	280	280	280	280
Imputed from linear regression	332	332	336	330	338	317	338
Hindcast from hydrodynamic model	--	--	--	--	--	--	--
Missing surface temperature	8	2	8	0	2	3	2
Total	620	614	624	610	620	600	620
	Bottom salinity						
Observed during sampling	280	280	280	280	280	280	280
Imputed from linear regression	330	333	336	325	337	316	338
Hindcast from hydrodynamic model	--	--	--	--	--	--	--
Missing surface salinity	10	1	8	5	3	4	2
Total	620	614	624	610	620	600	620
	MD Small Trawl: 1991 – 2019 (n=11,439)						
	Bottom temperature						
Observed during sampling	0	0	0	0	0	0	0
Imputed from linear regression	0	143	164	156	112	133	0
Hindcast from hydrodynamic model	0	1,862	2,340	2,162	2,186	2,100	0
Missing surface temperature	0	0	8	12	36	25	0
Total	0	2,005	2,512	2,330	2,334	2,258	0
	Bottom salinity						
Observed during sampling	0	0	0	0	0	0	0
Imputed from linear regression	0	122	164	155	106	123	0
Hindcast from hydrodynamic model	0	1,862	2,340	2,162	2,186	2,100	0
Missing surface salinity	0	21	8	13	42	35	0
Total	0	2,005	2,512	2,330	2,334	2,258	0

	VIMS Trawl: 1989 – 2019 (n=21,197)						
	Bottom temperature						
Observed during sampling	2,854	3,021	3,060	3,042	2,976	3,051	3,061
Imputed from linear regression	8	17	3	20	36	8	7
Hindcast from hydrodynamic model	0	0	0	0	0	0	0
Missing surface temperature	4	5	1	6	3	12	2
Total	2,866	3,043	3,064	3,068	3,015	3,071	3,070
	Bottom salinity						
Observed during sampling	2,854	3,003	3,057	3,026	2,989	3,034	3,060
Imputed from linear regression	6	18	4	19	24	14	8
Hindcast from hydrodynamic model	0	0	0	0	0	0	0
Missing surface salinity	6	22	3	23	2	23	2
Total	2,866	3,043	3,064	3,068	3,015	3,071	3,070

Table 3. Physicochemical parameters measured at the time of gear retrieval at Eastern Shore and Piankatank River sites in 2019 and 2020 for marsh, oyster, soft-bottom, and seagrass habitats. Values are means and standard error of the mean (in parentheses); values were averaged across replicate sampling sites within each habitat type. DO is dissolved oxygen concentration.

Habitat type	2019			2020		
	Temperature (°C)	Salinity (psu)	DO (mg/L)	Temperature (°C)	Salinity (psu)	DO (mg/L)
	Eastern Shore					
Marsh	23.6 (0.8)	31.1 (0.1)	6.9 (0.2)	23.3 (0.9)	30.9 (0.2)	7.3 (0.2)
Oyster	23.2 (0.8)	31.0 (0.1)	6.9 (0.2)	23.3 (0.9)	31.1 (0.1)	7.2 (0.2)
Soft-bottom	23.1 (0.8)	31.0 (0.1)	7.0 (0.2)	23.0 (0.9)	31.0 (0.1)	7.2 (0.2)
Seagrass	23.0 (0.8)	31.0 (0.1)	8.1 (0.3)	22.8 (0.9)	31.1 (0.1)	7.9 (0.2)
	Piankatank River					
Marsh	24.5 (0.8)	13.2 (0.5)	9.2 (0.3)	23.9 (0.9)	17.5 (0.1)	8.2 (0.2)
Oyster	24.2 (0.8)	13.2 (0.5)	8.6 (0.4)	23.7 (0.9)	17.6 (0.1)	7.6 (0.2)
Soft-bottom	23.6 (0.8)	13.3 (0.5)	8.7 (0.3)	23.4 (0.9)	17.7 (0.1)	7.9 (0.2)
Seagrass	23.8 (0.8)	13.1 (0.5)	9.6 (0.3)	23.2 (0.9)	17.4 (0.2)	8.3 (0.2)

Table 4. Metrics describing the seascape characteristics for each habitat type in Eastern Shore and Piankatank River areas, 2019-2020. "Distance to" denotes the distance (m) to the nearest specified habitat feature. Distance to open water refers to the distance between each sampling site and the Atlantic Ocean or Chesapeake Bay. Values are means and standard error of the mean (SE); distances and depths were averaged across replicate sampling sites in each habitat type.

Habitat type	Distance to open water (m)	Distance to marsh creek (m)	Distance to oysters (m)	Distance to seagrass (m)	Habitat diversity within 500 m	Habitat diversity within 1 km	Depth (m)
	Eastern Shore						
Marsh	3599 (952.1)	0	265 (59.9)	445.3 (113.9)	0.39 (0.07)	0.43 (0.05)	0.97 (0.13)
Oyster	3121.4 (1019.7)	237 (37.8)	0	362.7 (79.5)	0.27 (0.08)	0.42 (0.03)	1.01 (0.16)
Soft-bottom	3648.1 (1037.7)	214.4 (27.9)	167 (46.3)	394.3 (154.3)	0.3 (0.05)	0.42 (0.04)	1.03 (0.14)
Seagrass	3145.6 (527.7)	997.8 (126.7)	840 (72.3)	0	0.18 (0.09)	0.38 (0.03)	1.53 (0.05)
	Piankatank River						
Marsh	2589.8 (312.3)	6.7 (1.0)	827.5 (124.7)	1200.6 (389.8)	0.12 (0.05)	0.07 (0.02)	0.14 (0.02)
Oyster	1947 (607.9)	418 (142.8)	0	1102.2 (256.3)	0.07 (0.03)	0.07 (0.02)	0.59 (0.05)
Soft-bottom	1477.2 (699.5)	638 (92.4)	906.2 (113.4)	699.3 (262.2)	0.04 (0.02)	0.08 (0.01)	0.52 (0.05)
Seagrass	2040.5 (563.8)	1222.5 (178.3)	1145.2 (120.4)	0	0.19 (0.04)	0.13 (0.02)	0.69 (0.23)

Table 5. Cumulative counts of fish species and individuals captured in SMURFs and fyke nets during the field study in the Eastern Shore and Piankatank River, 2019-2020. Site refers to the replicate site location within a habitat type.

Eastern Shore				**Piankatank River**			
Habitat	Site	# Fish	# Species	Habitat	Site	# Fish	# Species
Marsh	A	2817	31	Marsh	A	3047	32
Marsh	B	1560	30	Marsh	B	4791	37
Marsh	C	1720	32	Marsh	C	2587	32
All marsh sites		**6097**	**41**	**All marsh sites**		**10425**	**43**
Oyster	A	7401	34	Oyster	A	4013	27
Oyster	B	4808	25	Oyster	B	1629	29
Oyster	C	619	23	Oyster	C	2339	28
All oyster sites		**12828**	**38**	**All oyster sites**		**7981**	**39**
Seagrass	A	2665	28	Seagrass	A	778	22
Seagrass	B	3393	27	Seagrass	B	572	24
Seagrass	C	1219	25	Seagrass	C	5179	31
All seagrass sites		**7277**	**40**	**All seagrass sites**		**6529**	**37**
Soft-bottom	A	2641	31	Soft-bottom	A	720	23
Soft-bottom	B	1807	25	Soft-bottom	B	2196	29
Soft-bottom	C	605	23	Soft-bottom	C	3392	33
All soft-bottom sites		**5035**	**36**	**All soft-bottom sites**		**6308**	**43**
All Sites and Habitats		**31,255**	**58**	**All Sites and Habitats**		**31,243**	**62**

Table 6. Comprehensive list of fishes and number of individuals captured in SMURFs and fyke nets during the small-scale field study (2019-2020) in the Eastern Shore and Piankatank River. Rows are in descending order of the number of individuals captured.

Eastern Shore			Piankatank River		
Species	**Common name**	**N**	**Species**	**Common name**	**N**
Anchoa mitchilli	bay anchovy	17510	*Menidia menidia*	Atlantic silverside	10123
Bairdiella chrysoura	silver perch	5471	*Anchoa mitchilli*	bay anchovy	8015
Leiostomus xanthurus	spot	2520	*Bairdiella chrysoura*	silver perch	6060
Membras martinica	rough silverside	1588	*Opisthonema oglinum*	Atlantic thread herring	1366
Fundulus heteroclitus	mummichog	1431	*Fundulus heteroclitus*	mummichog	1318
Opisthonema oglinum	Atlantic thread herring	909	*Brevoortia tyrannus*	Atlantic menhaden	805
Micropogonias undulatus	Atlantic croaker	309	*Leiostomus xanthurus*	spot	791
Paralichthys dentatus	summer flounder	181	*Menidia beryllina*	inland silverside	456
Centropristis striata	black seabass	137	*Anchoa hepsetus*	striped anchovy	320
Orthopristis chrysoptera	pigfish	134	*Trinectes maculatus*	hogchoker	289
Cynoscion nebulosus	spotted seatrout	115	*Chaetodipterus faber*	Atlantic spadefish	240
Brevoortia tyrannus	Atlantic menhaden	112	*Morone americana*	white perch	218
Alosa aestivalis	blueback herring	104	*Fundulus majalis*	striped killifish	160
Lagodon rhomboides	pinfish	104	*Anguilla rostrata*	American eel	138
Anguilla rostrata	American eel	78	*Menticirrhus americanus*	southern kingfish	129
Trinectes maculatus	hogchoker	71	*Micropogonias undulatus*	Atlantic croaker	120
Chaetodipterus faber	Atlantic spadefish	70	*Gobiosoma bosc*	naked goby	75
Gobiosoma bosc	naked goby	49	*Alosa pseudoharengus*	alewife	73
Cynoscion regalis	weakfish	39	*Paralichthys dentatus*	summer flounder	69
Fundulus majalis	striped killifish	36	*Cynoscion nebulosus*	spotted seatrout	54
Opsanus tau	oyster toadfish	31	*Synodus foetens*	inshore lizardfish	52
Symphurus plagiusa	blackcheek tonguefish	29	*Morone saxatilis*	striped bass	47
Sphyraena borealis	northern sennet	25	*Gobiesox strumosus*	skilletfish	42
Menticirrhus americanus	southern kingfish	18	*Orthopristis chrysoptera*	pigfish	38
Synodus foetens	inshore lizardfish	16	*Lagodon rhomboides*	pinfish	36
Caranx hippos	crevalle jack	15	*Cynoscion regalis*	weakfish	28
Menticirrhus saxatilis	northern kingfish	14	*Sciaenops ocellatus*	red drum	18
Mustelus canis	smooth dogfish	14	*Symphurus plagiusa*	blackcheek tonguefish	16
Pogonias cromis	black drum	13	*Sphoeroides maculatus*	northern puffer	16
Sphoeroides maculatus	northern puffer	12	*Opsanus tau*	oyster toadfish	16
Syngnathus fuscus	northern pipefish	11	*Strongylura marina*	Atlantic needlefish	14
Strongylura marina	Atlantic needlefish	8	*Pogonias cromis*	black drum	14
Selene vomer	lookdown	8	*Centropristis striata*	black seabass	12
Archosargus probatocephalus	sheepshead	8	*Syngnathus fuscus*	northern pipefish	10
Prionotus carolinus	northern searobin	6	*Cyprinodon variegatus*	sheepshead minnow	10
Sciaenops ocellatus	red drum	6	*Lutjanus griseus*	gray snapper	9
Carcharhinus plumbeus	sandbar shark	6	*Hippocampus erectus*	lined seahorse	7
Menidia menidia	Atlantic silverside	5	*Membras martinica*	rough silverside	5
Mugil cephalus	striped mullet	5	*Lepophidium brevibarbe*	blackedge cusk-eel	3
Pomatomus saltatrix	bluefish	4	*Syngnathus floridae*	dusky pipefish	3

Hypsoblennius hentz	feather blenny	4	*Hyporhamphus meeki*	halfbeak	3
Morone saxatilis	striped bass	4	*Fundulus diaphanus*	banded killifish	2
Seriola zonata	banded rudderfish	3	*Alosa aestivalis*	blueback herring	2
Lutjanus griseus	gray snapper	3	*Caranx hippos*	crevalle jack	2
Eucinostomus argenteus	spotfin mojarra	3	*Mugil cephalus*	striped mullet	2
Caranx crysos	blue runner	2	*Pomatomus saltatrix*	bluefish	1
Cyprinodon variegatus	sheepshead minnow	2	*Peprilus triacanthus*	butterfish	1
Prionotus evolans	striped searobin	2	*Syngnathus louisianae*	chain pipefish	1
Trichiurus lepturus	Atlantic cutlassfish	1	*Hypsoblennius hentz*	feather blenny	1
Fistularia commersonii	bluespotted cornetfish	1	*Dorosoma cepedianum*	gizzard shad	1
Peprilus triacanthus	butterfish	1	*Peprilus paru*	harvestfish	1
Hyporhamphus meeki	halfbeak	1	*Alosa mediocris*	hickory shad	1
Aluterus schoepfii	orange filefish	1	*Caranx latus*	horse-eye jack	1
Trachinotus falcatus	permit	1	*Selene vomer*	lookdown	1
Etropus microstomus	smallmouth flounder	1	*Prionotus carolinus*	northern searobin	1
Dasyatis americana	southern stingray	1	*Trachinotus falcatus*	permit	1
Diplodus holbrookii	spottail pinfish	1	*Lepomis gibbosus*	pumpkinseed	1
Chilomycterus schoepfi	striped burrfish	1	*Lucania parva*	rainwater killifish	1
			Archosargus probatocephalus	sheepshead	1
			Scomberomorus maculatus	Spanish mackerel	1
			Chasmodes bosquianus	striped blenny	1
			Mugil curema	white mullet	1

Table 7. Proportion of SMURFs and fyke net sets that captured juvenile summer flounder and juvenile black sea bass in marsh, oyster, soft-bottom, or seagrass habitats at the Eastern Shore and Piankatank River sampling sites, 2019-2020. SMURFs were deployed in April and May, and fyke nets were deployed from June to October.

Habitat type	Proportion of nets with summer flounder		Proportion of nets with black sea bass	
	SMURFs	Fyke nets	SMURFs	Fyke nets
	Eastern Shore			
Marsh	0	0.542	0.14	0.15
Oyster	0	0.063	0.04	0
Soft-bottom	0	0.208	0.26	0.21
Seagrass	0	0.083	0.07	0.10
	Piankatank River			
Marsh	0	0.298	0.19	0.25
Oyster	0	0.125	0	0
Soft-bottom	0	0.146	0	0.38
Seagrass	0	0.083	0	0.04

Table 8. Mean fish size (total length, mm), standard error of the means (SE), and number (N) of juvenile summer flounder and juvenile black sea bass captured in the Eastern Shore and Piankatank River in 2019 and 2020.

Year	Mean length (SE)			
	Summer flounder	**N**	**Black sea bass**	**N**
	Eastern Shore			
2019	152.1 (9.3)	36	94.6 (2.2)	98
2020	134.3 (7.1)	51	117.4 (4.2)	31
	Piankatank River			
2019	182.9 (7.7)	45	133.3 (14.6)	9
2020	152.0 (35.2)	4	145.0 (32.6)	3

Table 9. Mean relative body condition (K_n) and mean fish size (total length, mm), of juvenile summer flounder captured in the Eastern Shore and Piankatank River in marsh, oyster, soft-bottom, and seagrass habitats, 2019-2020. Standard error of the means (SE), and number (N) are also presented.

Habitat type	**Mean K_n (SE)**	**Mean length (SE)**	**N**
	Eastern Shore		
Marsh	1.01 (0.01)	141.4 (6.5)	65
Oyster	0.96 (0.06)	124.3 (42.0)	3
Soft-bottom	1.01 (0.03)	150.3 (14.4)	14
Seagrass	0.93 (0.02)	130.8 (26.5)	5
	Piankatank River		
Marsh	1.01 (0.02)	185.4 (10.1)	26
Oyster	1.00 (0.03)	186.7 (16.9)	9
Soft-bottom	1.00 (0.02)	173.1 (22.6)	8
Seagrass	1.04 (0.03)	159.2 (23.8)	6

Table 10. Mean fish size (total length, mm), standard error of the mean (SE), and number (N) of juvenile black sea bass captured in the Eastern Shore and Piankatank River in marsh, oyster, soft-bottom, and seagrass habitats in 2019 and 2020.

Habitat type	Mean length (SE)			
	2019	N	2020	N
	Eastern Shore			
Marsh	85.2 (8.2)	14	96.0	1
Oyster	93.3 (3.5)	33	110.2 (4.9)	5
Soft-bottom	92.8 (5.5)	16	104.4 (9.2)	7
Seagrass	100.3 (2.8)	35	125.7 (5.4)	18
	Piankatank River			
Marsh	46.0	1	--	0
Oyster	149.9 (10.9)	7	126.5 (46.5)	2
Soft-bottom	--	0	--	0
Seagrass	105.0	1	182.0	1

Table 11. Comparison of models estimating juvenile summer flounder relative condition. Models fit with maximum likelihood to compare fixed effects. AIC_c = Akaike Information Criterion corrected for small sample sizes, ΔAIC_c = difference in AIC values, df denotes the degrees of freedom associated with hypothesis testing.

Model	Fixed effects	Random effects	AIC_c	ΔAIC_c	Log likelihood	df
Null	--	Site nested in area-habitat type	-243.6	0.0	124.9	3
Full	Area-Habitat type	Site nested in area-habitat type	-232.6	11.0	127.2	10

Table 12. Estimated marginal mean difference in relative condition K_n and its standard error (SE) used for comparisons of relative condition of juvenile summer flounder from the Eastern Shore (ES) and Piankatank River (PK), 2019-2020. The *t* value is the statistic used to determine significance of the difference in mean relative condition specified by the contrast (i.e., *t* tests the null hypothesis that the difference in means is 0), and P is probability of observing a more extreme test statistic under the null hypothesis.

Contrast	**Marginal mean difference in K_n (SE)**	***t***	**P**
ES vs PK	-0.07 (0.08)	-0.89	0.384
ES Marsh vs ES Seagrass	0.02 (0.03)	0.50	0.622
PK Marsh vs PK Seagrass	-0.002 (0.04)	-0.06	0.952
ES Seagrass vs PK Seagrass	0.11 (0.06)	1.81	0.073

Table 13. Mean absolute and percent differences in otolith measurements recorded by two independent readers and the total distance measured for context; these measurements were taken from otoliths of juvenile summer flounder and juvenile black sea bass collected at the Eastern Shore and the Piankatank River, 2019-2020. Means and standard errors of the mean (SE) are shown. This excludes otoliths that were co-read by both readers. Distances were measured from the otolith's edge to the 7th daily increment in microns (µm).

Otolith metrics	Summer flounder	Black sea bass
Between-reader difference in distance measured (µm)	0.91 (0.07)	1.01 (0.08)
Between-reader percent difference in distance measured (%)	8.97 (0.64)	9.13 (0.76)
Distance measured (µm)	10.25 (0.25)	11.41 (0.21)

Table 14. Ordinary least-squares regressions relating fish size (total length TL, in mm) to otolith size (microns, µm) of juvenile summer flounder and juvenile black sea bass captured from the Eastern Shore and Piankatank River, 2019-2020. Otolith size was quantified using two measures, the longitudinal maximum diameter and the edge to core radial distance. R^2 = variation explained by the model, and N = number of otoliths used to fit regressions.

Otolith measure	Model	R^2	N
Summer flounder			
Longitudinal	TL = -31.4341 + 0.095832 * longitudinal distance	0.93	115
Radial	TL = 56.5338 + 0.2662853 * radial distance	0.33	115
Black sea bass			
Longitudinal	TL = -7.7166 + 0.06004 * longitudinal distance	0.91	100
Radial	TL = 0.2751 + 0.25076 * radial distance	0.41	100

Table 15. Likelihood-based comparisons of models to estimate recent growth of juvenile summer flounder from the Eastern Shore and Piankatank River, 2019-2020. AIC_c is Akaike's Information Criterion corrected for small sample sizes, ΔAIC_c is the difference in AIC_c values between a given model and the model with the lowest AIC_c, and df denotes the degrees of freedom associated with hypothesis testing.

Model	**Fixed effects**	**Random effects**	**AIC_c**	**ΔAIC_c**	**Log likelihood**	**df**
Null	--	Sampling event	215.6	0.0	-104.7	3
Area-Habitat type	Area-Habitat type	Sampling event	224.0	8.4	-101.0	10
Full	Area-Habitat type, Length	Sampling event	226.4	10.9	-100.9	11

Table 16. Estimated marginal mean differences in recent growth (mm accrued during the 7-day period before capture) and its standard error (SE) used for comparisons of recent growth of juvenile summer flounder from the Eastern Shore (ES) and Piankatank River (PK), 2019-2020. The *t* value is the statistic used to determine significance of the difference in mean recent growth specified by the contrast (i.e., *t* tests the null hypothesis that the difference in means is 0), and P is the probability of observing a more extreme test statistic under the null hypothesis.

Contrast	**Marginal mean difference in 7-day growth (SE)**	***t***	**P**
ES vs PK	-0.54 (0.51)	-1.06	0.298
PK Marsh vs PK Soft-bottom	0.34 (0.22)	1.54	0.127
PK Marsh vs PK Seagrass	0.03 (0.26)	0.71	0.904
ES Seagrass vs PK Seagrass	0.58 (0.49)	1.18	0.239

Table 17. Mean relative body condition (K_n) of juvenile black sea bass captured in the Eastern Shore and Piankatank River in marsh, oyster, soft-bottom, and seagrass habitats, 2019-2020. Standard error of the means (SE), and number (N) are also presented.

Habitat type	**Mean K_n (SE)**	**N**
	Eastern Shore	
Marsh	1.01 (0.03)	15
Oyster	1.05 (0.03)	38
Soft-bottom	0.95 (0.03)	23
Seagrass	0.99 (0.01)	53
	Piankatank River	
Marsh	1.09	1
Oyster	1.04 (0.03)	9
Soft-bottom	--	0
Seagrass	0.98 (0.01)	2

Table 18. Likelihood-based comparisons of models to estimate relative condition (K_n) of juvenile black sea bass from the Eastern Shore, 2019-2020. Small sample size from the Piankatank River precluded inclusion of observations from those individuals in these models. AIC_c is Akaike's Information Criterion corrected for small sample sizes, ΔAIC_c is the difference in AIC_c values between a given model and the model with the lowest AIC_c, and df denotes the degrees of freedom associated with hypothesis testing.

Model	Fixed effects	Random effect	AIC_c	ΔAIC_c	Log likelihood	df
Null	--	Site nested in habitat type	-180.0	0.0	93.1	3
Habitat	Habitat type	Site nested in habitat type	-178.7	1.3	95.7	6
Year	Year	Site nested in habitat type	-178.4	1.7	93.4	4
Full	Habitat type, Year	Site nested in habitat type	-176.7	3.4	95.8	7

Table 19. Likelihood-based comparisons of models to estimate recent growth of juvenile black sea bass from the Eastern Shore, 2019-2020. Small sample size from the Piankatank River precluded inclusion of observations from those individuals in these models. AIC_c is Akaike's Information Criterion corrected for small sample sizes, ΔAIC_c is the difference in AIC_c values between a given model and the model with the lowest AIC_c, and df denotes the degrees of freedom associated with hypothesis testing.

Model	Fixed effects	Random effects	AIC_c	ΔAIC_c	Log likelihood	df
Year + Length	Year, Length	Sampling event, Site nested in habitat type	152.4	0.0	-69.8	6
Null	--	Sampling event, Site nested in habitat type	152.9	0.5	-72.2	4
Full	Habitat type, Year, Length	Sampling event, Site nested in habitat type	157.5	5.0	-68.7	9
Habitat type + Length	Habitat type, Length	Sampling event, Site nested in habitat type	158.3	5.9	-70.4	8

Table 20. Significance of seascape features for describing habitat quality (as measured by relative condition and recent growth) of juvenile summer flounder and juvenile black sea bass from the Eastern Shore and Piankatank River, 2019-2020. Results presented are from generalized additive models (GAMs) in descending order of the percent deviance explained by each predictor. Models in which the smoothed term (seascape feature) was significant are in bold. All habitat diversity and percent area seascape features were calculated within a spatial range of either 1 km for summer flounder, or 500 m for black sea bass. *F* is the *F*-statistic, P is the P value, and N is the number of observations in each model.

Model	Seascape feature	F	P	% deviance explained	N
	Summer flounder				
Relative condition	Percent area of marsh	2.690	0.084	5.42	136
	Percent area of soft-bottom	1.198	0.337	3.84	136
	Habitat diversity	1.423	0.241	3.28	136
	Distance to marsh creek	0.072	0.790	0.05	136
Recent growth	Habitat diversity	2.627	0.108	2.25	116
	Percent area of marsh	2.153	0.145	1.86	116
	Percent area of soft-bottom	1.892	0.172	1.63	116
	Distance to marsh creek	1.389	0.241	1.20	116
	Black sea bass				
Relative condition	**Percent area of oyster habitat**	**9.509**	**<0.001**	**19.70**	**141**
	Percent area of soft-bottom	1.065	0.261	2.37	141
	Distance to seagrass	1.173	0.265	2.36	141
	Distance to oyster habitat	2.963	0.087	2.09	141
	Percent area of seagrass	0.788	0.318	1.86	141
	Distance to marsh creek	2.161	0.144	1.53	141
	Percent area of marsh	1.646	0.520	1.18	141
	Habitat diversity	0.480	0.686	1.02	141
Recent growth	**Distance to seagrass**	**3.066**	**0.027**	**8.87**	**106**
	Percent area of soft-bottom	**2.708**	**0.039**	**8.77**	**106**
	Percent area of seagrass	**3.829**	**0.034**	**8.52**	**106**
	Habitat diversity	1.870	0.141	6.60	106
	Distance to marsh creek	2.556	0.113	2.40	106
	Distance to oyster habitat	2.269	0.135	2.14	106
	Percent area of marsh	1.828	0.179	1.73	106
	Percent area of oyster habitat	0.264	0.600	0.98	106

Table 21. Akaike's Information Criterion (AIC) and generalized R^2 values for multiple models fitted to juvenile summer flounder abundances from three fishery-independent surveys (MD Coastal Bays, MD Small Trawl Survey, and VIMS Juvenile Fish Trawl Survey), 1989 – 2019. Predictors considered in the models included water temperature, salinity, depth, and categorical predictors indicating sampling locations within a given distance to structure (within either 500 or 1000 m). For these models, "cs" indicates the predictor's effect was modeled as an additive cubic-spline smooth function, and "re" indicates random model terms. The model with the lowest AIC was selected as the best model and is indicated in bold. DNC indicates that the model did not converge.

Survey	Models		AIC	R^2
MD Coastal Bays				
	1	cs(Temperature) + cs(Salinity) + cs(Depth) + Struct500	45353.1	0.08
	2	cs(Temperature) + cs(Salinity) + cs(Depth) + Struct500 + re(Year)	45058.8	0.16
	3	cs(Temperature) + cs(Salinity) + cs(Depth) + Struct500 + re(Year) sigma: cs(Temperature) + cs(Salinity)	45017.9	0.32
	4	cs(Temperature) + cs(Salinity) + cs(Depth) + Struct500 + re(Year) sigma: cs(Temperature) + cs(Salinity) nu: cs(Temperature) + cs(Salinity)	44335.9	0.17
	5	**cs(Temperature) + cs(Salinity) + cs(Depth) + re(Struct500|Year) sigma: cs(Temperature) + cs(Salinity) nu: cs(Temperature) + cs(Salinity)**	**44315.0**	**0.33**
	6	cs(Temperature) + cs(Salinity) + cs(Depth) + re(Struct1000|Year) sigma: cs(Temperature) + cs(Salinity) nu: cs(Temperature) + cs(Salinity)	44330.0	0.32
MD Small Trawl				
	1	cs(Temperature) + cs(Salinity) + cs(Depth) + Struct500	16205.3	0.02
	2	cs(Temperature) + cs(Salinity) + cs(Depth) + Struct500 + re(Year)	16109.6	0.05
	3	cs(Temperature) + cs(Salinity) + cs(Depth) + Struct500 + re(Year) sigma: cs(Temperature) + cs(Salinity)	16097.4	0.05
	4	**cs(Temperature) + cs(Salinity) + cs(Depth) + Struct500 + re(Year) sigma: cs(Temperature) + cs(Salinity) nu: cs(Temperature) + cs(Salinity)**	**15713.6**	**0.12**
	5	cs(Temperature) + cs(Salinity) + cs(Depth) + re(Struct500|Year) sigma: cs(Temperature) + cs(Salinity) nu: cs(Temperature) + cs(Salinity)	15719.8	0.12
	6	cs(Temperature) + cs(Salinity) + cs(Depth) + re(Struct1000|Year) sigma: cs(Temperature) + cs(Salinity) nu: cs(Temperature) + cs(Salinity)	DNC	
VIMS				
	1	cs(Temperature) + cs(Salinity) + cs(Depth) + Struct500	91189.8	0.01
	2	cs(Temperature) + cs(Salinity) + cs(Depth) + Struct500 + re(Year)	90679.2	0.05
	3	cs(Temperature) + cs(Salinity) + cs(Depth) + Struct500 + re(Year) sigma: cs(Temperature) + cs(Salinity)	90667.2	0.05
	4	cs(Temperature) + cs(Salinity) + cs(Depth) + Struct500 + re(Year) sigma: cs(Temperature) + cs(Salinity) nu: cs(Temperature) + cs(Salinity)	88058.5	0.19
	5	cs(Temperature) + cs(Salinity) + cs(Depth) + re(Struct500|Year) sigma: cs(Temperature) + cs(Salinity) nu: cs(Temperature) + cs(Salinity)	88064.3	0.20
	6	**cs(Temperature) + cs(Salinity) + cs(Depth) + re(Struct1000|Year) sigma: cs(Temperature) + cs(Salinity) nu: cs(Temperature) + cs(Salinity)**	**88052.8**	**0.20**

Table 22. Results from the selected generalized additive models for location, scale, and shape (GAMLSS) describing abundance of juvenile summer flounder in three fishery-independent surveys (MD Coastal Bays Survey, MD Small Trawl Survey, and VIMS Juvenile Fish Trawl Survey), 1989-2019. Significance of final model terms was tested using the *stepGAIC* function in R. df is the degrees of freedom, AIC is Akaike's Information Criterion, LRT is the likelihood ratio test statistic, which is assumed to be distributed as a χ^2 random variable, and $P(\chi^2)$ is the probability of observing a greater value of the χ^2 statistic under the null hypothesis. Structure 500 is a categorical predictor indicating that structured habitat was present within 500 m of the sampling site. Re(struct500|year) is the random effect of the categorical structure predictor nested within year. Re(year) is the random effect of year, and Re(struct100|year) is the random effect of the predictor indicating that structured habitat was present within 1000 m of the sampling site nested within year.

Survey	Predictor	df	AIC	LRT	$P(\chi^2)$
MD Coastal Bays	Water temperature	4.7	44424	118.23	<0.001
	Salinity	10.5	44573	278.84	<0.001
	Depth	6.2	44319	16.35	0.014
	re(struct500|year)	42.2	44646	415.90	<0.001
MD Small Trawl	Water temperature	6.2	15741	39.80	<0.001
	Salinity	6.2	15763	61.45	<0.001
	Depth	6.2	15721	19.68	0.004
	Structure 500	1.0	15712	0.38	0.538
	re(year)	26.7	15806	146.23	<0.001
VIMS	Water temperature	5.6	88077	35.63	<0.001
	Salinity	6.0	88061	20.33	0.003
	Depth	5.3	88105	62.68	<0.001
	re(struct1000|year)	52.4	88569	621.15	<0.001

Table 23. Akaike's Information Criterion (AIC) and generalized R^2 values for multiple models fitted to juvenile black sea bass abundances from three fishery-independent surveys (MD Coastal Bays, MD Small Trawl Survey, and VIMS Juvenile Fish Trawl Survey), 1989 – 2019. Predictors considered in the models included water temperature, salinity, depth, and categorical predictors indicating sampling locations within a given distance to structure (within either 500 or 1000 m). For these models, "cs" indicates the predictor's effect was modeled as an additive cubic-spline smooth function, and "re" indicates random model terms. Predictors that explained variation in the variance (σ), or skewness and kurtosis (ν) are designated 'sigma:' and 'nu:". The model with the lowest AIC was selected as the best model and is indicated in bold. DNC indicates that the model did not converge.

Survey	Models		AIC	R^2
MD Coastal Bays				
	1	cs(Temperature) + cs(Salinity) + cs(Depth) + Struct500	17519.45	0.01
	2	cs(Temperature) + cs(Salinity) + cs(Depth) + Struct500 + re(Year)	17459.55	0.04
	3	cs(Temperature) + cs(Salinity) + cs(Depth) + Struct500 + re(Year) sigma: cs(Temperature) + cs(Salinity)	17458.96	0.05
	4	cs(Temperature) + cs(Salinity) + cs(Depth) + Struct500 + re(Year) sigma: cs(Temperature) + cs(Salinity) nu: cs(Temperature) + cs(Salinity)	17187.57	0.12
	5	**cs(Temperature) + cs(Salinity) + cs(Depth) + re(Struct500|Year) sigma: cs(Temperature) + cs(Salinity) nu: cs(Temperature) + cs(Salinity)**	**17157.21**	**0.14**
	6	cs(Temperature) + cs(Salinity) + cs(Depth) + re(Struct1000|Year) sigma: cs(Temperature) + cs(Salinity) nu: cs(Temperature) + cs(Salinity)	17191.41	0.13
VIMS				
	1	cs(Temperature) + cs(Salinity) + cs(Depth) + Struct500	55415.89	0.02
	2	cs(Temperature) + cs(Salinity) + cs(Depth) + Struct500 + re(Year)	54929.68	0.07
	3	cs(Temperature) + cs(Salinity) + cs(Depth) + Struct500 + re(Year) sigma: cs(Temperature) + cs(Salinity)	54890.04	0.08
	4	cs(Temperature) + cs(Salinity) + cs(Depth) + Struct500 + re(Year) sigma: cs(Temperature) + cs(Salinity) nu: cs(Temperature) + cs(Salinity)	54774.02	0.09
	5	cs(Temperature) + cs(Salinity) + cs(Depth) + re(Struct500|Year) sigma: cs(Temperature) + cs(Salinity) nu: cs(Temperature) + cs(Salinity)	54765.87	0.09
	6	**cs(Temperature) + cs(Salinity) + cs(Depth) + re(Struct1000|Year) sigma: cs(Temperature) + cs(Salinity) nu: cs(Temperature) + cs(Salinity)**	**54758.47**	**0.09**

Table 24. Results from the selected generalize additive models for location, scale, and shape (GAMLSS) describing abundance of juvenile black sea bass in two fishery-independent surveys (MD Coastal Bays Survey, and VIMS Juvenile Fish Trawl Survey), 1989-2019. Significance of the final model terms was tested using the *stepGAIC* function in R. df is the degrees of freedom, AIC is Akaike's Information Criterion, LRT is the likelihood ratio test statistic, which is assumed to be distributed as a χ^2 random variable, and $P(\chi^2)$ is the probability of observing a greater value of the χ^2 statistic under the null hypothesis. Re(struct500|year) is the random effect of the predictor indicating that structured habitat was present within 500 m of the sampling site nested within year. Re(struct100|year) is the random effect of the predictor indicating that structured habitat was present within 1000 m of the sampling site nested within year.

Survey	Predictor	df	AIC	LRT	$P(\chi^2)$
MD Coastal Bays	Water temperature	6.3	17157	12.48	0.060
	Salinity	6.3	17159	14.70	<0.001
	Depth	6.6	17175	31.22	<0.001
	re(struct500|year)	45.4	17247	181.03	<0.001
VIMS	Water temperature	6.5	54808	62.11	<0.001
	Salinity	6.5	54777	32.07	<0.001
	Depth	6.6	54799	53.86	<0.001
	re(struct1000|year)	51.0	55273	616.17	<0.001

Table 25. Effect of stratum, distance to structure, temperature, day of year, depth, salinity, density and tow on mean length of juvenile summer flounder from the best fitting generalized additive mixed model. Observations include fish captured by three fishery-independent trawl surveys, 1989 – 2019. The model intercept (representing the overall mean length) and estimated mean effects for the categorical factors are shown in section A, with associated standard errors, *t* statistics, and approximate significance (*P*). Stratum estimates are relative to those found in the Chester River and in habitats nearest structure (0 – 250 m). The continuous smooth terms are shown in section B, with associated estimated degrees of freedom (edf), *F* values, and approximate significance (*P*). EBY is the Eastern Bay, James is the James River, MD Coast N is Assawoman Sound and Isle of Wight Bay, MD Coast S is Sinepuxent Bay and Chincoteague Bay, POC is Pocomoke Sound, Rapp is the Rappahannock River, TNG is Tangier Sound, VALower_bay, VAMid_bay, VAUpper_bay correspond with Virginia lower bay, Virginia middle bay and Virginia upper bay, and York is the York River.

A

Parameter	**Estimate**	**Standard error**	**t-value**	***P***
Intercept	160.5145	3.2866	48.839	<0.001
Stratum: EBY	2.2722	3.9709	0.572	0.567
Stratum: James	-11.6529	2.9552	-3.943	0.000
Stratum: MD Coast N	-44.4654	3.2883	-13.522	<0.001
Stratum: MD Coast S	-47.442	3.1416	-15.101	<0.001
Stratum: POC	-24.1031	3.142	-7.671	<0.001
Stratum: Rapp	-11.128	2.8732	-3.873	<0.001
Stratum: TNG	-19.3245	2.9823	-6.48	<0.001
Stratum: VALower_bay	-10.3761	3.1037	-3.343	0.001
Stratum: VAMid_bay	-11.6662	3.0324	-3.847	<0.001
Stratum: VAUpper_bay	-11.2248	2.9929	-3.75	<0.001
Stratum: York	-21.7629	2.9439	-7.393	<0.001
Marsh: 251 - 500	-2.272	2.6082	-0.871	0.384
Marsh: 501 - 750	-5.4827	2.1124	-2.596	0.009
Marsh: 751 - 1000	-5.103	2.4192	-2.109	0.035
Marsh: GT 1000	-1.7895	1.6068	-1.114	0.265
SAV: 251 - 500	-0.9284	1.833	-0.507	0.612
SAV: 501 - 750	-4.7955	1.8259	-2.626	0.009
SAV: 751 - 1000	-4.7918	1.8849	-2.542	0.011
SAV: GT 1000	-6.2771	1.5358	-4.087	<0.001
Oyster: 251 - 500	0.6741	1.2903	0.522	0.601
Oyster: 501 - 750	3.1155	1.377	2.262	0.024
Oyster: 751 - 1000	-1.0861	1.397	-0.777	0.437
Oyster: GT 1000	4.2243	0.9666	4.37	<0.001
Shore: 251 - 500	-1.5389	1.2806	-1.202	0.229
Shore: 501 - 750	-0.0685	1.4543	-0.047	0.962
Shore: 751 - 1000	0.6486	1.7064	0.38	0.704
Shore: GT 1000	2.4122	1.379	1.749	0.080

B

Smooth terms	**edf**	***F***	***P***
s(Temperature)	7	307.228	<0.001
s(Day of year)	9	35111.074	<0.001
s(Salinity)	7	115.656	<0.001
s(Density)	7	447.656	<0.001
s(Tow)	7097	3.536	<0.001

Table 26. Effect of stratum, distance to structure, temperature, day of year, depth, salinity, density and tow on black sea bass length from the best fitting generalized additive mixed model. Observations include fish captured by three fishery-independent trawl surveys, 1989 – 2019. The model intercept (representing the overall mean length) and estimated mean effects for the categorical factors are shown in section A, with associated standard errors, *t* statistics, and approximate significance (*P*). Stratum estimates are relative to those found in the James River and in habitats nearest structure (0 – 250 m). The continuous smooth terms are shown in section B, with associated estimated degrees of freedom (edf), *F* statistics, and approximate significance (*P*). EBY is the Eastern Bay, James is the James River, MD Coast N is Assawoman Sound and Isle of Wight Bay, MD Coast S is Sinepuxent Bay and Chincoteague Bay, POC is Pocomoke Sound, Rapp is the Rappahannock River, TNG is Tangier Sound, VALower_bay, VAMid_bay, VAUpper_bay correspond with Virginia lower bay, Virginia middle bay and Virginia upper bay, and York is the York River.

A

Parameter	Estimate	Standard error	t-value	*P*
Intercept	130.5878	2.9855	43.74	<0.001
Stratum: MD Coast N	6.633	1.7387	3.815	<0.001
Stratum: MD Coast S	-1.6887	1.6318	-1.035	0.301
Stratum: POC	-1.415	5.7064	-0.248	0.804
Stratum: TNG	7.9579	4.7765	1.666	0.096
Stratum: VALower_bay	-8.9118	0.7589	-11.74	<0.001
Stratum: VAMid_bay	-7.1268	0.7709	-9.245	<0.001
Stratum: VAUpper_bay	-8.1343	0.8553	-9.51	<0.001
Marsh: 251 - 500	4.4913	3.18	1.412	0.158
Marsh: 501 - 750	9.478	2.5192	3.762	<0.001
Marsh: 751 - 1000	11.1286	4.2346	2.628	0.009
Marsh: GT 1000	5.2935	2.125	2.491	0.013
SAV: 251 - 500	5.7051	2.2041	2.588	0.010
SAV: 501 - 750	0.1518	2.3849	0.064	0.949
SAV: 751 - 1000	2.0164	2.351	0.858	0.391
SAV: GT 1000	-0.2862	2.0681	-0.138	0.890
Oyster: 251 - 500	-1.0818	2.5358	-0.427	0.670
Oyster: 501 - 750	-5.8429	3.5272	-1.657	0.098
Oyster: 751 - 1000	2.4835	2.6565	0.935	0.350
Oyster: GT 1000	-3.2956	1.7327	-1.902	0.057
Shore: 251 - 500	-6.0231	2.0883	-2.884	0.004
Shore: 501 - 750	-7.8765	2.0674	-3.81	<0.001
Shore: 751 - 1000	-7.9973	2.5162	-3.178	0.001
Shore: GT 1000	-8.5399	1.8241	-4.682	<0.001

B

Smooth terms	edf	*F*	*P*
s(Temperature)	7	0.00	0.269
s(Day of year)	9	3812.00	<0.001
s(Depth)	9	9.73	<0.001
s(Salinity)	7	0.00	0.520
s(Density)	7	6.93	0.006
s(Tow)	3366	0.33	<0.001

Figure 1. Monthly length-frequency histograms for all ages of black sea bass captured in the Eastern Shore and the Piankatank River in 2019 and 2020. Number of fish captured (N) given in the upper right corner of each panel.

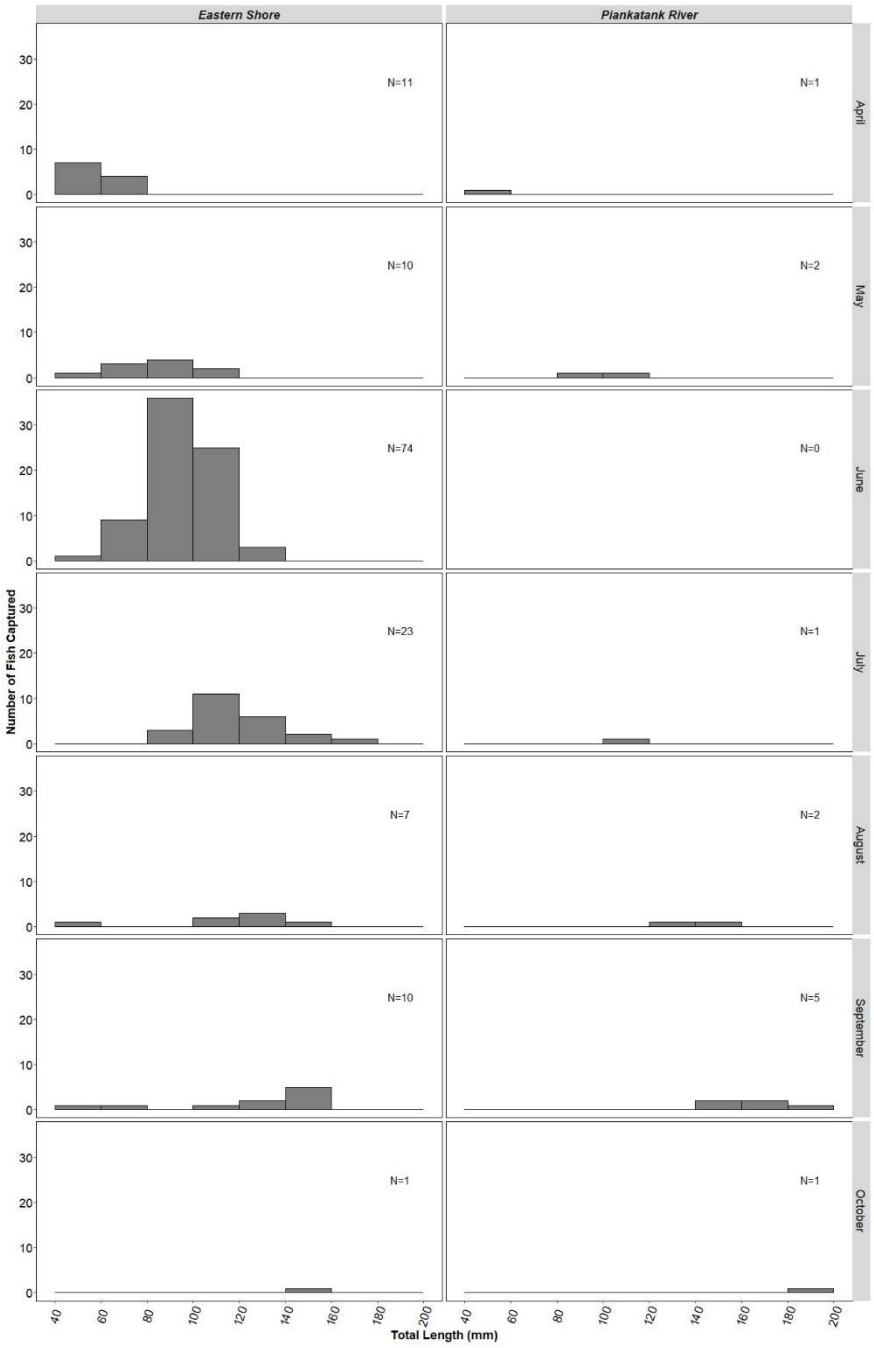

Figure 2. Location of 2019 and 2020 sampling sites (dark triangles) in the lower Piankatank River in Chesapeake Bay (PK) and in South Bay on the Eastern Shore (ES).

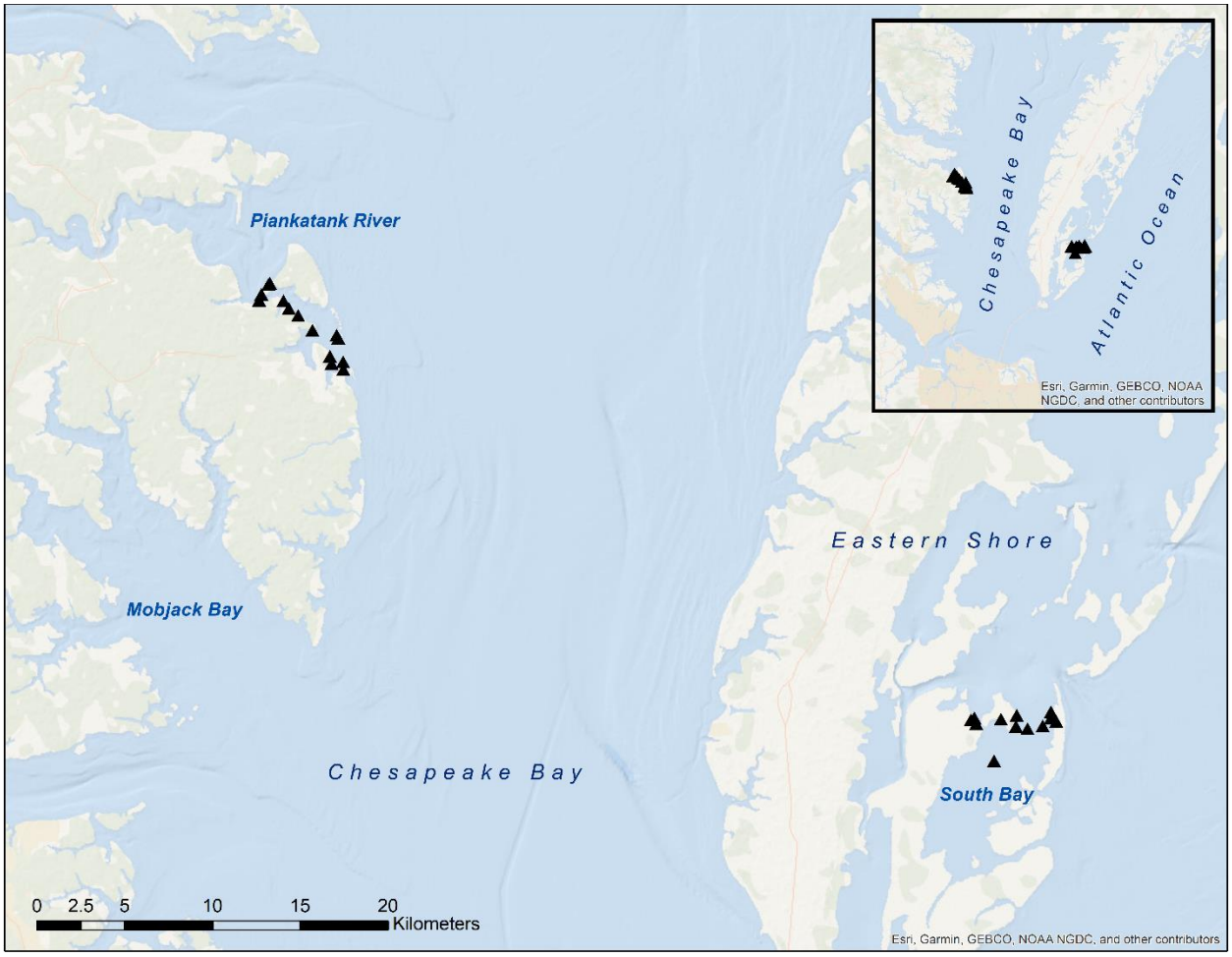

Figure 3. Example of an otolith from a juvenile summer flounder. The top panel shows a summer flounder otolith under 40x magnification; the white box indicates the area from which daily increments were measured. The bottom panel is an example depicting daily otolith increments (red "+") at 200x magnification; each of the seven daily increments from the edge to the core were measured (µm) by two independent readers along the axis depicted by the solid red line.

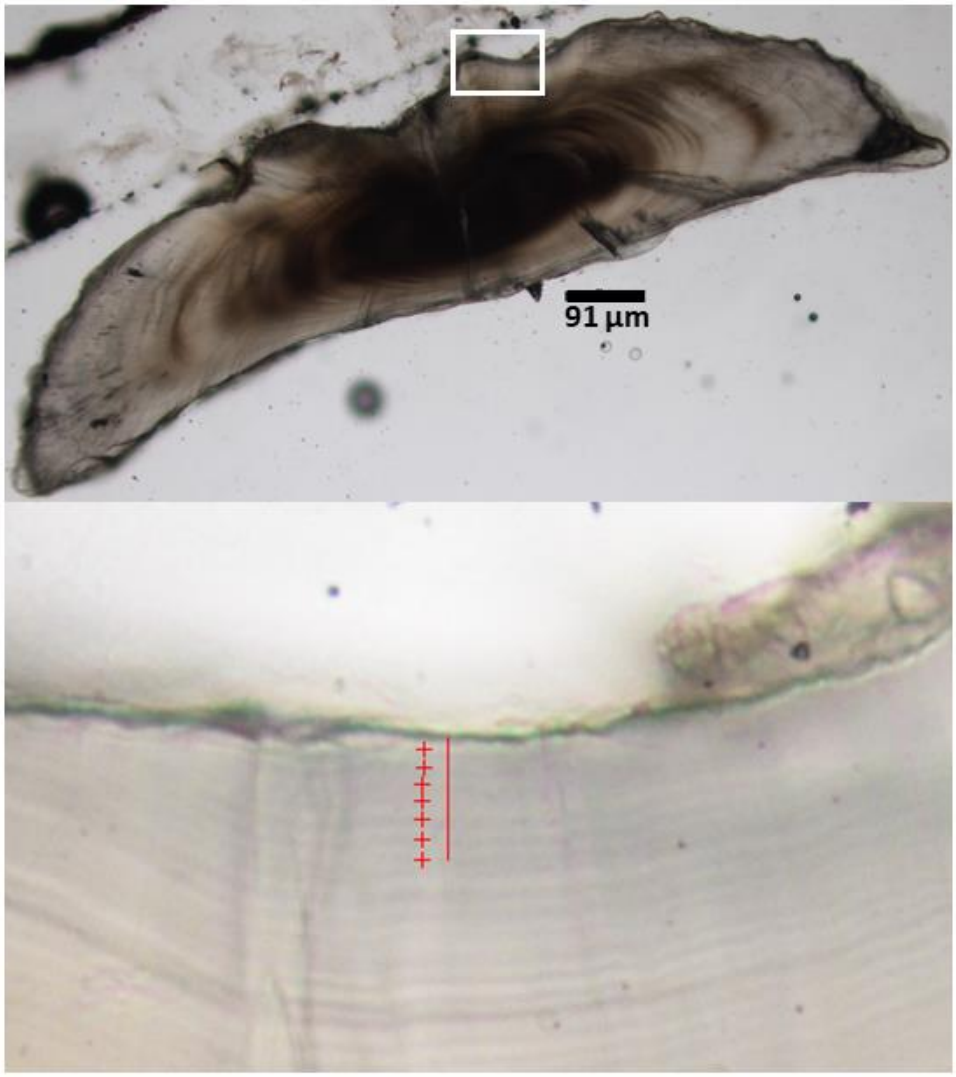

Figure 4. Locations of trawl survey sites in Chesapeake Bay and the coastal lagoons; in Virginia, sites are randomly selected each month, hence, sites sampled in only one month are depicted.

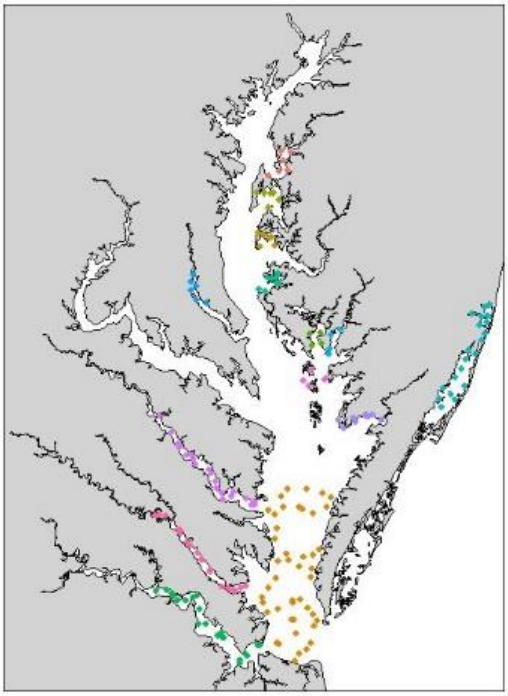

Figure 5. Monthly mean suitable habitat extents (filled circles) in June to November for juvenile summer flounder in Chesapeake Bay, 1996 to 2019; means were averages of daily extents (hectares). The line is a fitted linear regression.

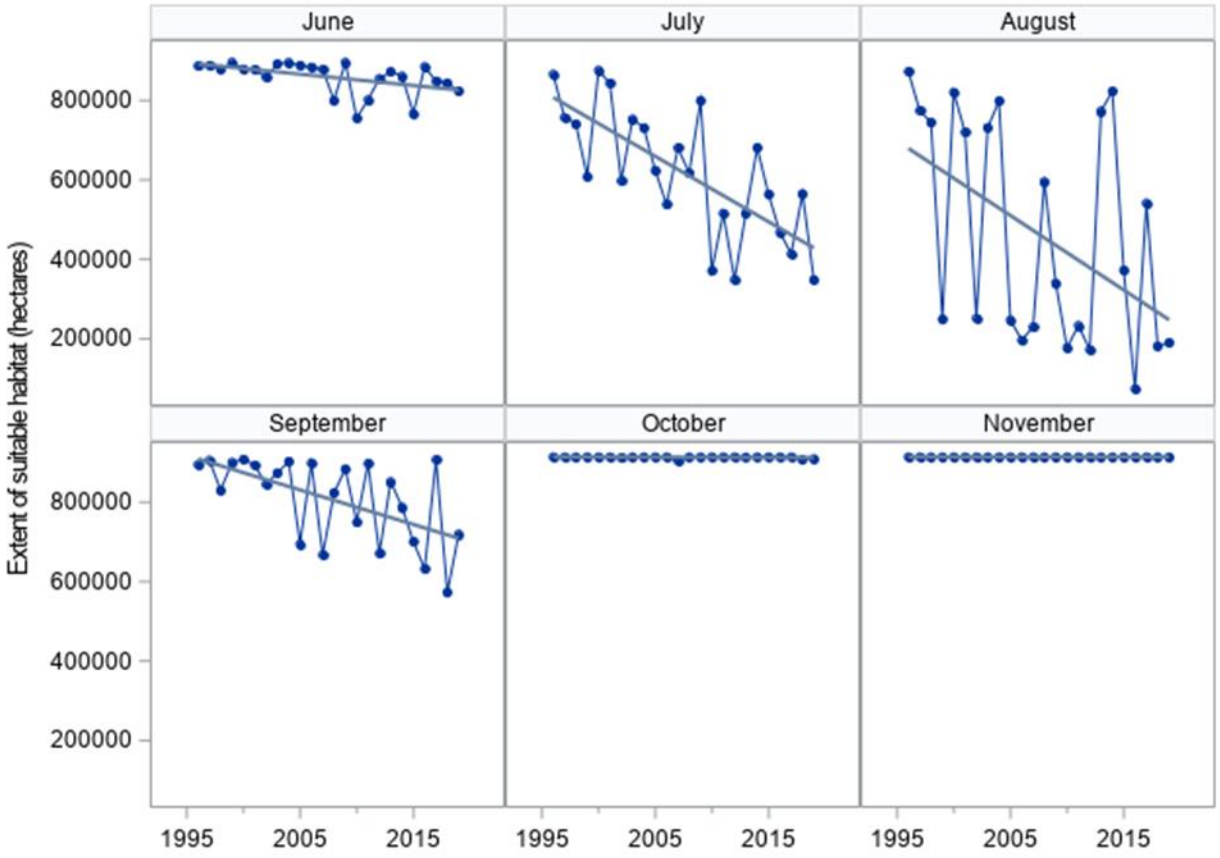

Figure 6. Boxplots of salinity (psu) measured at the Eastern Shore (light gray) and Piankatank River (dark gray) in marsh, oyster, soft-bottom, and seagrass habitats in 2019 and 2020. Black horizontal lines denote the median salinity.

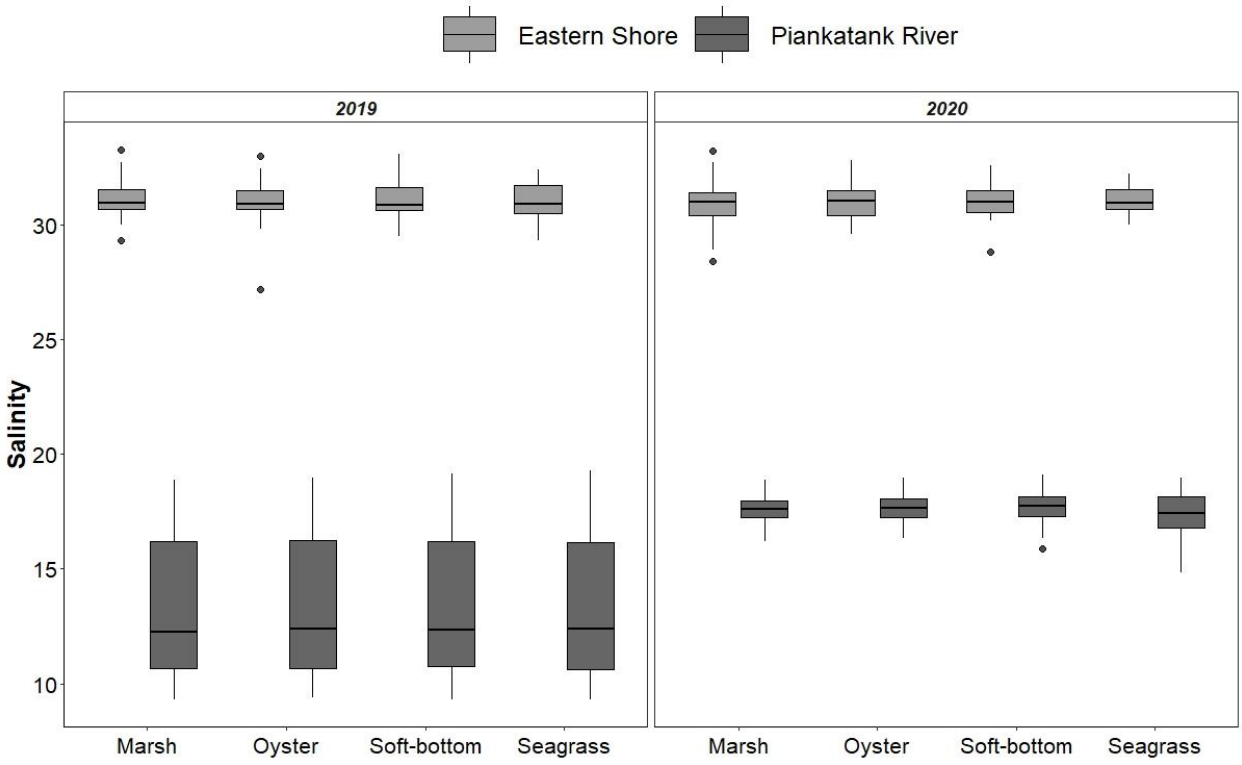

Figure 7. Boxplots of water temperature (°C) from marsh, oyster, soft-bottom, and seagrass habitats in the Eastern Shore (light gray) and Piankatank River (dark gray) in 2019 and 2020. Values are from temperature loggers that recorded temperature every five minutes, and thus captured fluctuations in water temperature during the duration of gear deployment. Black horizontal lines denote the median.

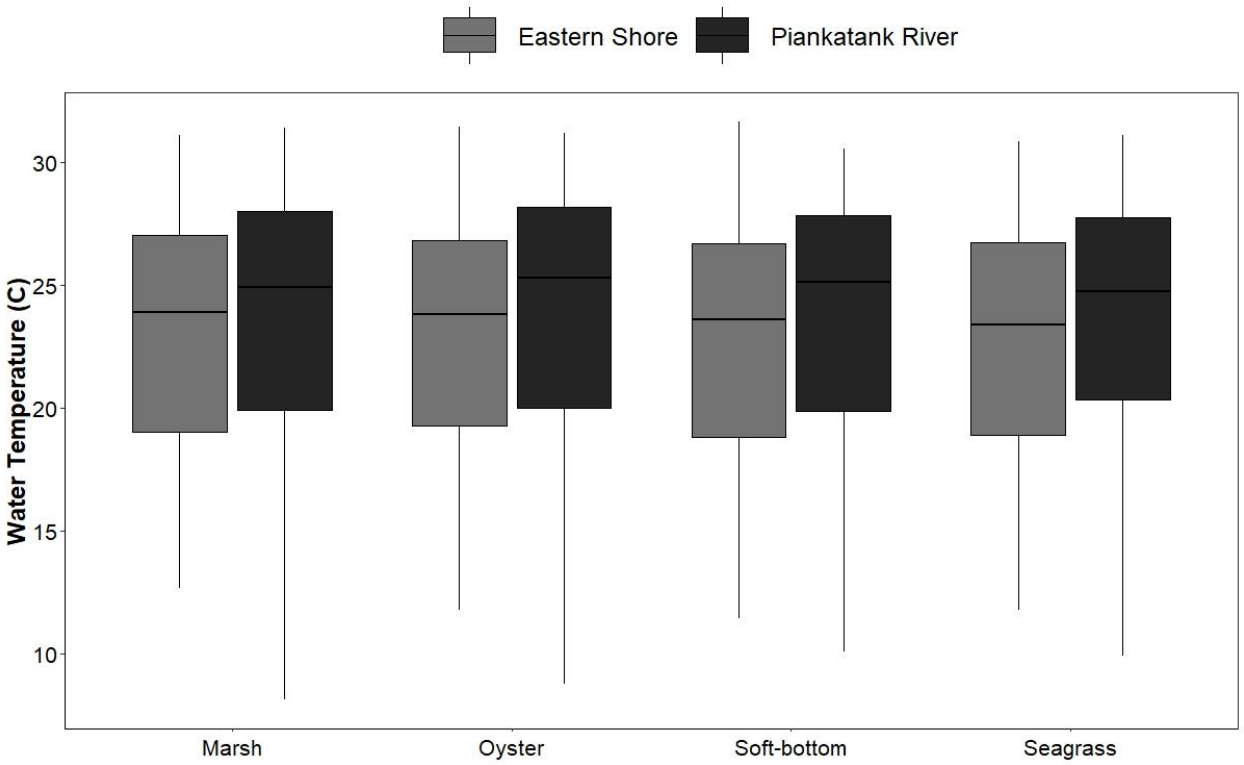

Figure 8. Boxplots of dissolved oxygen (mg/L) from marsh, oyster, soft-bottom, and seagrass habitats in the Eastern Shore (light gray) and Piankatank River (dark gray) in 2019 and 2020. Black horizontal lines denote the median.

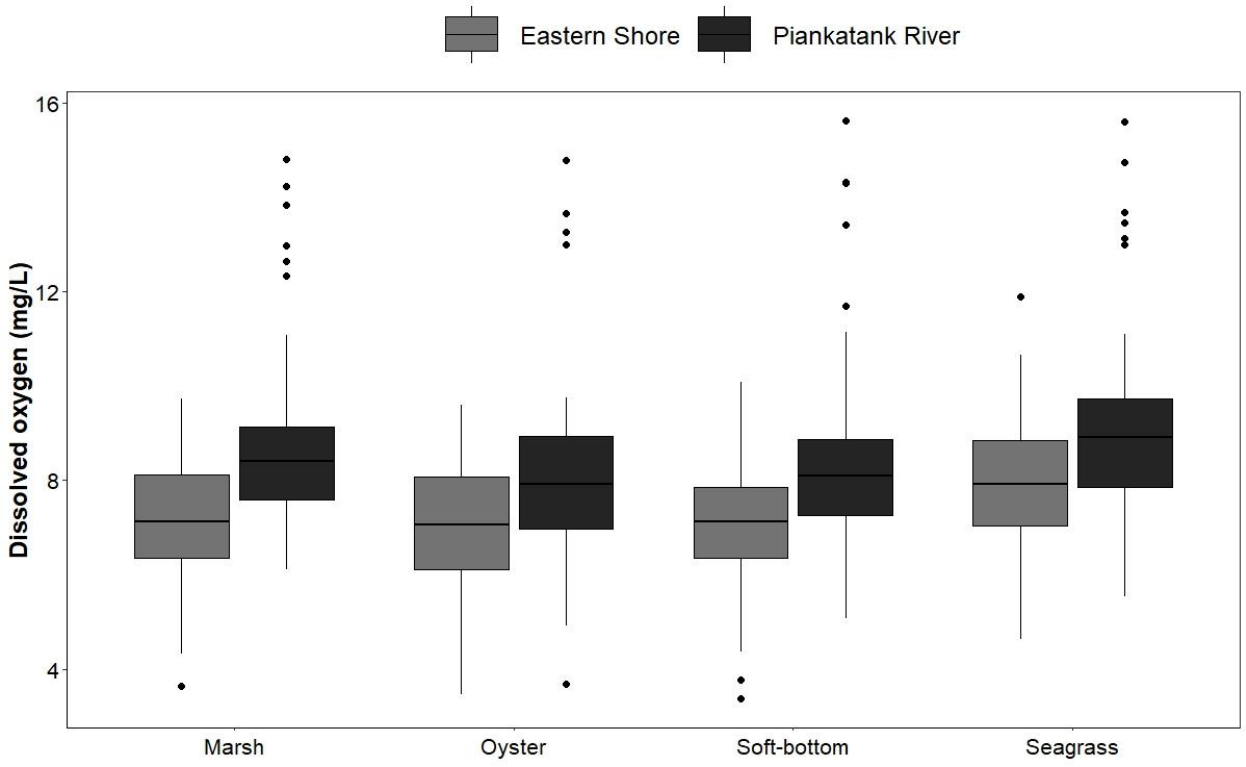

Figure 9. Habitat composition of sampling sites on the Eastern Shore and Piankatank River, 2019 - 2020. Percent habitat composition is the average from three replicate sites within each habitat type (marsh, oyster, seagrass or soft-bottom). The top row depicts habitat composition within 500 m of sampling sites; the bottom row depicts habitat composition within 1 km of sampling sites. Green denotes marsh creek habitat, orange denotes oyster habitat, gold denotes soft-bottom habitat, and purple denotes seagrass habitat.

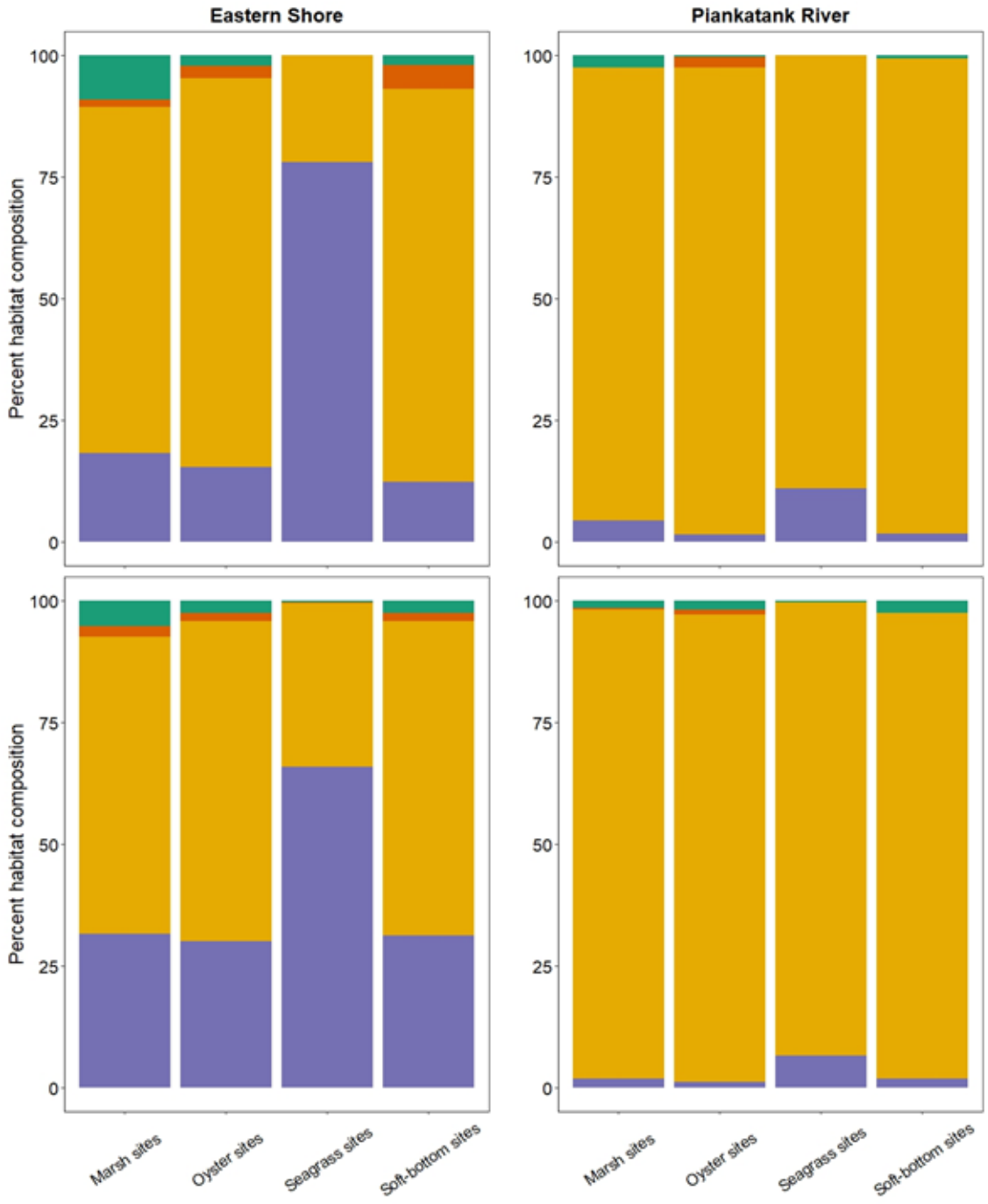

Figure 10. Length-frequency (total length, mm) histograms for all juvenile and adult summer flounder (top row, SF) and black sea bass (bottom row, BSB) captured in the Eastern Shore and Piankatank River, 2019-2020. Number of fish captured (N) is provided in the upper right corner of each panel.

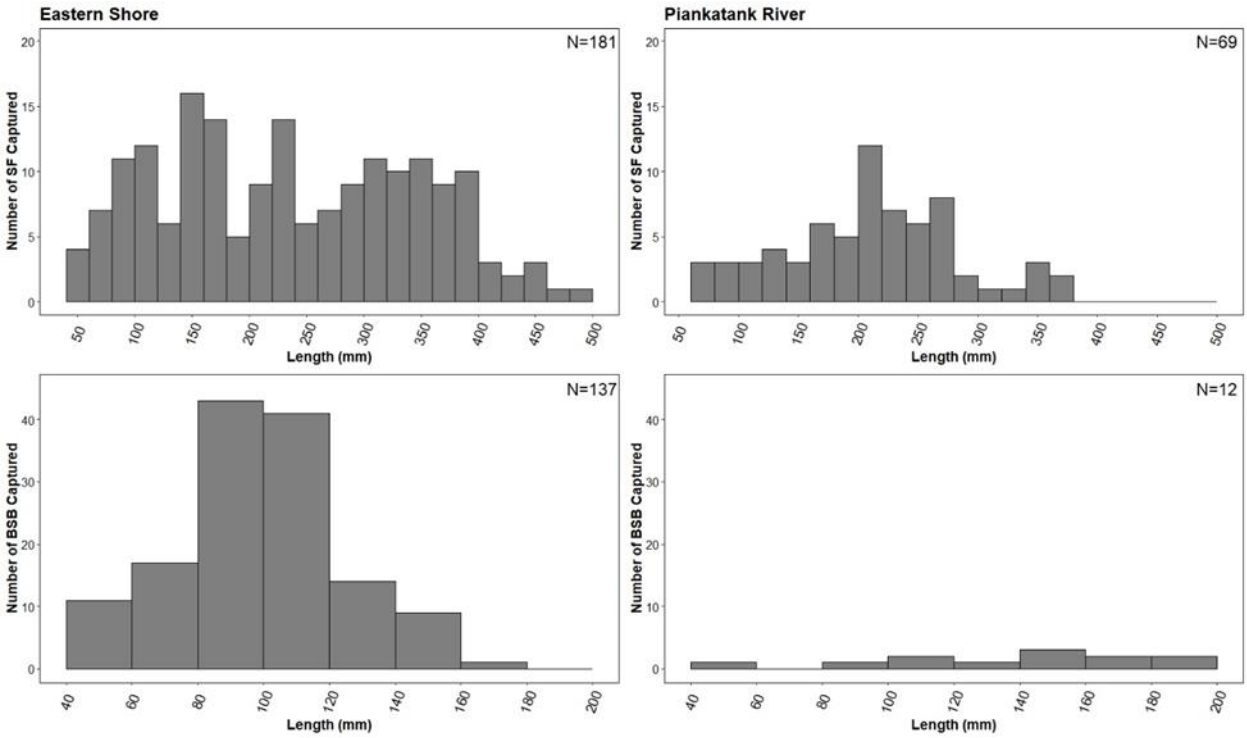

Figure 11. Monthly (June to October) length-frequency (total length, mm) histograms for juvenile summer flounder captured in the Eastern Shore and the Piankatank River in 2019-2020. No evidence of multiple sub-cohorts was detected in either year. Number of fish captured (N) is provided in the upper right corner of each panel.

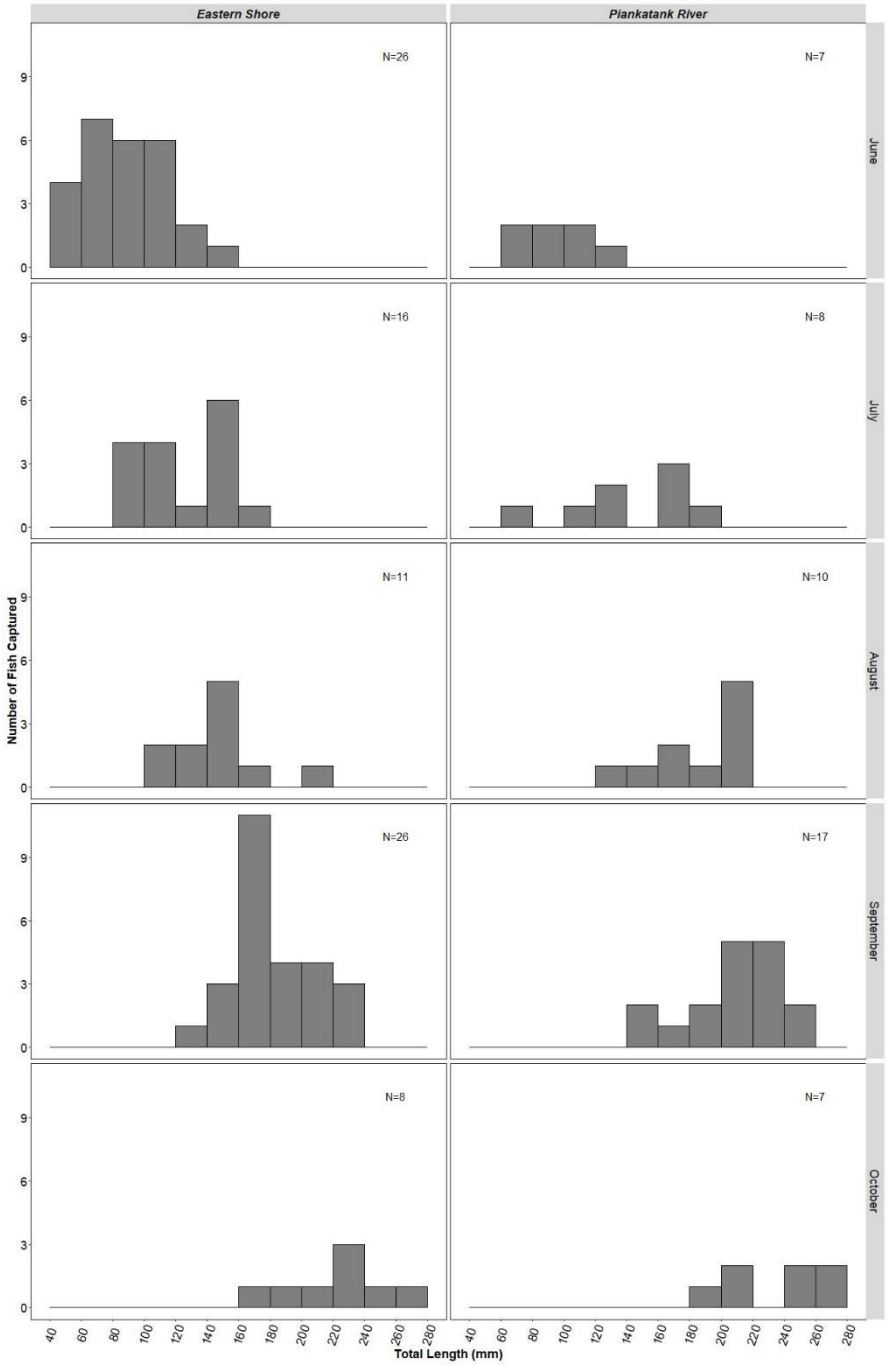

Figure 12. Proportion of fyke nets deployed in June-October that captured juvenile summer flounder (SF) in marsh, oyster, soft-bottom, and seagrass habitats in the Eastern Shore (light gray) and Piankatank River (dark gray) 2019-2020.

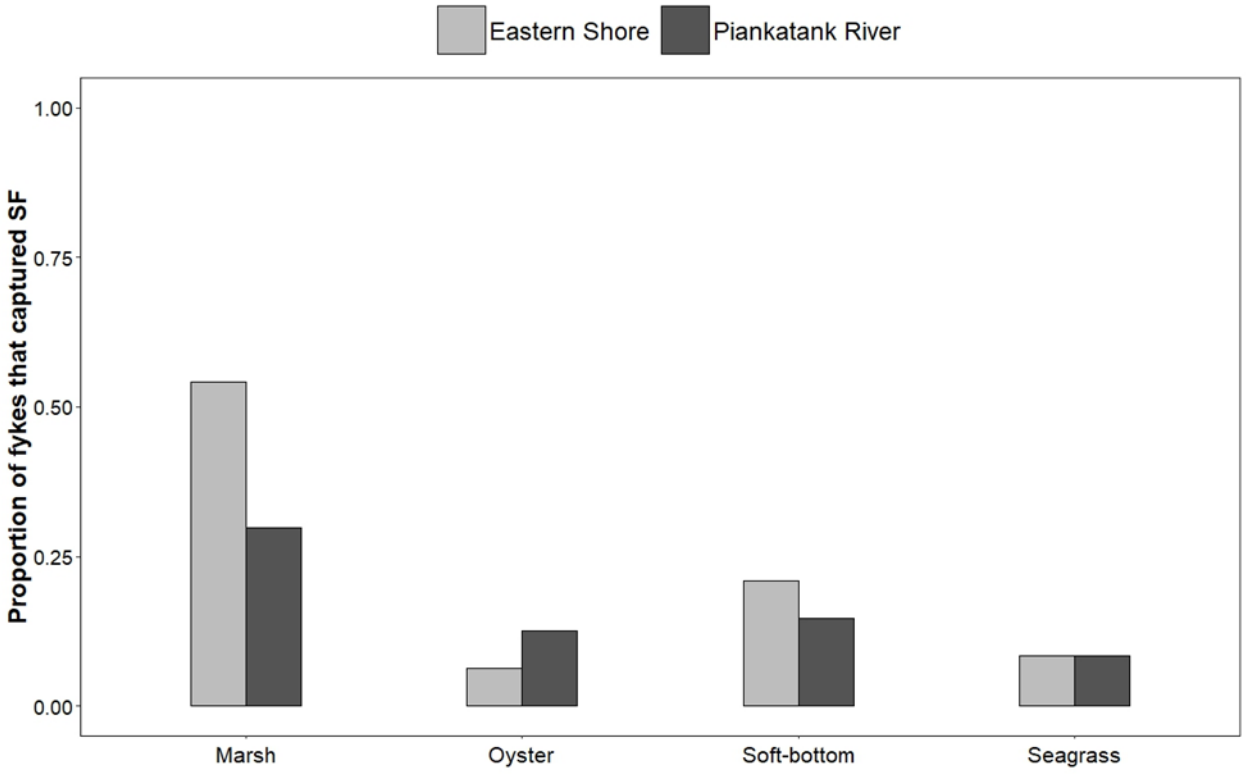

Figure 13. Mean relative abundance estimates of juvenile summer flounder at Eastern Shore (●) and Piankatank River (▲) sites in marsh, oyster, soft-bottom, and seagrass habitats, 2019-2020. Relative abundance was estimated using the delta-lognormal method; vertical bars denote the 95% confidence limits on the means. Dashed line depicts zero mean abundance.

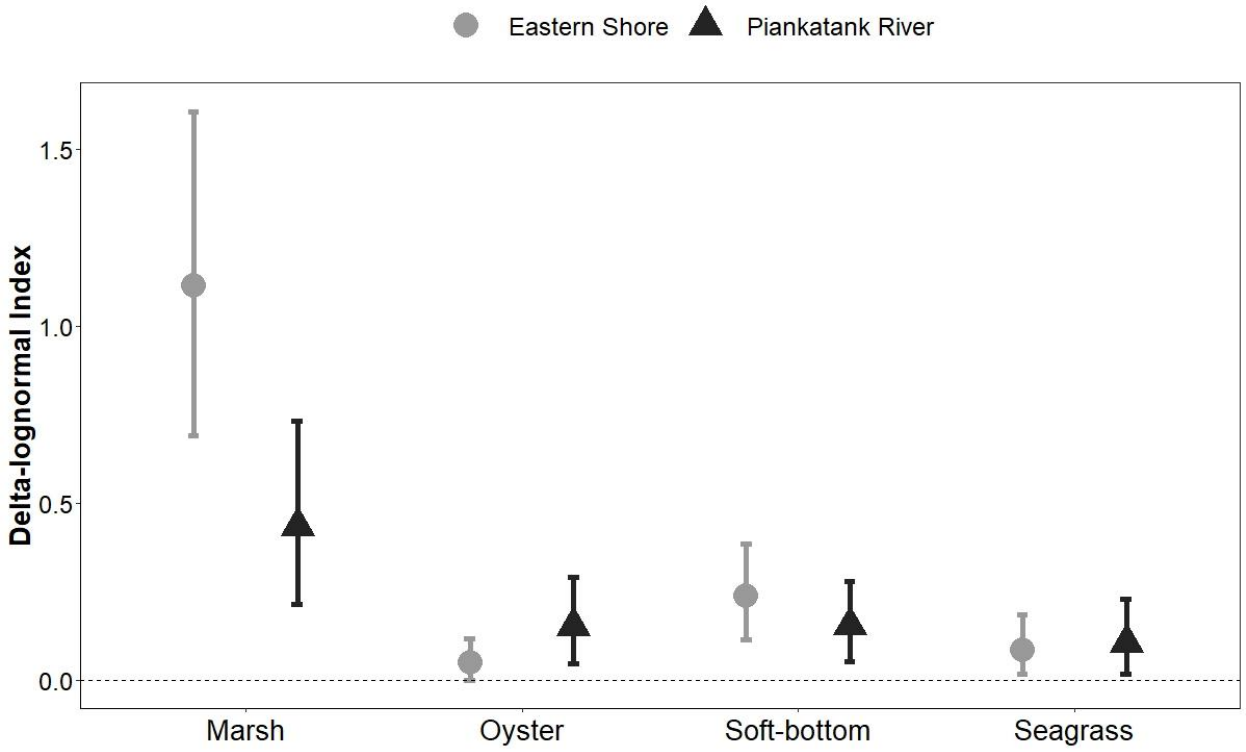

Figure 14. (A) Proportion of SMURFs deployed in April-May that captured juvenile black sea bass (BSB) in Eastern Shore (light gray) and Piankatank River (dark gray) sampling sites in marsh, oyster, soft-bottom, and seagrass habitats, 2019-2020. No juvenile black sea bass were captured in Piankatank River soft-bottom or seagrass habitats or in Eastern Shore seagrass habitats in April-May. (B) Proportion of fyke nets deployed in June-October that captured juvenile black sea bass (BSB) Eastern Shore (light gray) and Piankatank River (dark gray) sampling sites in marsh, oyster, soft-bottom, and seagrass habitats, 2019-2020. No juvenile black sea bass were captured in Piankatank River marsh or soft-bottom habitats in June-October.

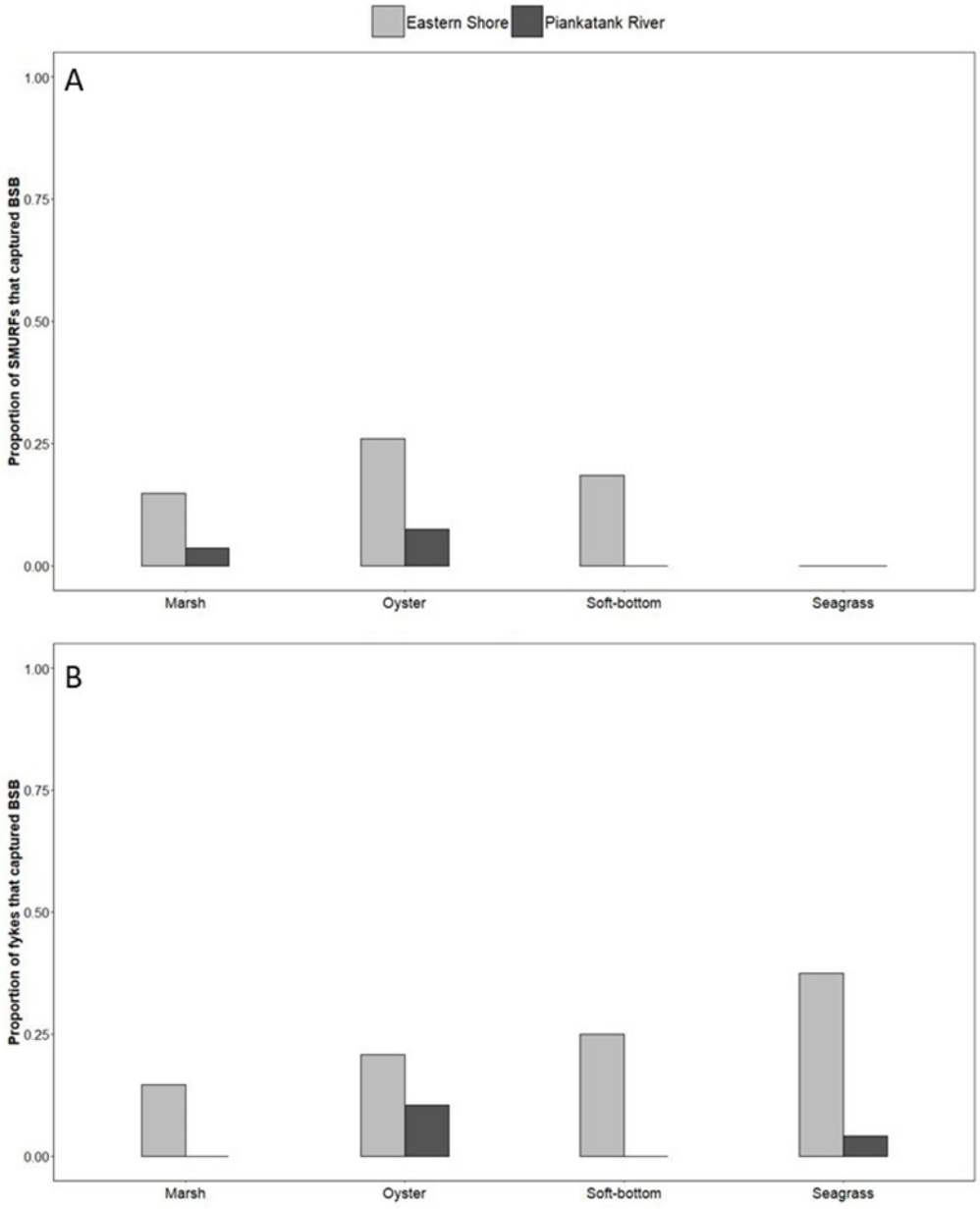

Figure 15. Mean relative abundance estimates of juvenile black sea bass at Eastern Shore (●) and Piankatank River (▲) sites in marsh, oyster, soft-bottom, and seagrass habitats, 2019-2020. Relative abundance was estimated using the delta-lognormal method; vertical bars denote the 95% confidence limits on the means. Dashed line depicts zero mean abundance.
(A) April-May abundance estimated from SMURFs. (B) June-October abundance estimated from fyke nets. No juvenile black sea bass were captured in Piankatank River soft-bottom or seagrass habitats or in Eastern Shore seagrass habitats in April-May. No juvenile black sea bass were captured in Piankatank River marsh or soft-bottom habitats in June-October.

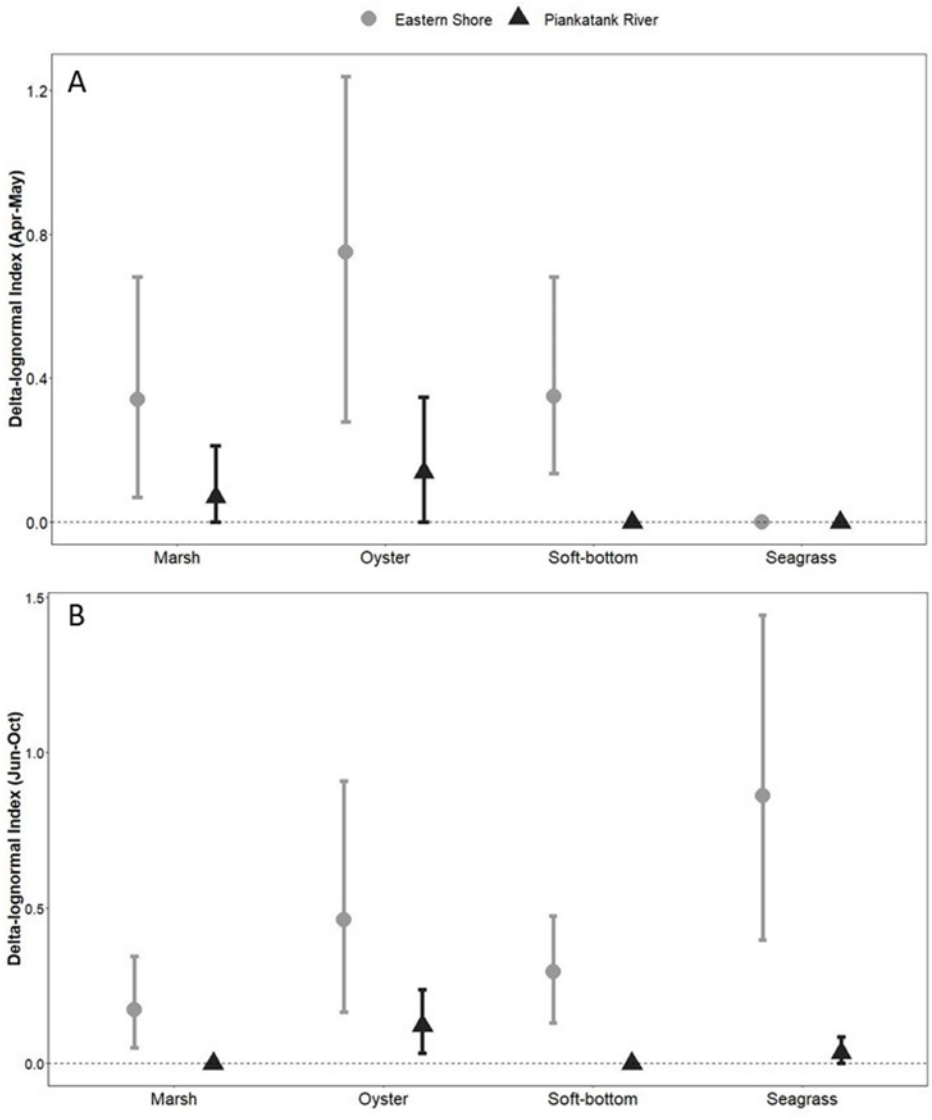

Figure 16. Marginal mean-scaled estimates of relative body condition (K_n) for juvenile summer flounder in Eastern Shore (●) and Piankatank River (▲) sites in marsh, oyster, soft-bottom, and seagrass habitats, 2019-2020. Vertical lines denote 95% confidence limits.

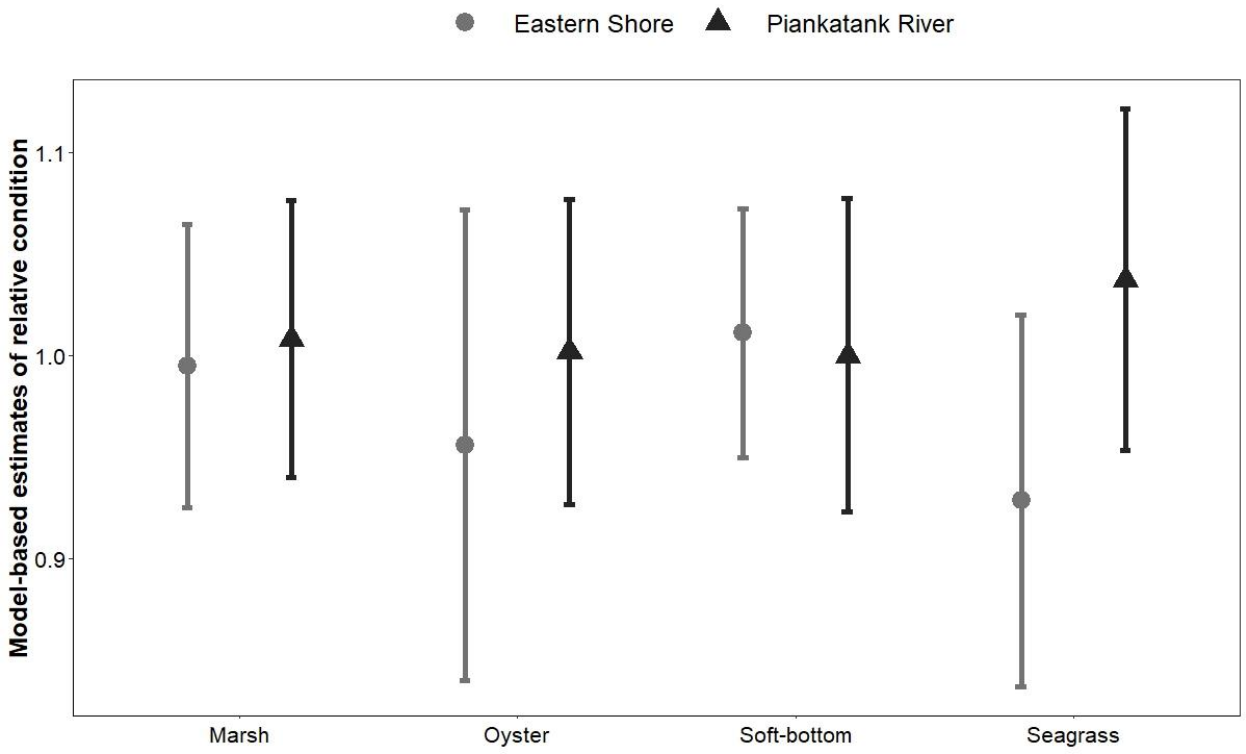

Figure 17. Bland-Altman plots depicting the between-reader difference in the distance (µm) measured from the otolith's edge to the seventh daily increment versus the mean of the two readers' distances measured from the otolith's edge to the seventh daily increment. The black dashed line denotes a zero difference, the solid red line indicates the mean between-reader difference, and the dashed red lines indicate the 95% confidence limits on the mean difference. (A) Juvenile summer flounder. (B) Juvenile black sea bass.

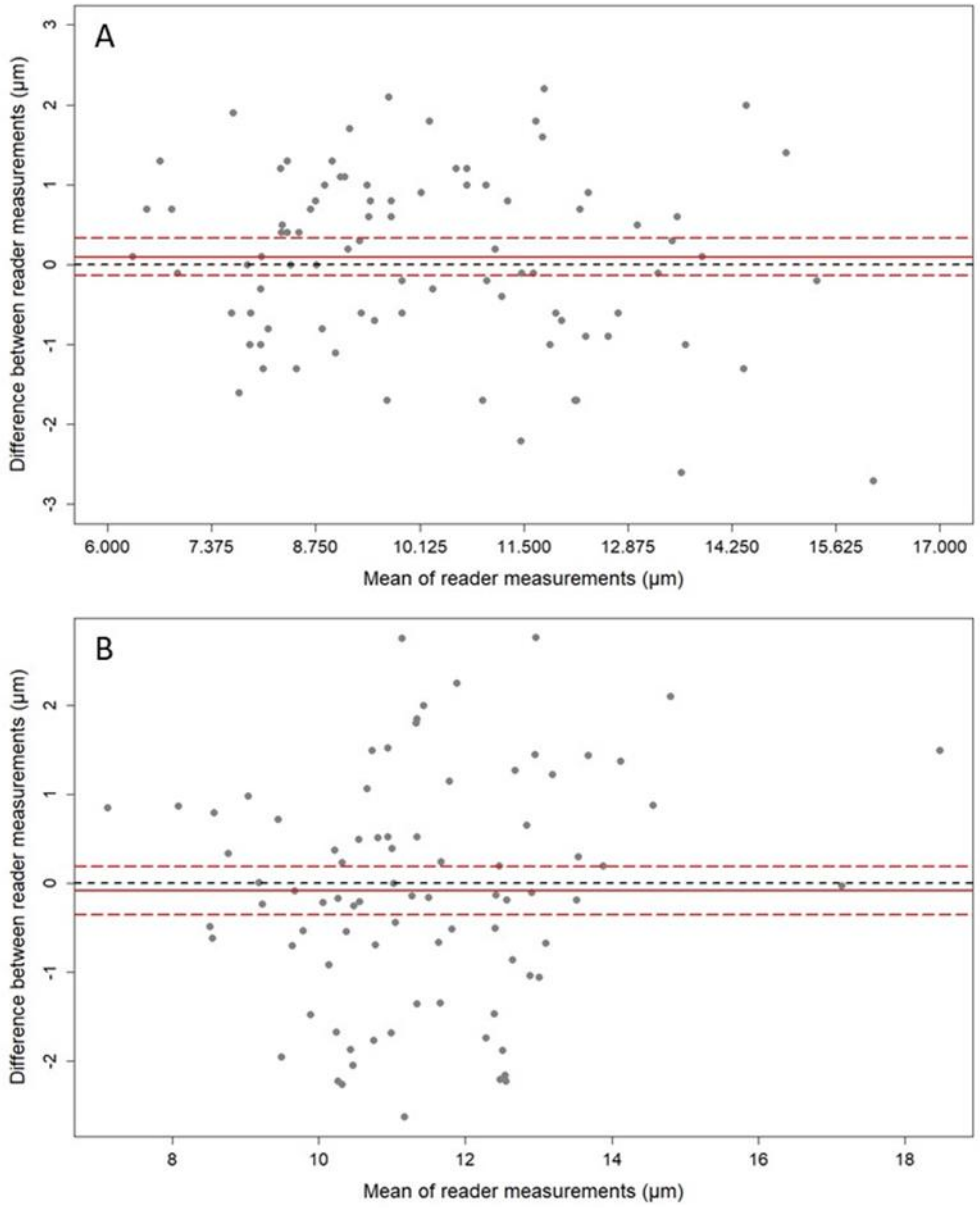

Figure 18. Body size (total length, mm) of juvenile summer flounder plotted against their corresponding otolith radial distance (µm). Juvenile summer flounder were captured at Eastern Shore and Piankatank River sites in 2019 - 2020. The solid black line is the regression line fitted to the individual observations of length (●). Dark grey shading indicates 95% confidence limits.

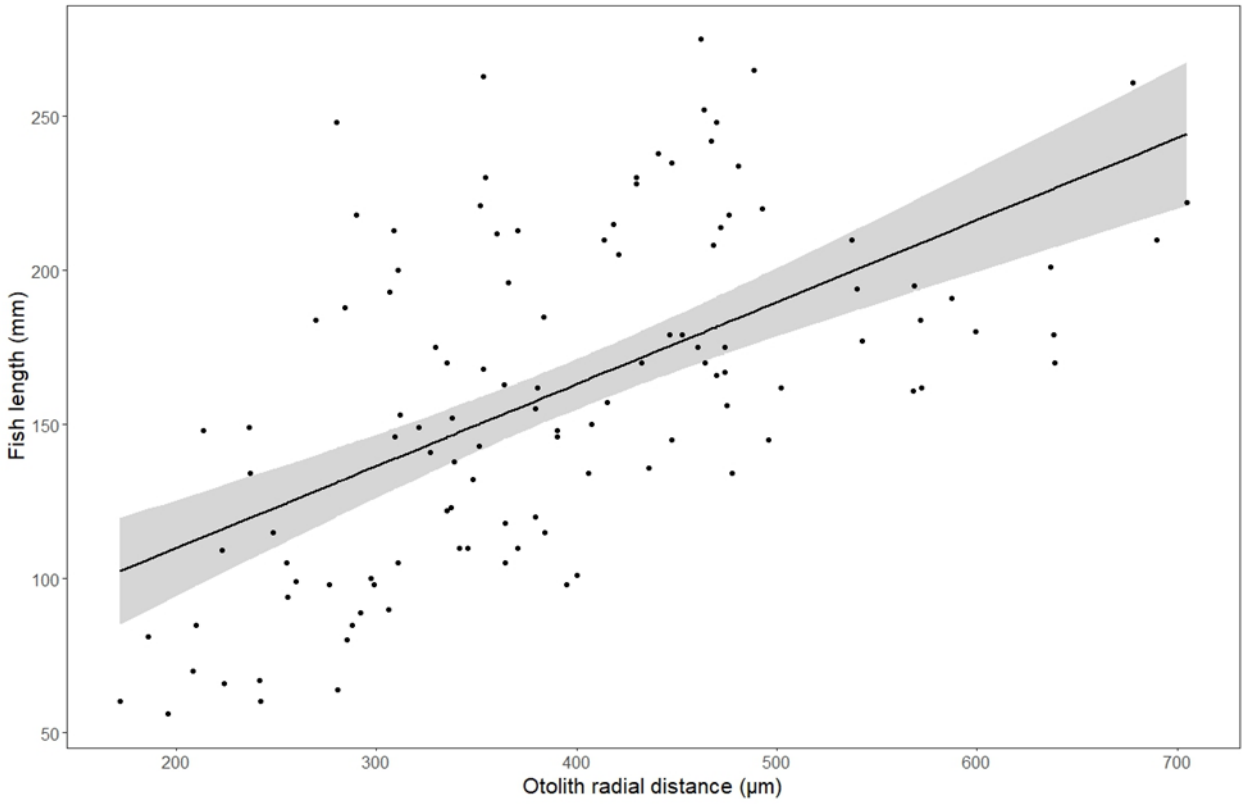

Figure 19. Marginal mean-scaled estimates of recent growth (mm of growth in 7 days) of juvenile summer flounder in Eastern Shore (●) and Piankatank River (▲) sites in marsh, oyster, soft-bottom, and seagrass habitats, 2019-2020. Vertical lines denote 95% confidence limits.

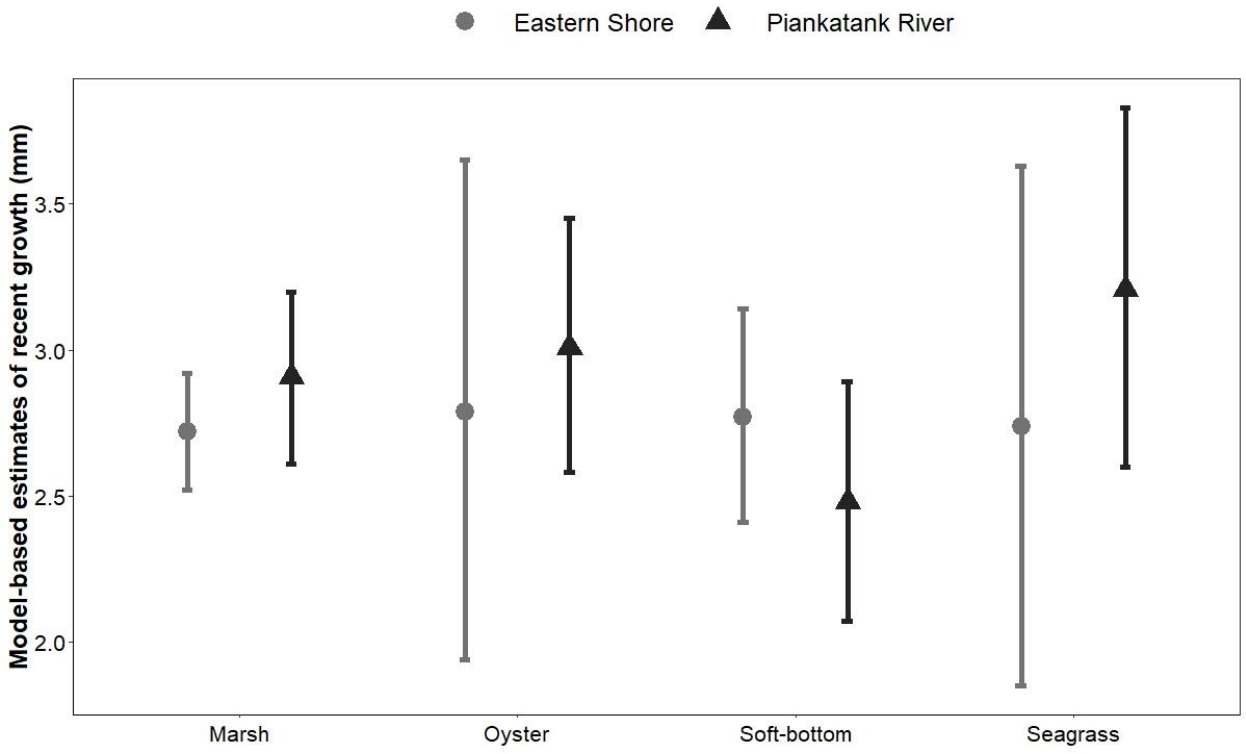

Figure 20. Marginal mean-scaled estimates of relative condition (K_n) for juvenile black sea bass captured in Eastern Shore habitats (left panel) and between 2019 and 2020 at the Eastern Shore, (right panel). Vertical lines denote 95% confidence limits.

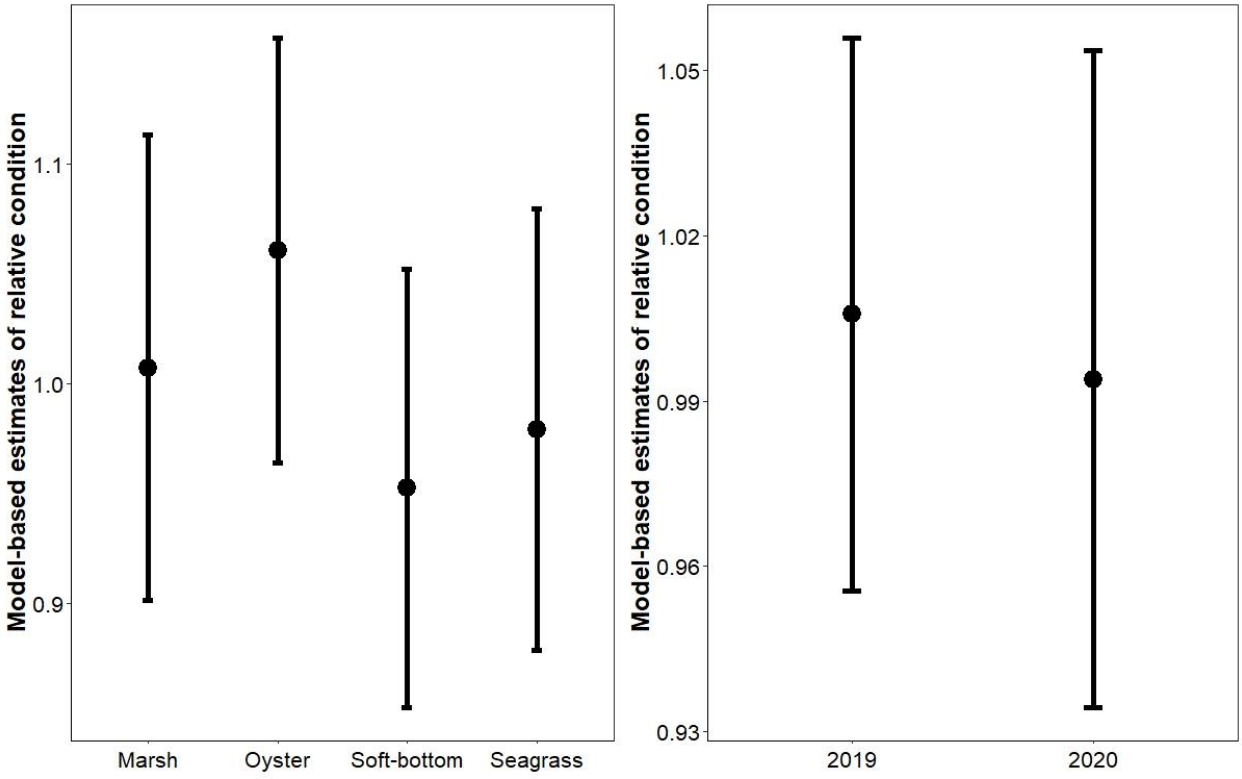

Figure 21. Body size (total length, mm) of juvenile black sea bass plotted against their corresponding otolith radial distance (µm). Juvenile black sea bass were captured from Eastern Shore and Piankatank River sites in 2019-2020. The solid black line is the regression fitted to the individual observations of length (●); dark grey shading indicates 95% confidence limits.

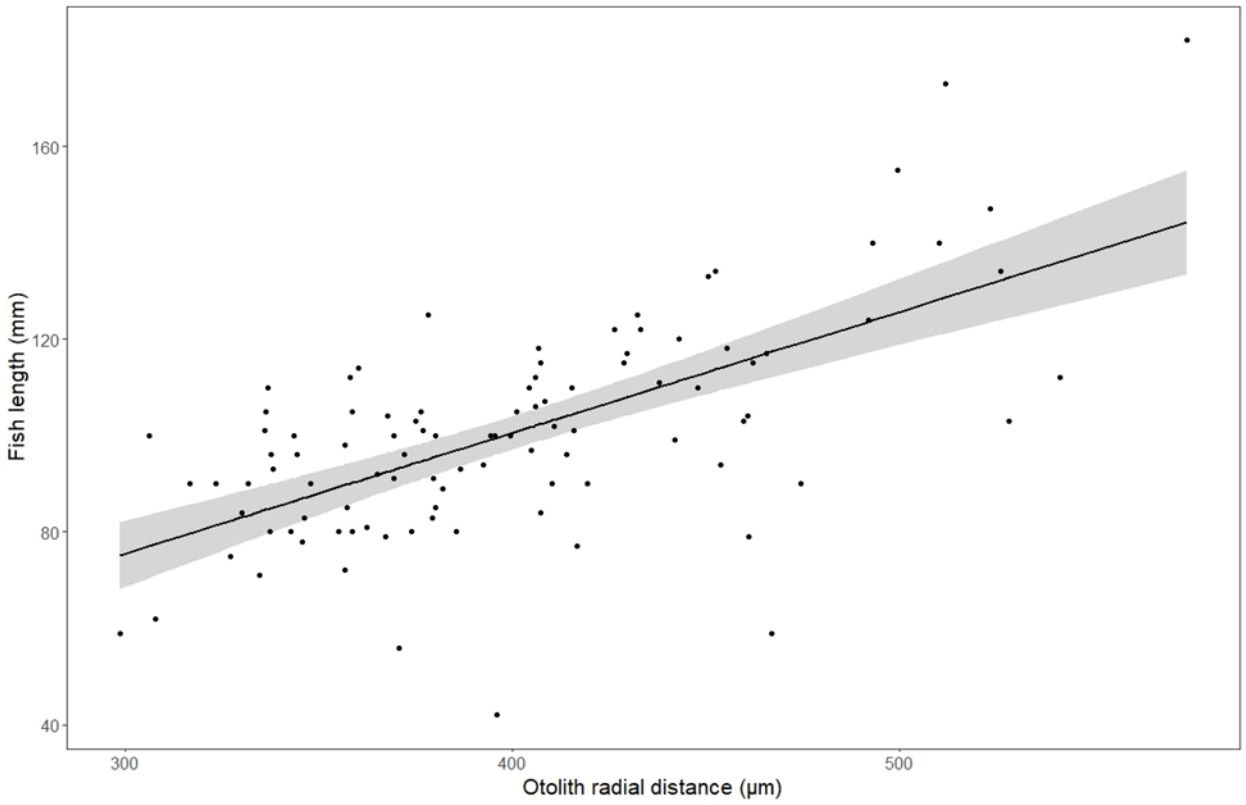

Figure 22. Marginal mean-scaled estimates of recent growth for juvenile black sea bass captured in Eastern Shore habitats (left panel) and between 2019 and 2020 at Eastern Shore sites (right panel). Vertical black lines denote 95% confidence limits.

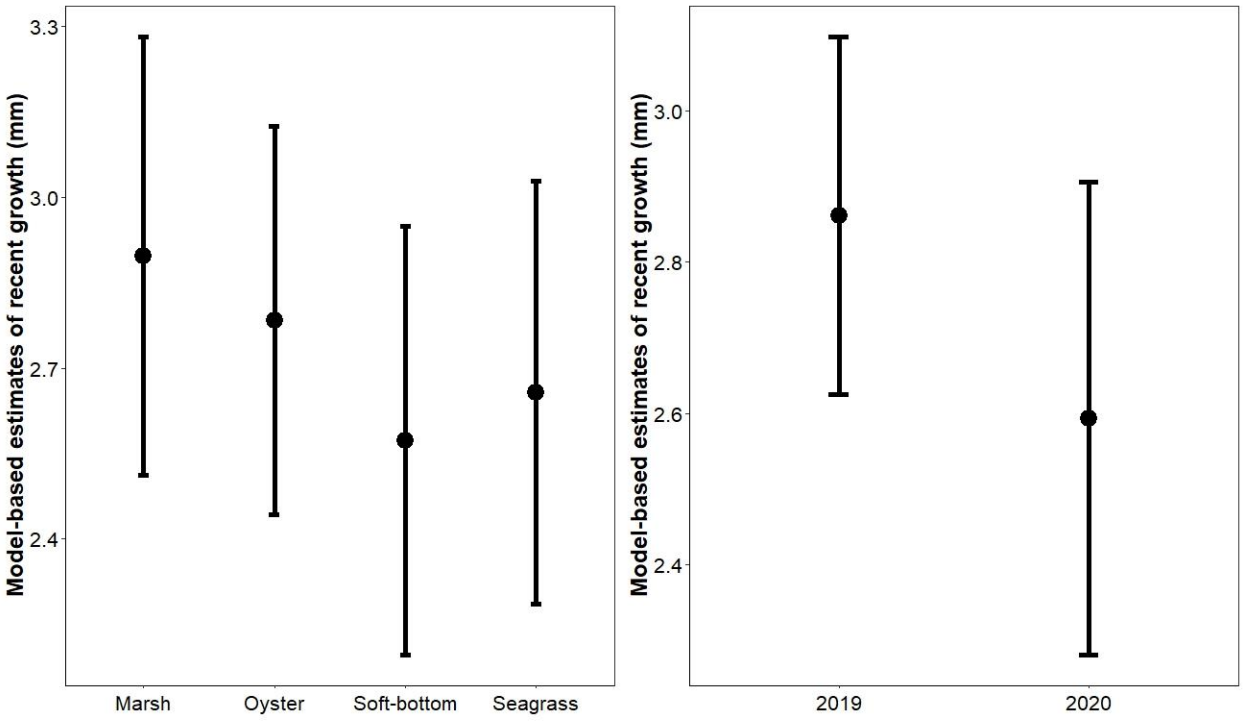

Figure 23. The effect of the percent of oyster habitat within 500 m of a fish's capture location on relative condition (K_n) of juvenile black sea bass captured at Eastern Shore and Piankatank River sites, 2019-2020. The figure depicts the fit of the generalized additive model to observed K_n values of individual fish; red filled circles (●) are Eastern Shore fish and blue filled circles (●) are Piankatank River fish.

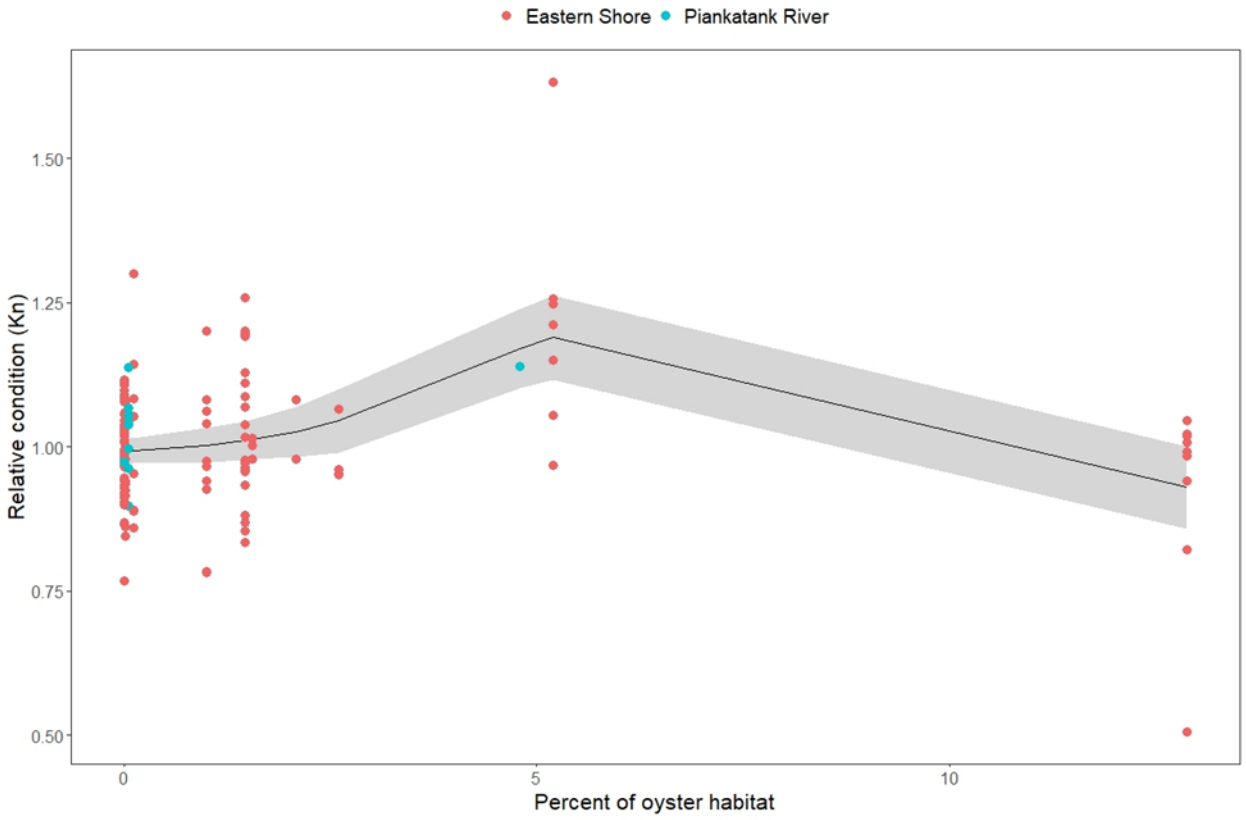

Figure 24. The effect of seascape features on recent growth of juvenile black sea bass captured at Eastern Shore and Piankatank River sites, 2019-2020. Seascape features include (A) percent of soft-bottom habitat, (B) percent of seagrass habitat, and (C) distance to the nearest seagrass habitat. The figure depicts the fit of the generalized additive model to observed recent growth values of individual fish; red filled circles (●) are Eastern Shore fish and blue filled circles (●) are Piankatank River fish.

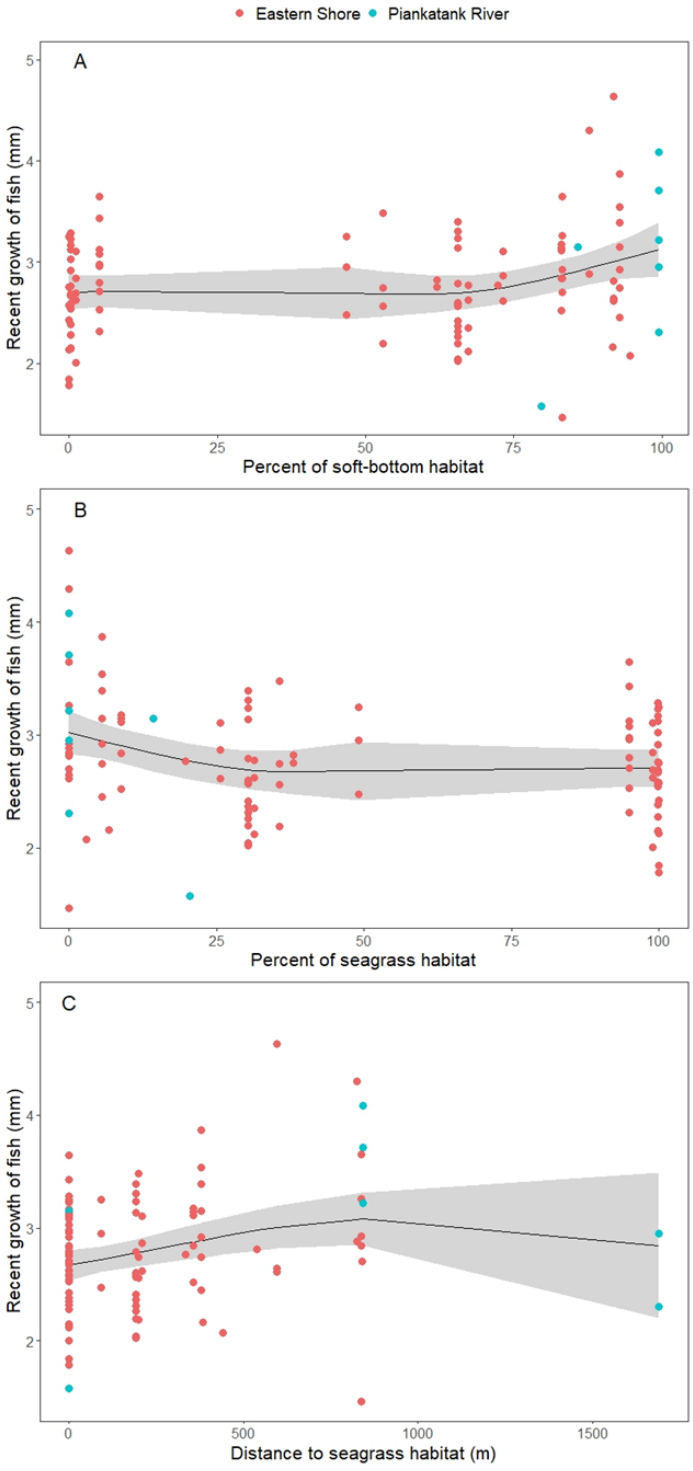

Figure 25. Number of tows that sampled for (A) juvenile summer flounder and (B) juvenile black sea bass each year by three fishery-independent surveys. The number of tows in the MD Coastal Bays Survey for summer flounder and black sea bass ranged from 69 to 100; the number of tows in the MD Small Trawl Survey ragned from 105 to 265 for summer flounder and from 48 to 65 for black sea bass; the number of tows conducted by the VIMS Juvenile Fish Trawl Survey ranged from 290 to 400 tows for summer flounder and from 185 to 260 tows for black sea bass.

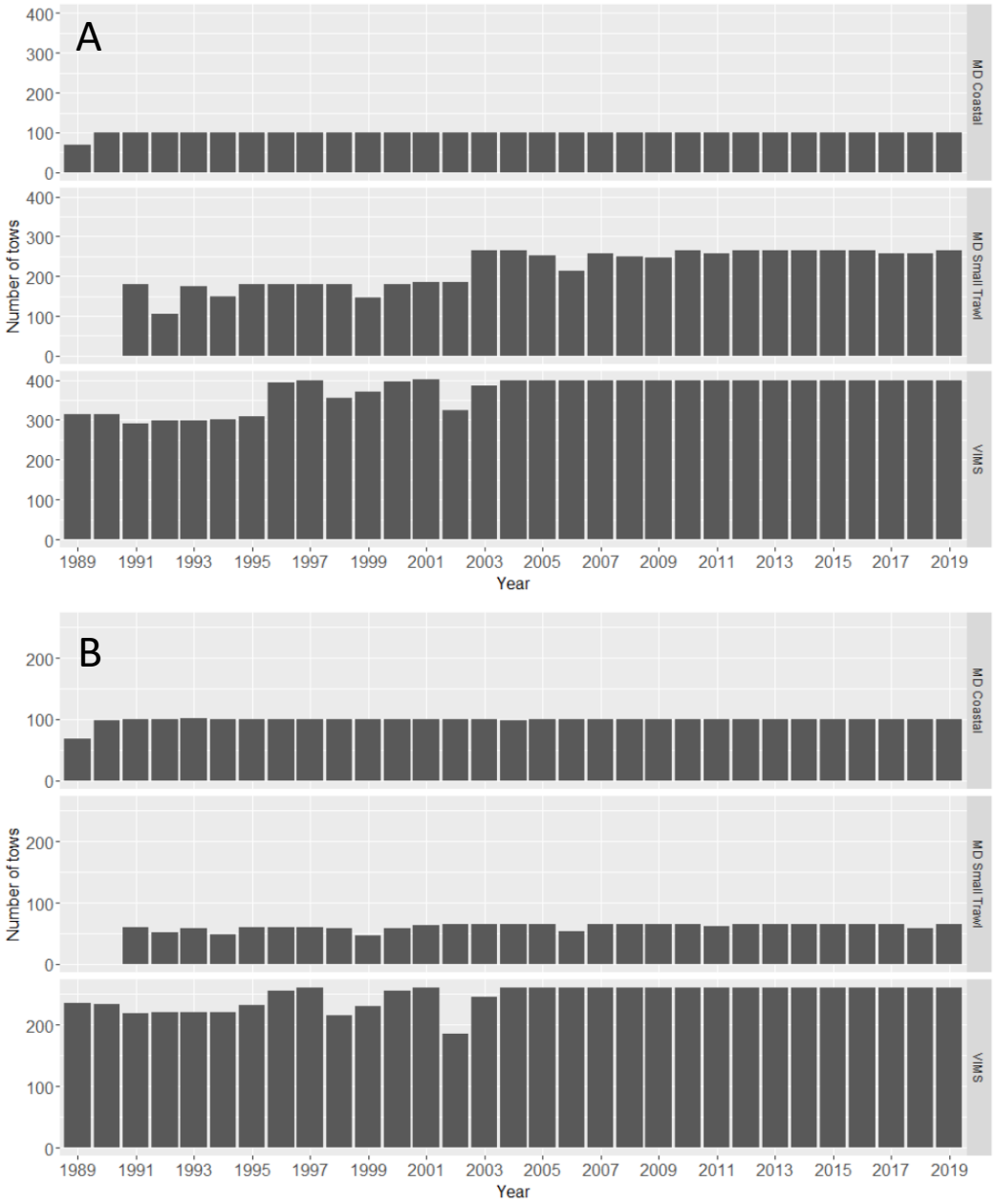

Figure 26. Numbers of (A) juvenile summer flounder and (B) juvenile black sea bass captured annually by the MD Coastal Bays (1989 – 2019), MD Small Trawl (1991 – 2019), and the VIMS Juvenile Fish Trawl (1989 – 2019) surveys. The MD Coastal Bays Survey observed 11,862 summer flounder and 1,965 black sea bass; the MD Small Trawl Survey observed 1,714 summer flounder and 32 black sea bass; the VIMS Juvenile Fish Trawl Survey observed 12,849 summer flounder and 7,697 black sea bass. For clarity, zero catches were omitted from the plots.

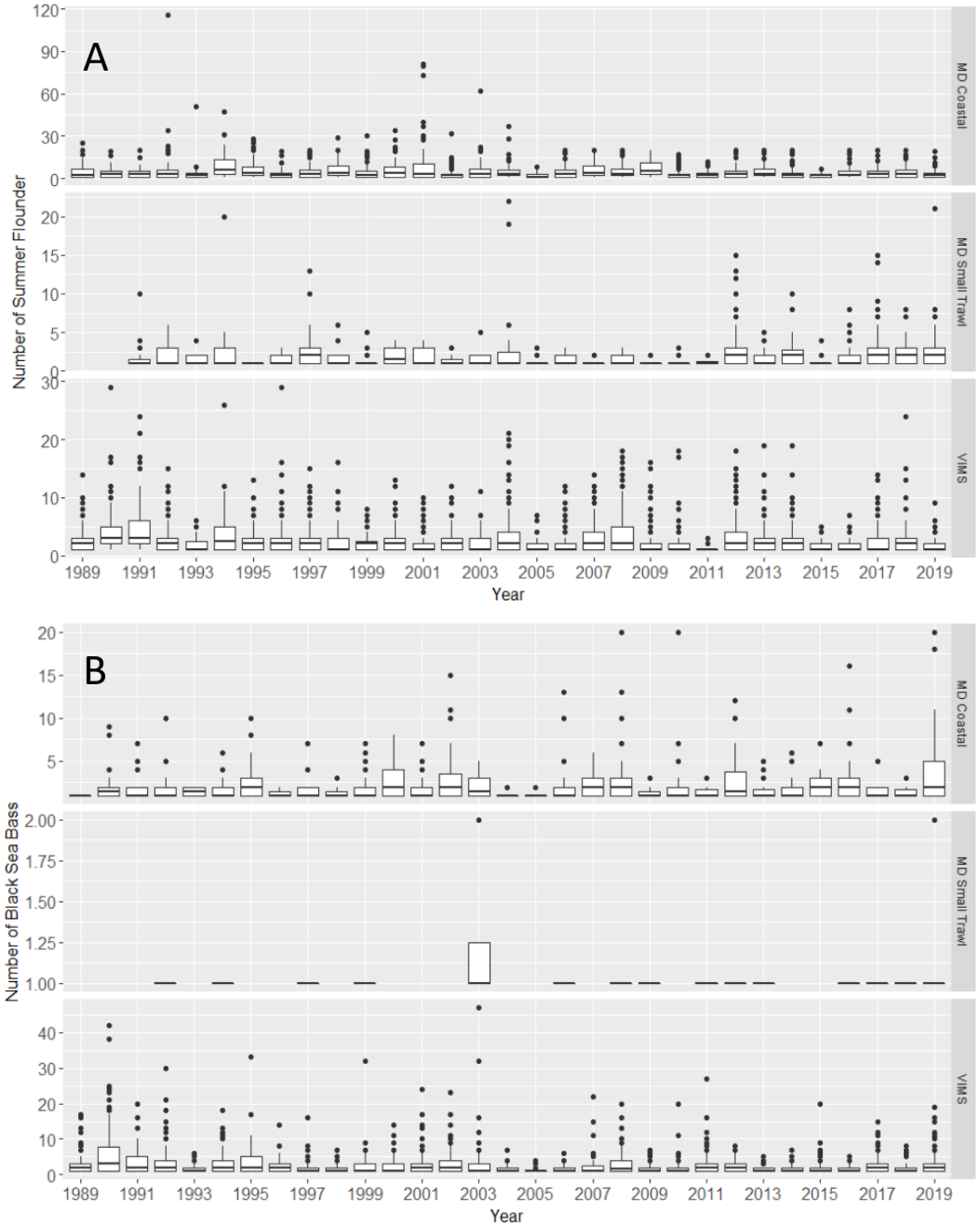

Figure 27. Effect of (A) bottom water temperature (°C), (B) bottom salinity (psu), and (C) depth (m) on relative abundance of juvenile summer flounder in the MD Coastal Bays Survey, 1989 - 2019. The horizontal line at zero on the y-axis indicates no effect. The solid red line is the fit of the generalized additive model and the gray shaded area denotes the 95% confidence interval.

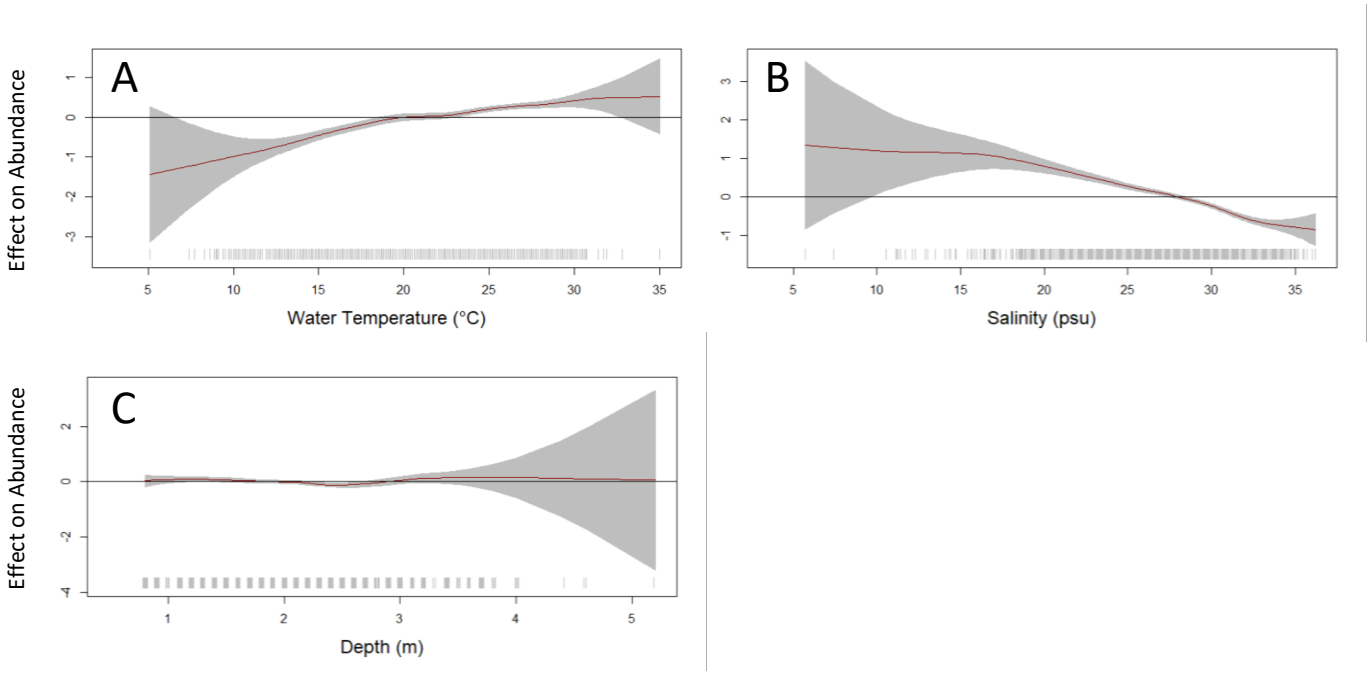

Figure 28. Effect of (A) bottom water temperature (°C), (B) bottom salinity (psu), and (C) depth (m) on relative abundance of juvenile summer flounder in the VIMS Juvenile Fish Trawl Survey, 1989 - 2019. The horizontal line at zero on the y-axis indicates no effect. The solid red line is the fit of the generalized additive model and the gray shaded area denotes the 95% confidence interval.

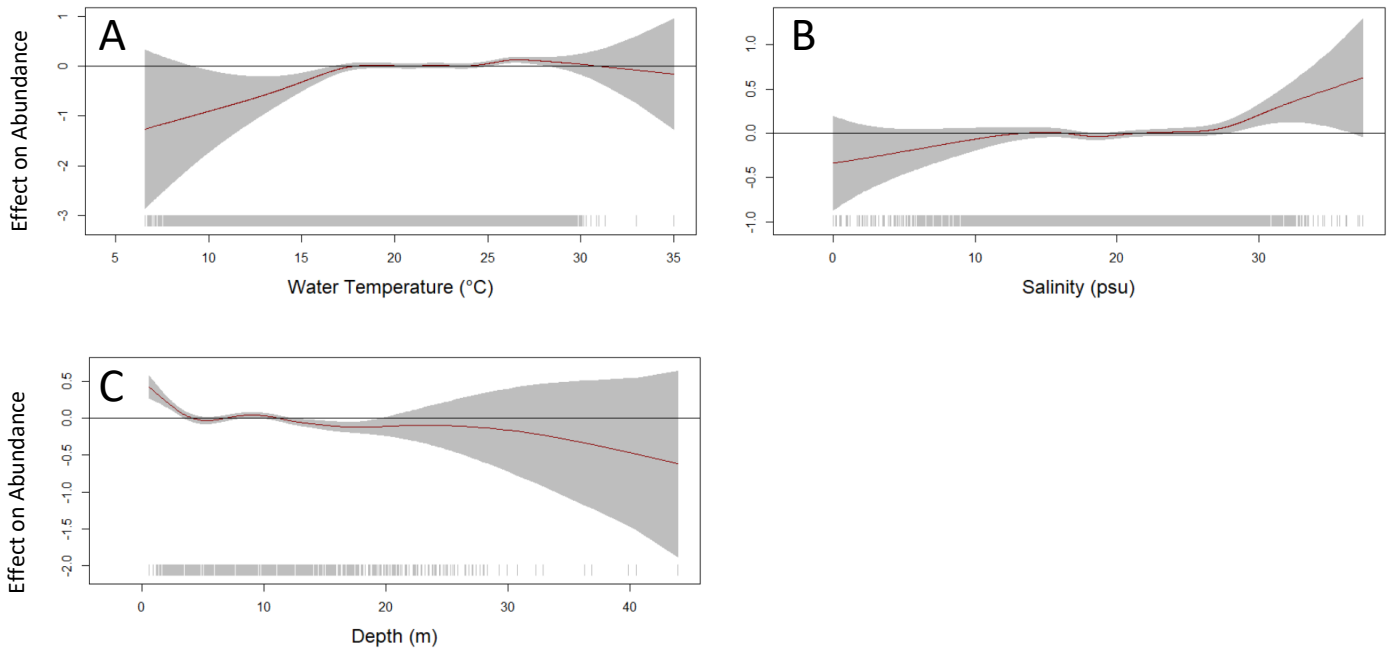

Figure 29. Effect of (A) bottom water temperature (°C), (B) bottom salinity (psu), and (C) depth (m) on relative abundance of juvenile summer flounder in the MD Small Trawl Survey, 1991 - 2019. The horizontal line at zero on the y-axis indicates no effect. The solid red line is the fit of the generalized additive model and the gray shaded area denotes the 95% confidence interval.

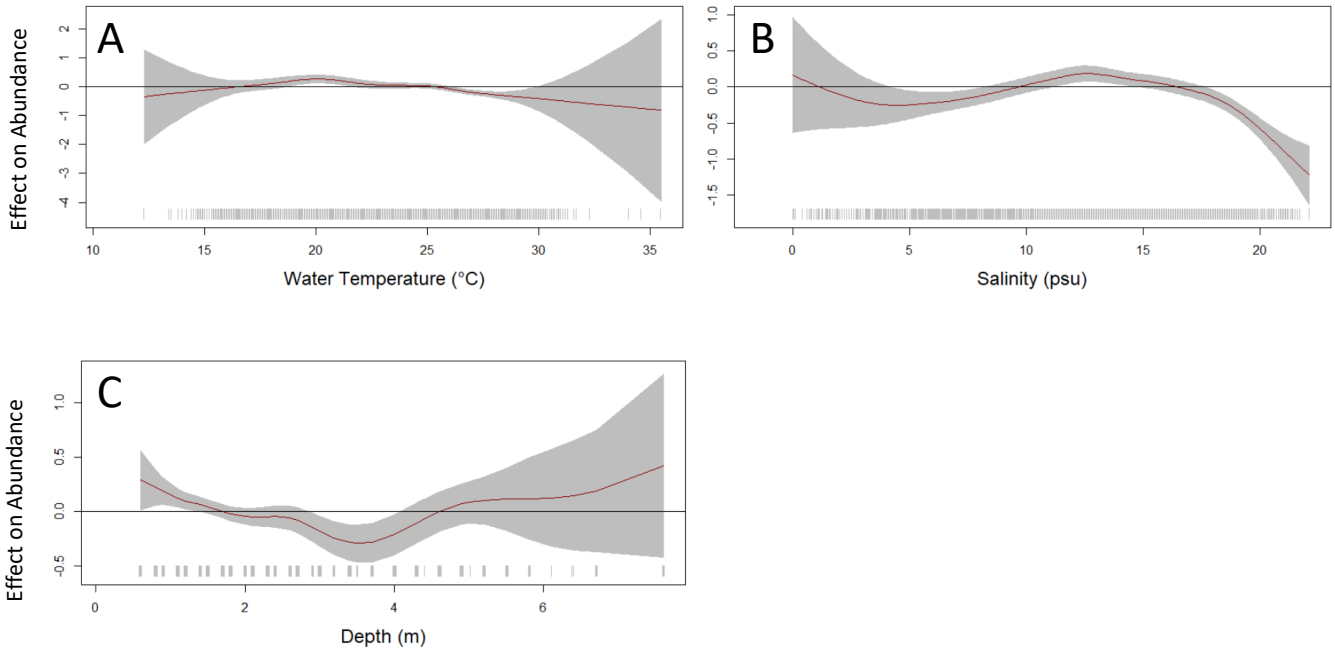

Figure 30. Effect of (A) bottom water temperature (°C), (B) bottom salinity (psu), and (C) depth (m) on relative abundance of juvenile black sea bass in the MD Coastal Bays Survey, 1989 - 2019. The horizontal line at zero on the y-axis indicates no effect. The solid red line is the fit of the generalized additive model and the gray shaded area denotes the 95% confidence interval.

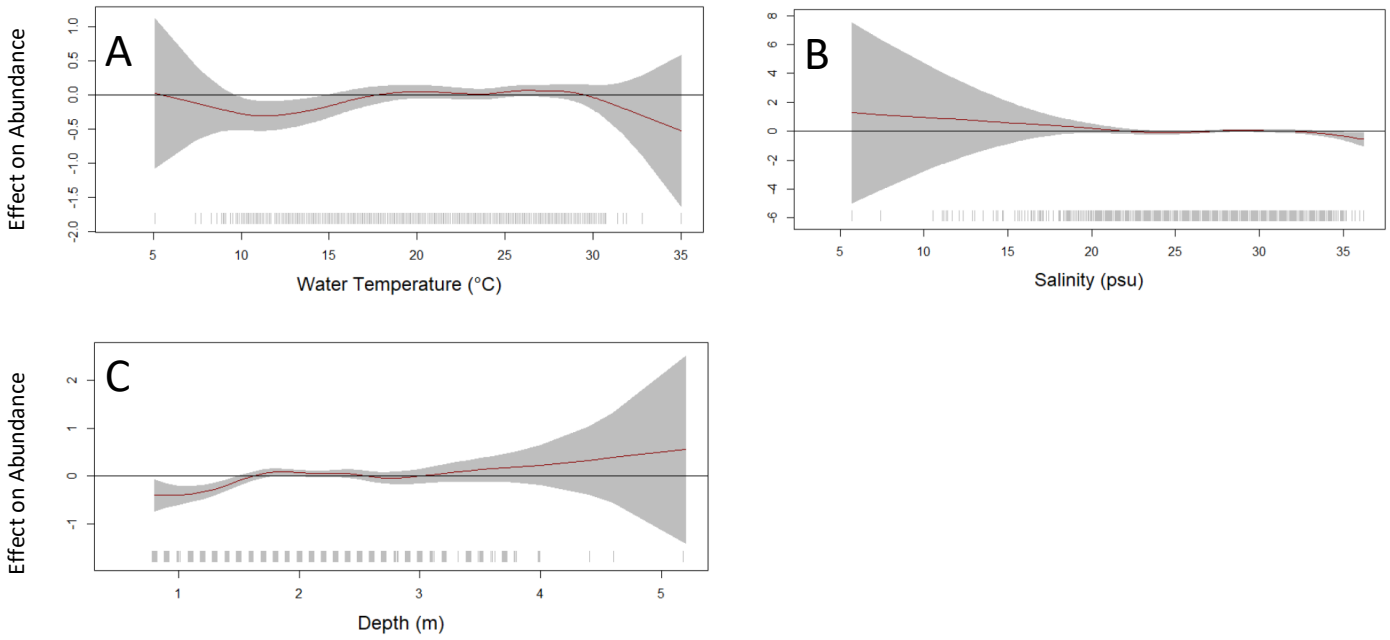

Figure 31. Effect of (A) bottom water temperature (°C), (B) bottom salinity (psu), and (C) depth (m) on relative abundance of juvenile black sea bass in the VIMS Juvenile Fish Trawl Survey, 1989 - 2019. The horizontal line at zero on the y-axis indicates no effect. The solid red line is the fit of the generalized additive model and the gray shaded area denotes the 95% confidence interval.

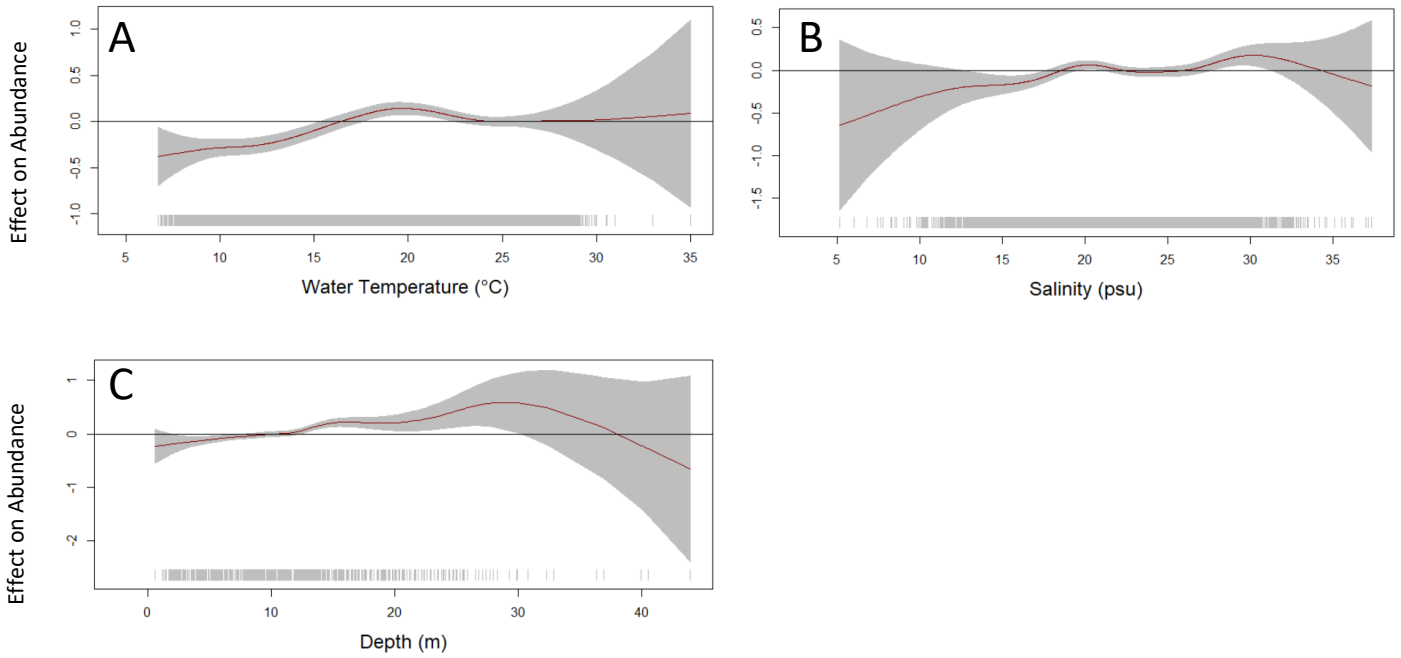

Figure 32. Effect of (A) bottom water temperature, (B) capture date, (C) bottom salinity, (D) mean-centered density, (E) distance to marsh, (F) distance to seagrass (SAV), (G) distance to oyster, and (H) distance to shore on mean length of juvenile summer flounder, 1989 to 2019 in Chesapeake Bay and the MD Coastal Bays. The black line represents the smooth function fitted to the observations (gray shading indicates ± 2 standard errors). The horizontal line at zero indicates no effect on mean length; values above the zero-line indicate a postive effect. Panels E – H show the effect of categorical distances (m) to structure, where GT indicates "greater than."

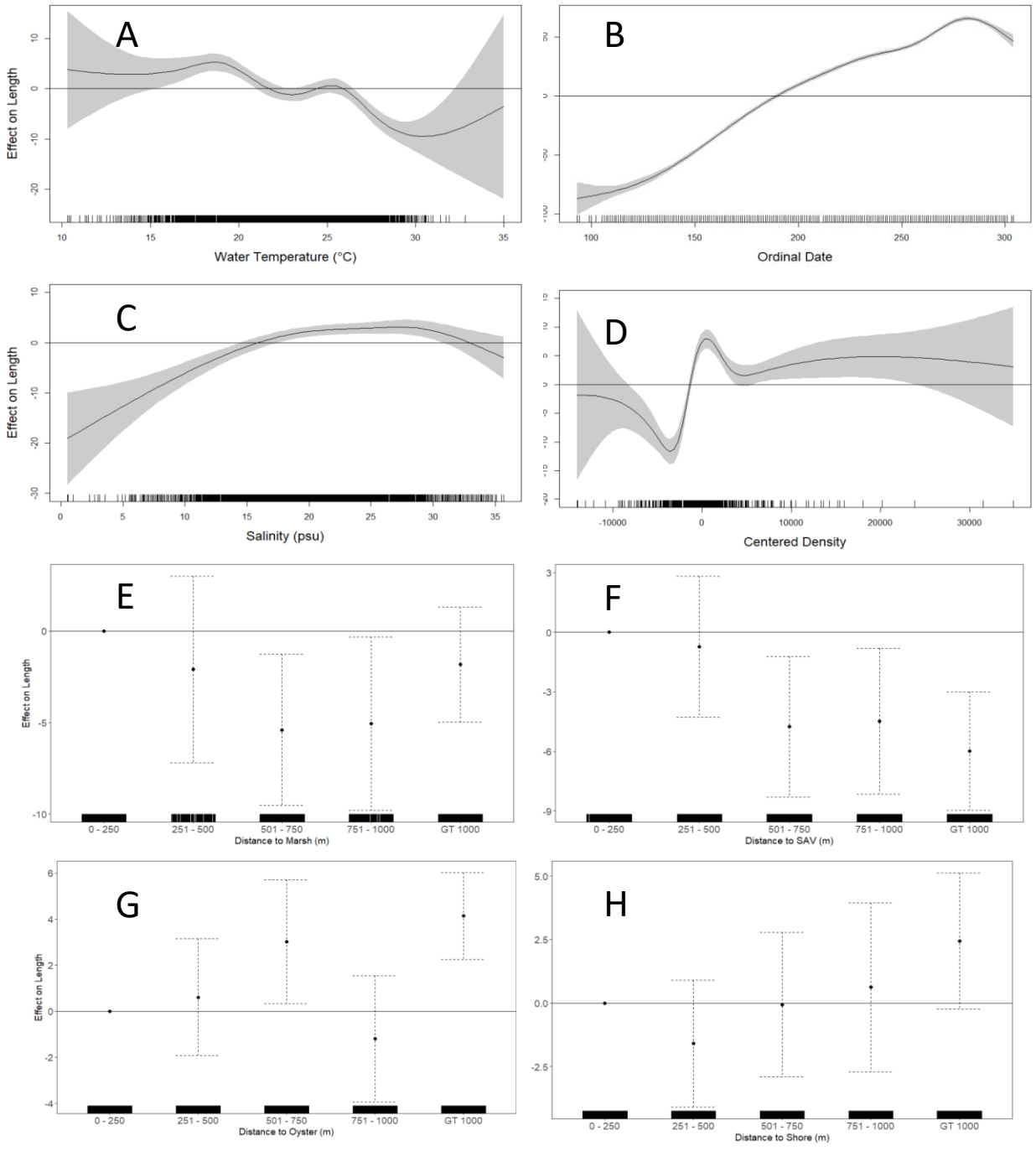

Figure 32 continued. Effect of survey stratum on mean length of juvenile summer flounder from 1989 to 2019 in Chesapeake Bay and the MD Coastal Bays. The horizontal line at zero indicates no effect on mean length; values above the zero line indicate a postive effect. CPR is the Choptank River (reference stratum), EBY is the Eastern Bay, James is the James River, MD_C_North is Assawoman Sound and Isle of Wight, MD_C_South is Sinepuxent Bay and Chincoteague Bay, POC is Pocomoke Sound, Rapp is the Rappahannock River, TNG is Tangier Sound, VALower_bay, VAMid_bay, VAUpper_bay correspond with Virginia lower bay, Virginia middle bay and Virginia upper bay, and York is the York River.

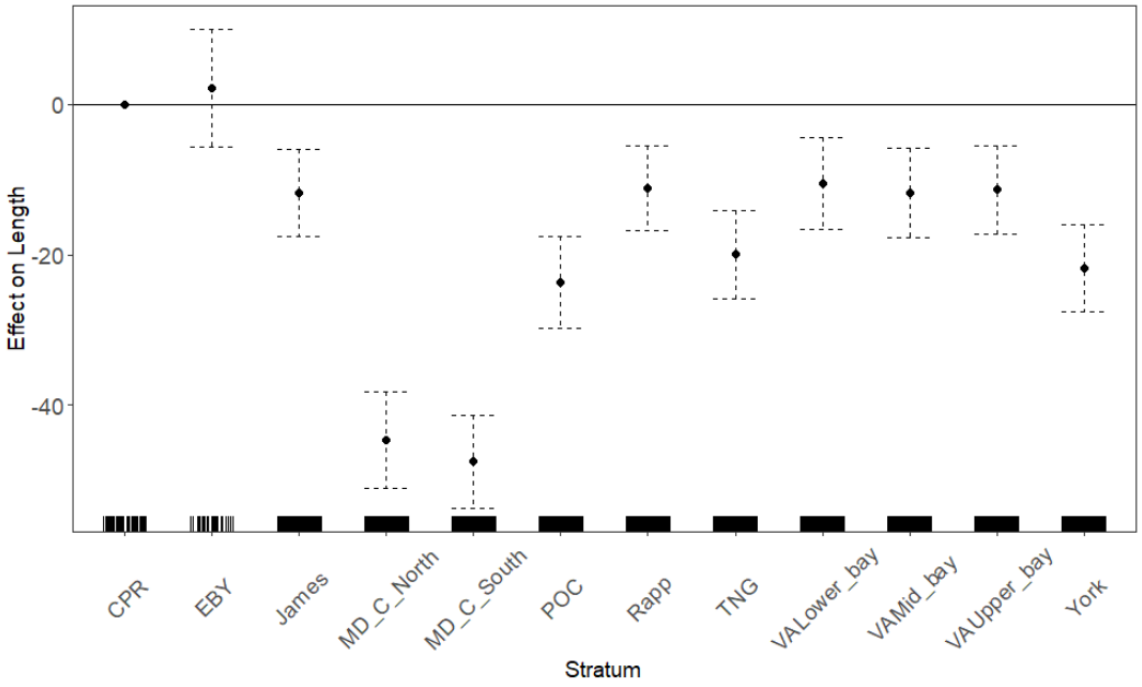

Figure 33. Effect of (A) capture date, (B) depth (m), and (C) stratum on the mean length of juvenile black sea bass from 1989 to 2019 in Chesapeake Bay and the MD Coastal Bays. The black line represents the smooth function (gray shading indicates ± 2 standard errors). The horizontal line at zero indicates no effect on mean length; values above the zero line indicate a postive effect. James is the James River, MD_C_North is Assawoman Sound and Isle of Wight, MD_C_South is Sinepuxent Bay and Chincoteague Bay, POC is Pocomoke Sound, TNG is Tangier Sound, and VALower_bay, VAMid_bay, VAUpper_bay correspond with Virginia lower bay, Virginia middle bay, and Virginia upper bay.

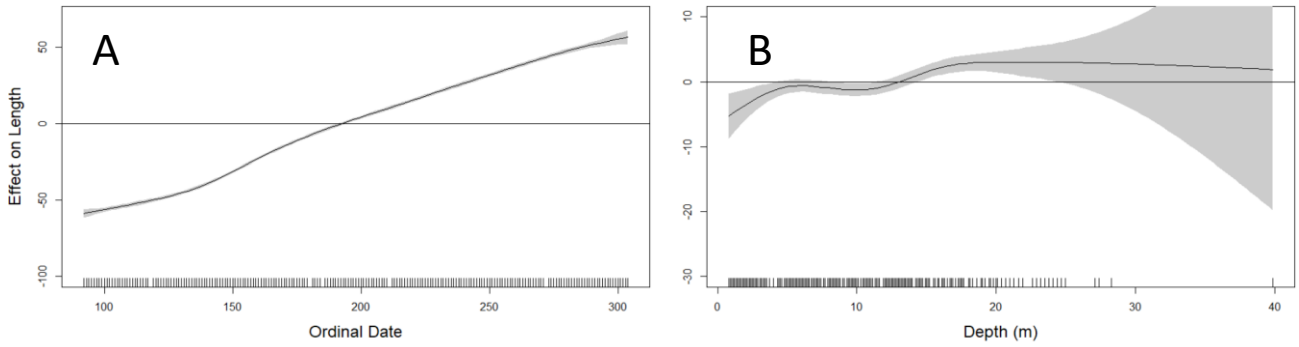

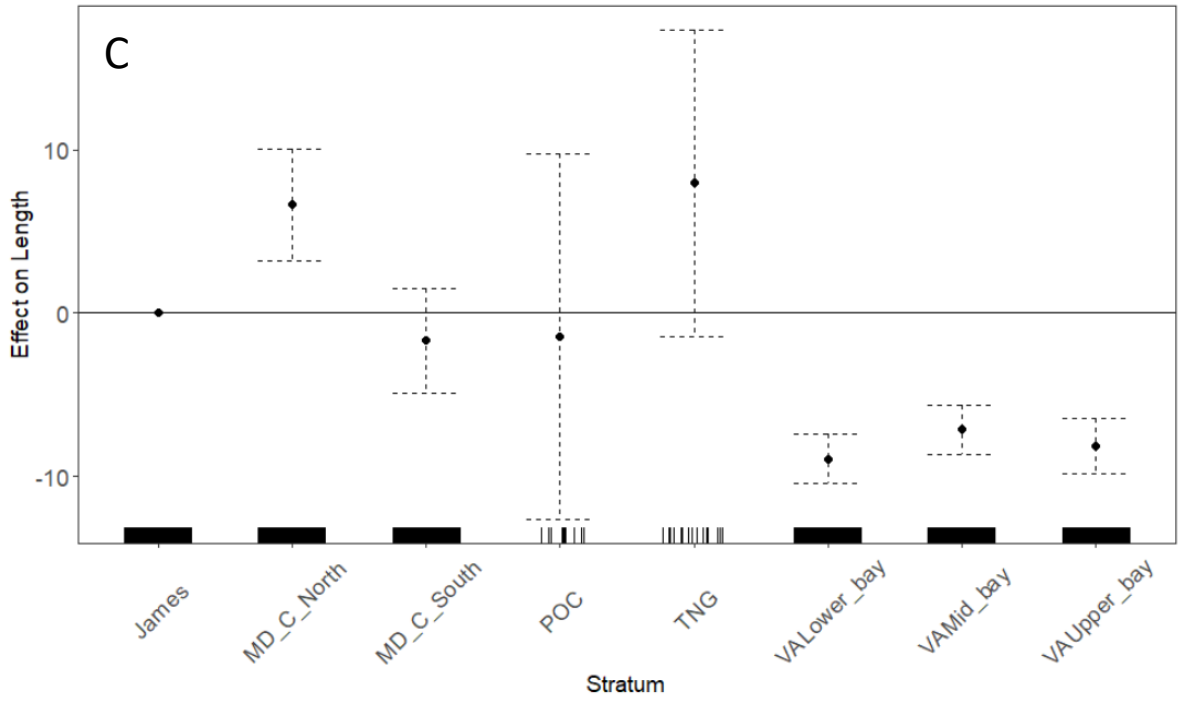

Figure 34. Estimated daily baywide extents (hectares) of suitable thermal habitat that supports summer flounder growth in Chesapeake Bay for each year, 1996 to 2019. Day of the year ranges between 1 May and 30 November, with minimum extents observed on average on day 225, which occurs on 13 August (12 August in leap years); minimum extents were observed between calendar day 205 (late July) and 249 (early September).

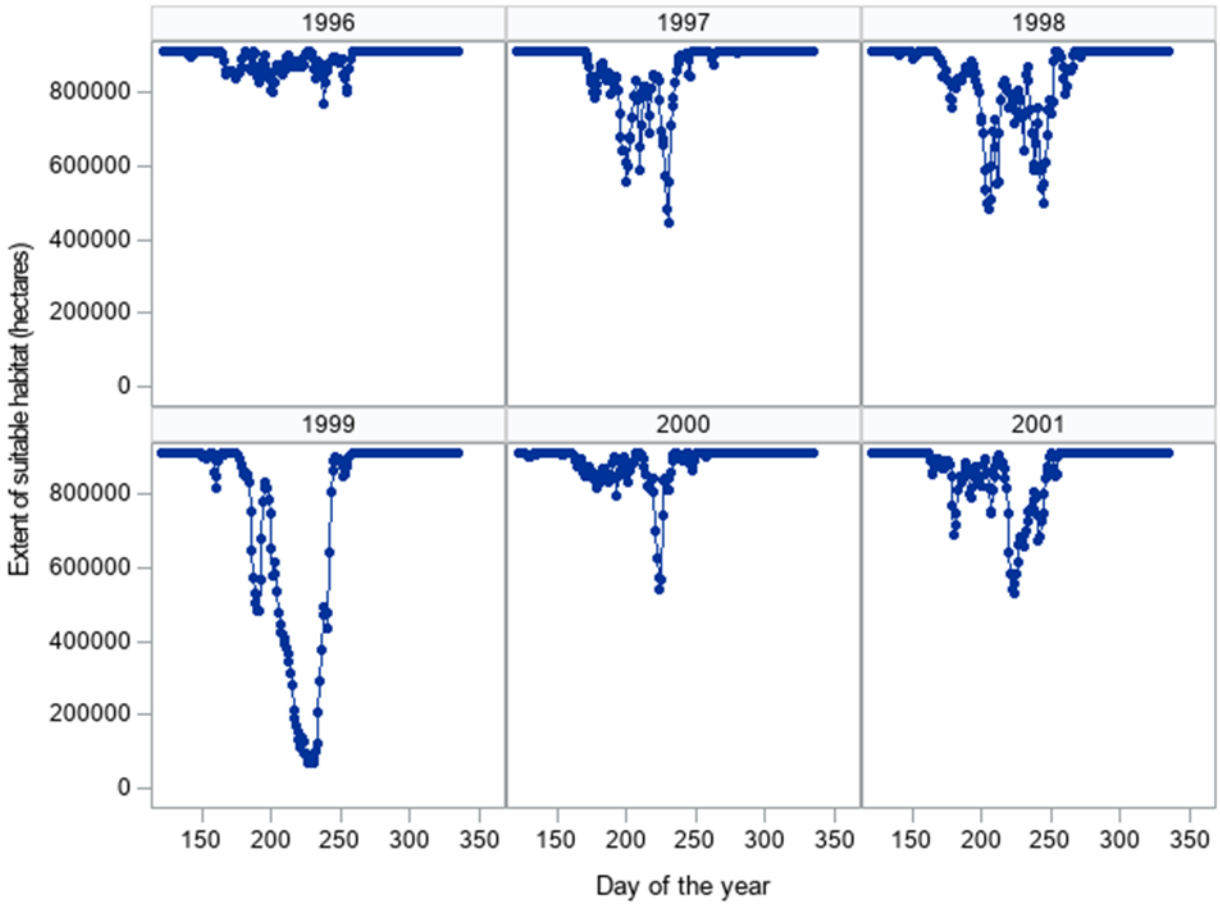

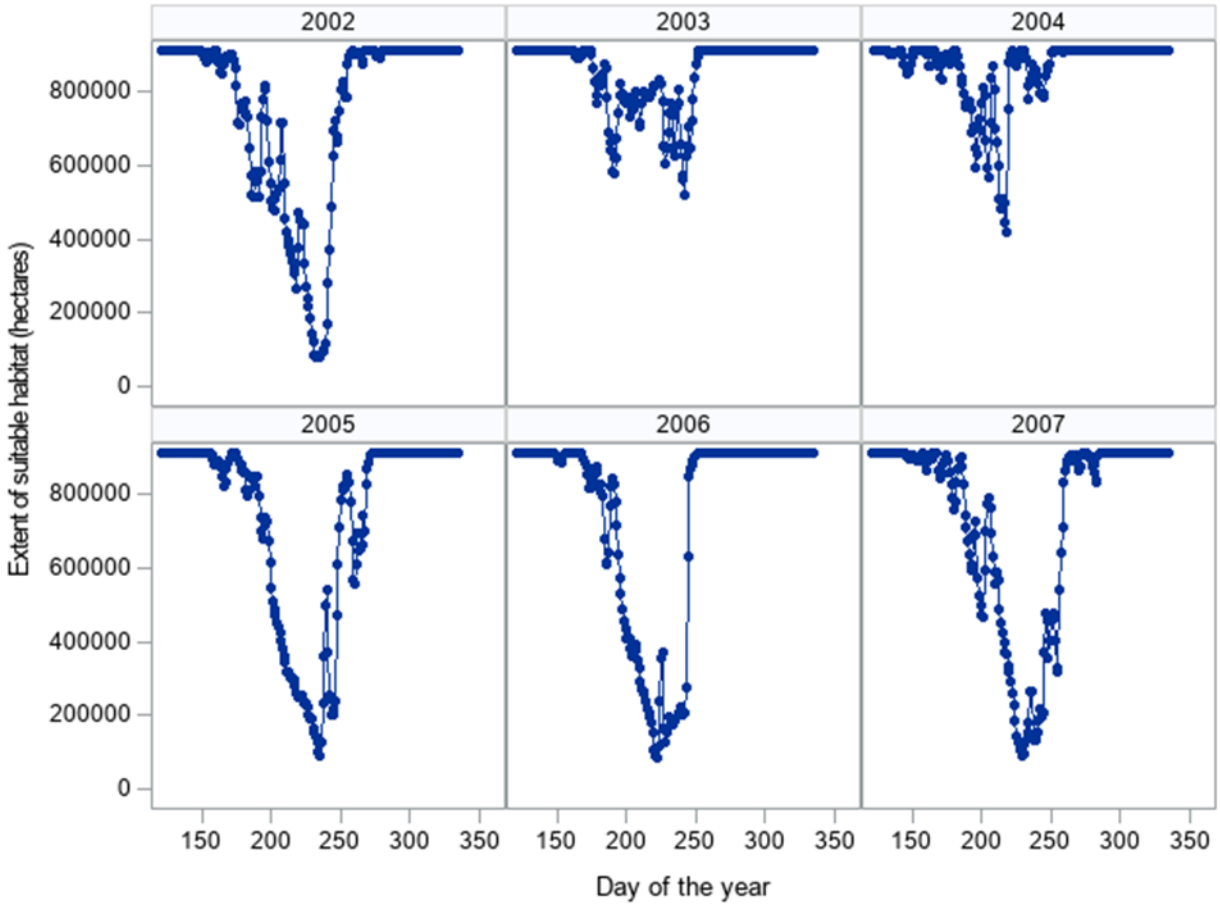
2002
2003
2004
2005
2006
2007
Extent of suitable habitat (hectares)
800000
600000
400000
200000
0
150
200
250
300
350
Day of the year

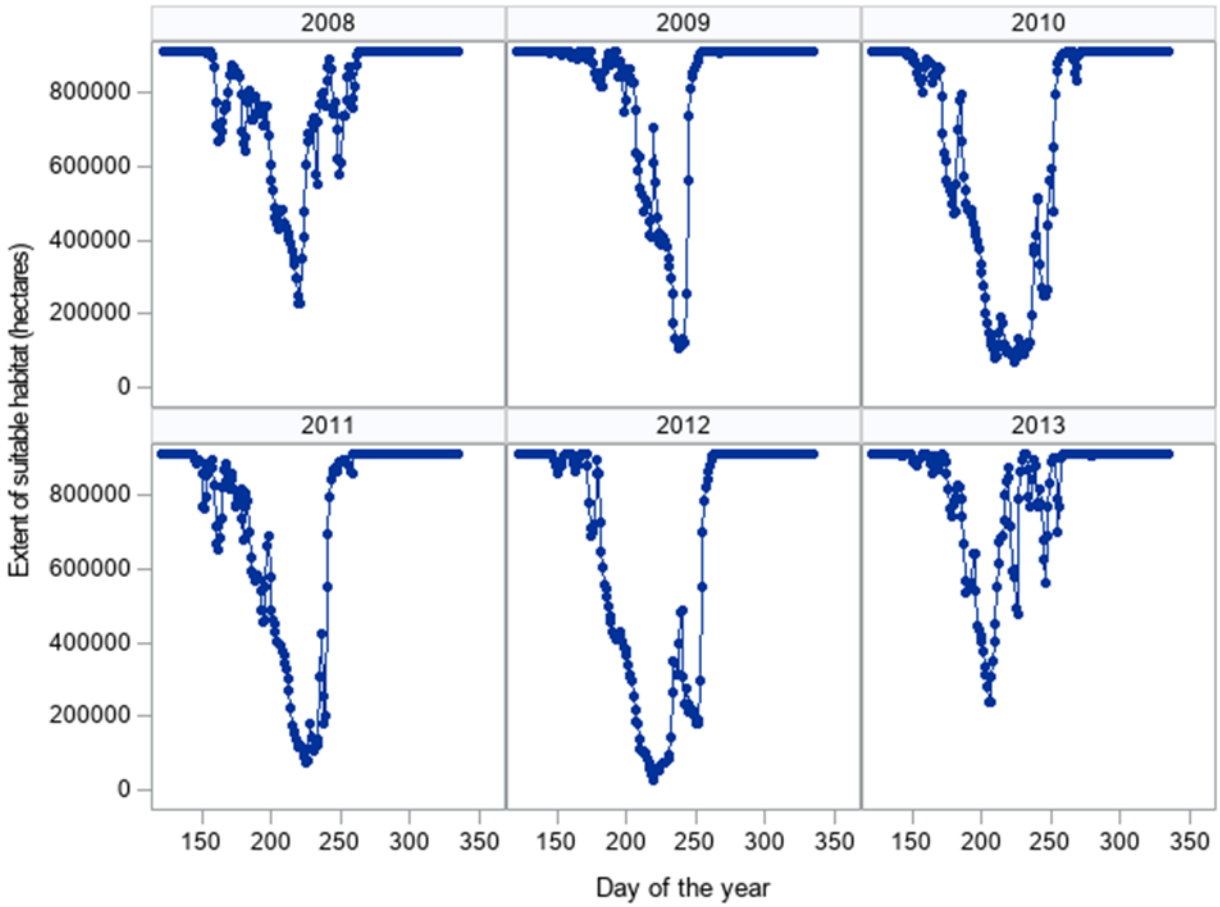
2008
2009
2010
2011
2012
2013
Extent of suitable habitat (hectares)
800000
600000
400000
200000
0
150
200
250
300
350
Day of the year

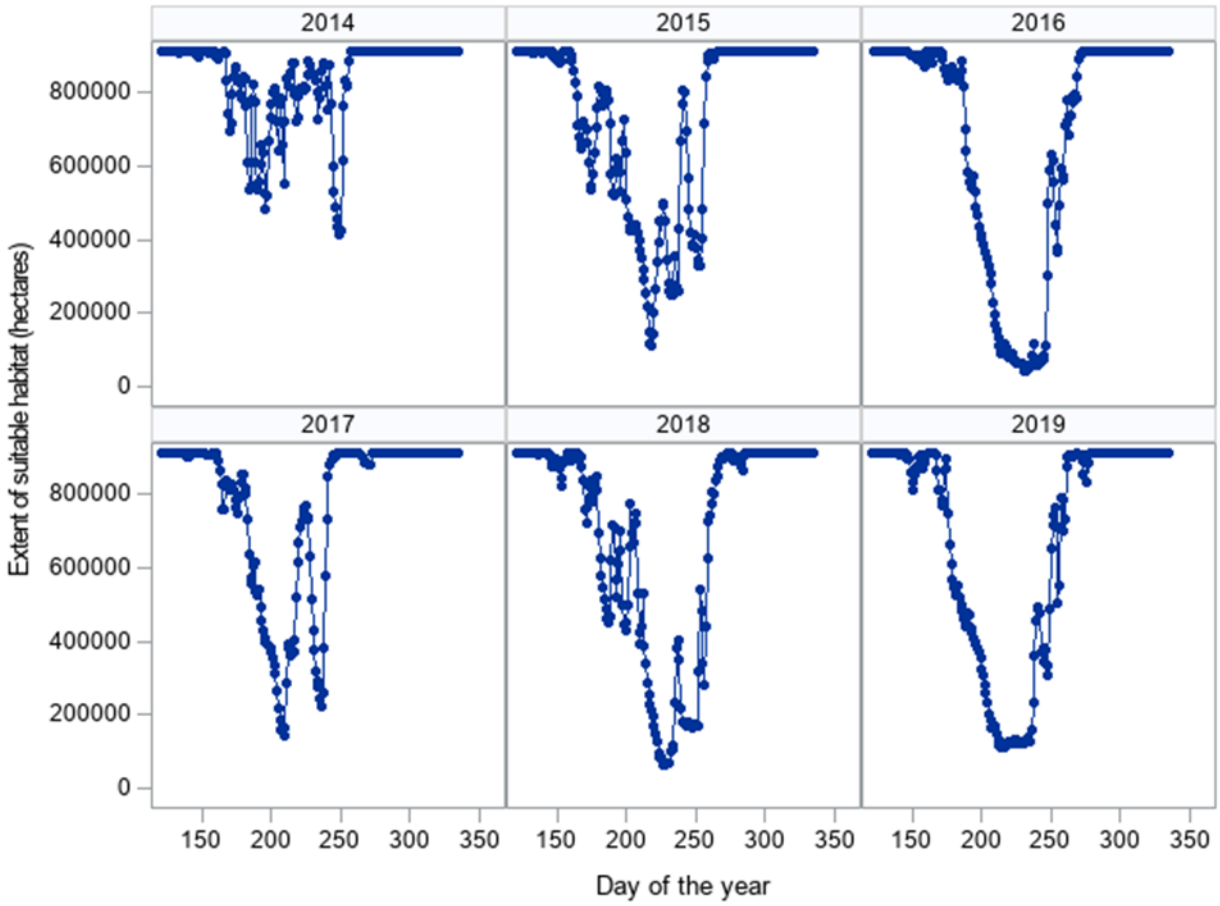
2014
2015
2016
2017
2018
2019
Extent of suitable habitat (hectares)
800000
600000
400000
200000
0
150
200
250
300
350
Day of the year

Figure 35. Model-based estimates of the annual extent (hectares) of suitable habitat for juvenile summer flounder growth in Chesapeake Bay, 1996 to 2019; the slopes for each month are significantly different from zero (t_{Jun}=-2.68, P_{Jun}=0.014; t_{Jul}=-4.98, P_{Jul}<0.001; t_{Aug}=-2.54, P_{Aug}=0.019; t_{Sep}=-3.40, P_{Sep}=0.003), whereas non-significant slopes were observed in May (t_{May}=-1.70, P_{May}=0.103) and October (t_{Oct}=-1.32, P_{Oct}=0.199), when almost the entirety of the bay supported suitable habitats for growth.

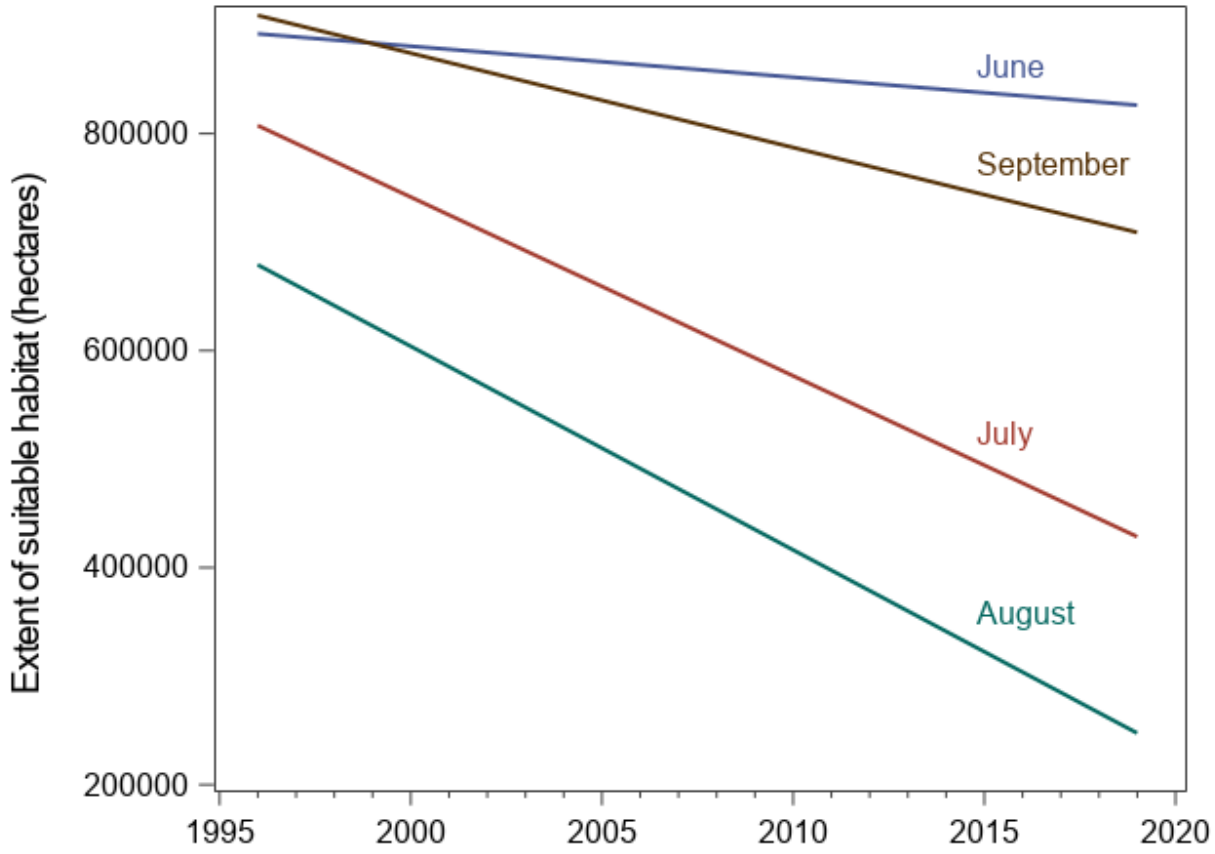

Figure 36. Median percent suitable habitat (< 25.9 °C) in Chesapeake Bay for growth of juvenile summer flounder, 1996 – 2019; the filled circles represent medians from the distribution of daily values observed between 1 June and 31 October each year. The line is a simple regression line and the shaded region denotes the 95% confidence limit; the slope is significant (*t*=-3.96, P<0.001) and indicates a 0.75% annual decrease in the median across years.

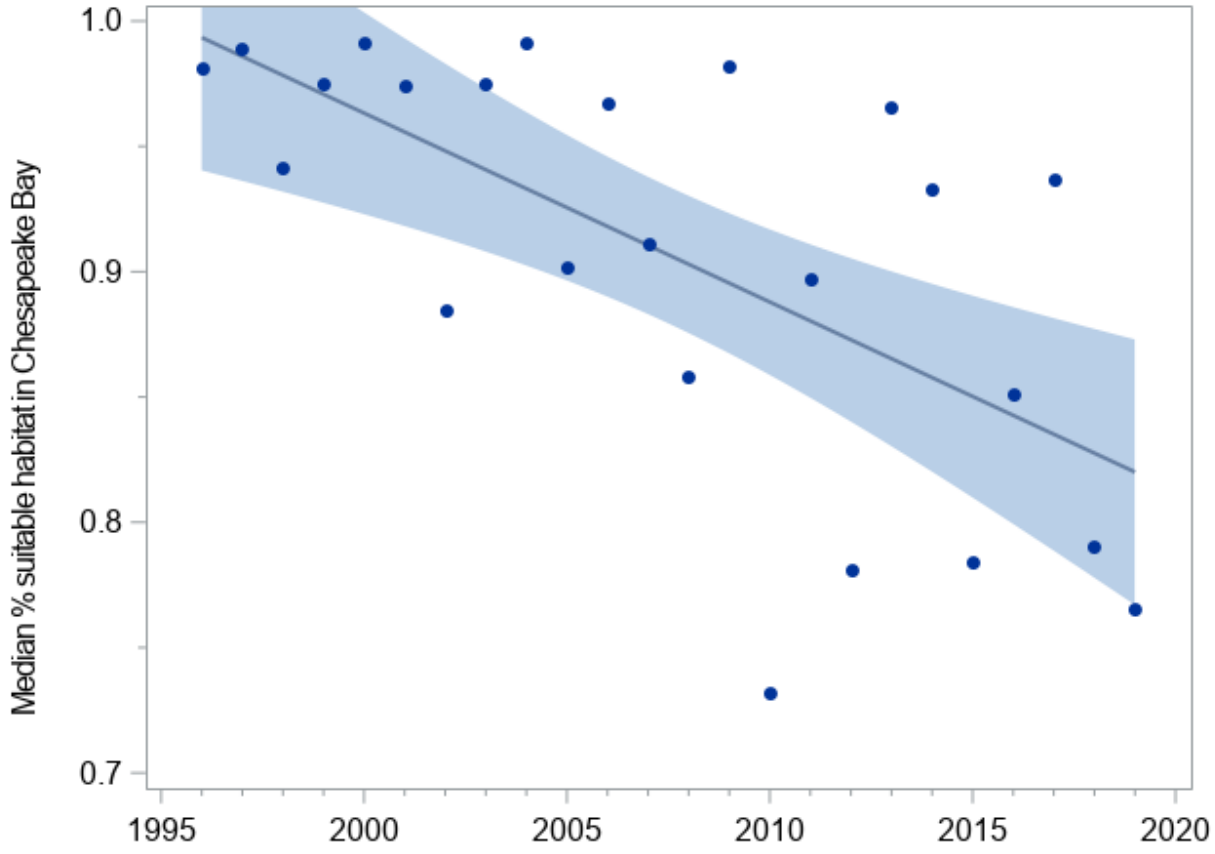

Figure 37. Percent of Chesapeake Bay exhibiting suitable thermal habitat (< 25.9 °C) for growth of juvenile summer flounder in June, July, August, and September, 1996-2019. Gray filled circles (●) are daily observations (N=2,928) that were jittered to enhance clarity, and the blue line is a loess curve fitted to the data with a smoothing parameter of 0.2.

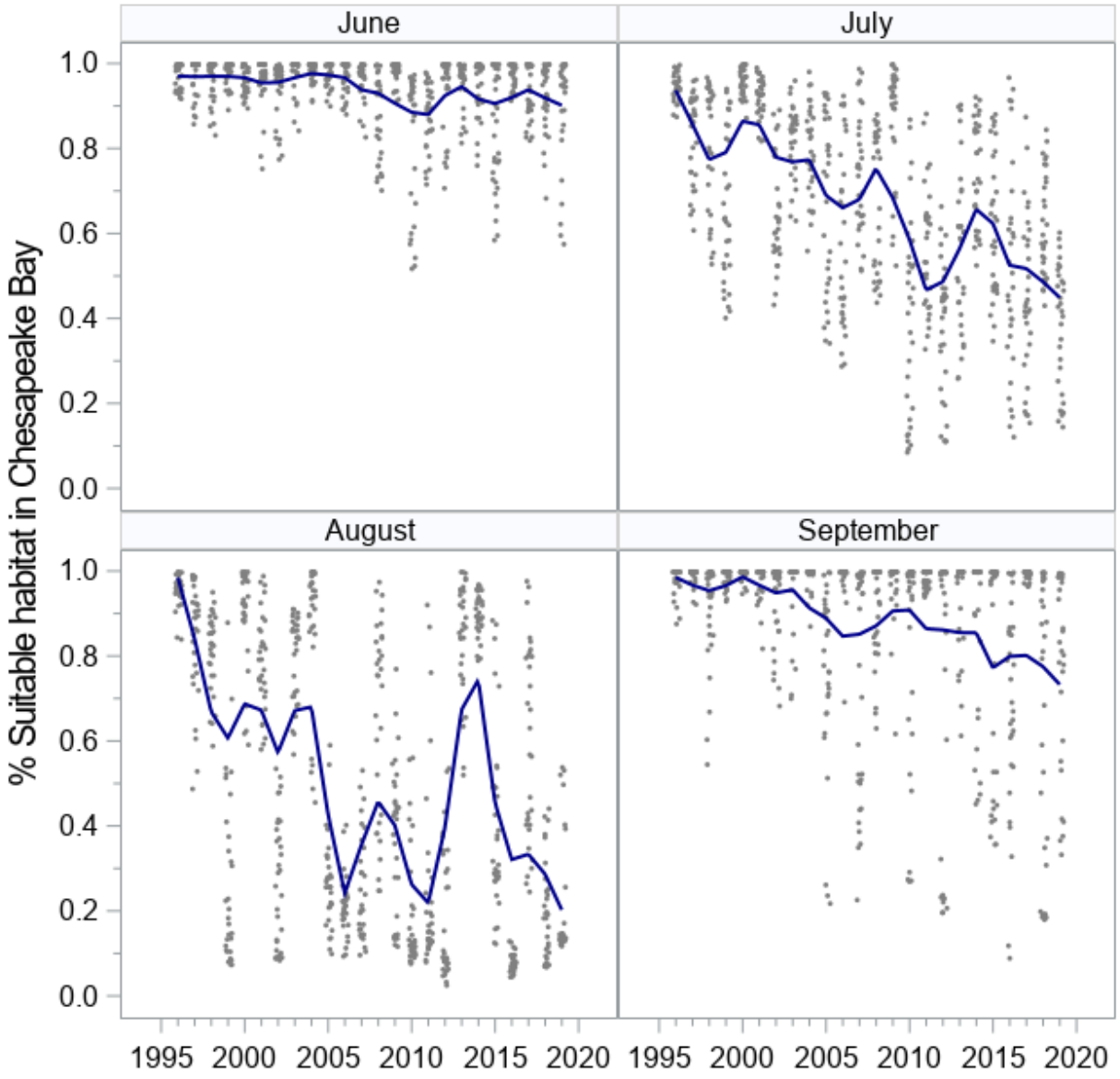

Figure 38. Relationship between the percent of suitable thermal habitat (< 25.9 °C) for growth of juvenile summer flounder in Maryland and Virginia, for early summer (June-July) and late summer (August-September), 1996 to 2019. Open circles (○) are daily observations (N=2,928); the dashed gray line is the one-to-one line, and the solid green line is a loess curve fitted to the data with a smoothing parameter of 0.2.

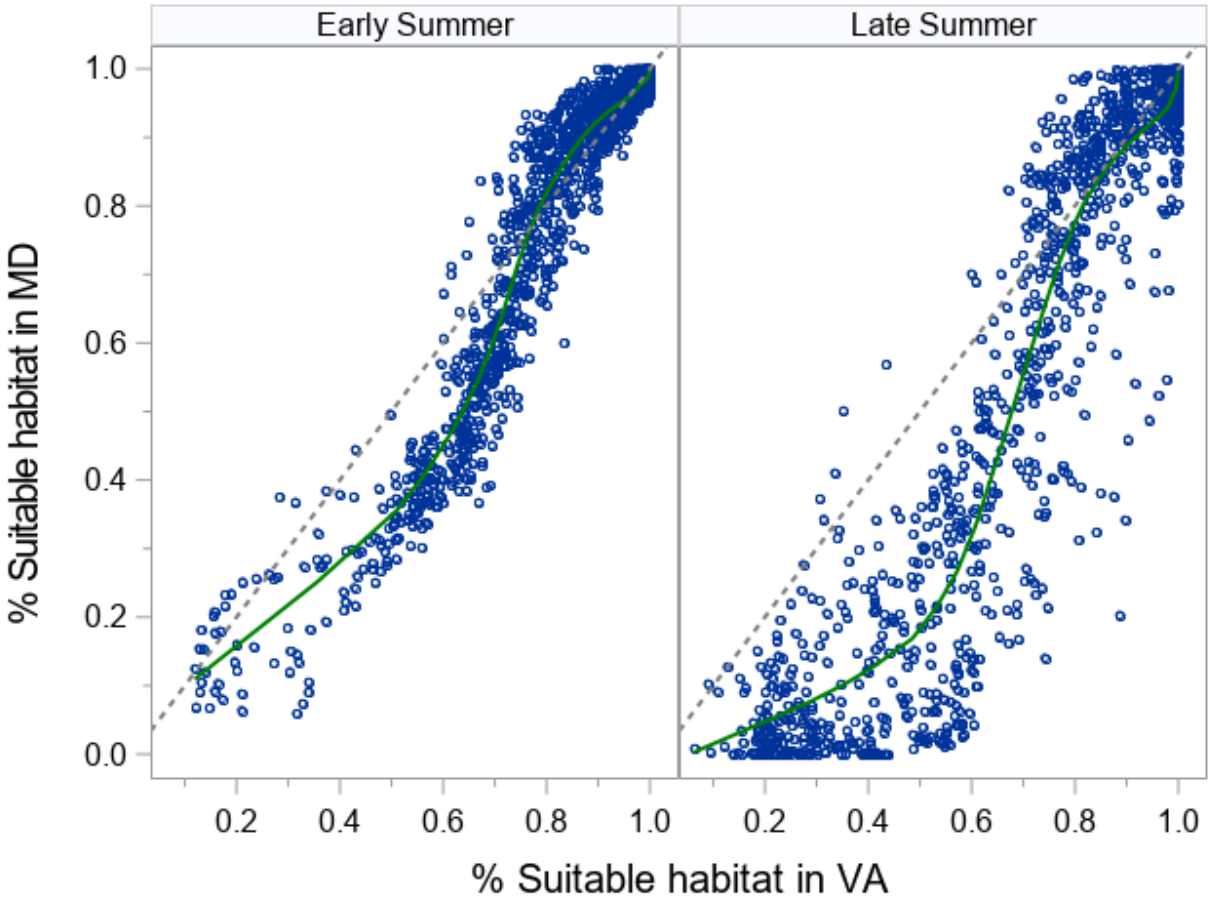

Figure 39. Baywide relative abundance of juvenile summer flounder (●) and the baywide extent of suitable thermal (<25.9 °C) habitat (green line) from 1996 -2019. The index of abundance is based on the Conn method of combining indices from the VIMS Juvenile Fish Trawl survey and the MD Small Trawl survey. Habitat extents are in hectares. We were unable to detect an effect of suitable habitat extent on relative baywide abundance (F=0.93, P=0.346).